

**REPORT
133**

**TECTONIC LINKS BETWEEN PROTEROZOIC
SEDIMENTARY CYCLES, BASIN FORMATION AND
MAGMATISM IN THE ALBANY–FRASER OROGEN,
WESTERN AUSTRALIA**

by CV Spaggiari, CL Kirkland, RH Smithies,
and MTD Wingate





Government of **Western Australia**
Department of **Mines and Petroleum**

REPORT 133

TECTONIC LINKS BETWEEN PROTEROZOIC SEDIMENTARY CYCLES, BASIN FORMATION AND MAGMATISM IN THE ALBANY–FRASER OROGEN, WESTERN AUSTRALIA

by

CV Spaggiari, CL Kirkland, RH Smithies, and MTD Wingate

Perth 2014



**Geological Survey of
Western Australia**

MINISTER FOR MINES AND PETROLEUM
Hon. Bill Marmion MLA

DIRECTOR GENERAL, DEPARTMENT OF MINES AND PETROLEUM
Richard Sellers

EXECUTIVE DIRECTOR, GEOLOGICAL SURVEY OF WESTERN AUSTRALIA
Rick Rogerson

REFERENCE

The recommended reference for this publication is:

Spaggiari, CV, Kirkland, CL, Smithies, RH and Wingate, MTD 2014, Tectonic links between Proterozoic sedimentary cycles, basin formation and magmatism in the Albany–Fraser Orogen: Geological Survey of Western Australia, Report 133, 63p.

National Library of Australia Cataloguing-in-Publication entry:

Author: Spaggiari, C. V., author.
Title: Tectonic links between proterozoic sedimentary cycles, basin formation and magmatism in the Albany–Fraser Orogen, Western Australia / CV Spaggiari, CL Kirkland, RH Smithies, and MTD Wingate.
ISBN: 9781741685596 (ebook)
Subjects: Geology--Western Australia--Goldfields-Esperance Region.
Plate tectonics--Western Australia--Albany Region.

Other Authors/Contributors: Kirkland, C. L., author.
Smithies, R. H., author.
Wingate, M. T. D. (Michael Thomas David), author.
Geological Survey of Western Australia, issuing body.

Dewey Decimal Classification: 599.412

ISSN 1834-2280

Grid references in this publication refer to the Geocentric Datum of Australia 1994 (GDA94). Locations mentioned in the text are referenced using Map Grid Australia (MGA) coordinates, Zones 50, 51 and 52. All locations are quoted to at least the nearest 100 m.



U–Pb measurements were conducted using the SHRIMP II ion microprobes at the John de Laeter Centre of Isotope Research at Curtin University in Perth, Australia. Isotope analyses were funded in part by the Western Australian Government Exploration Incentive Scheme (EIS). Lu–Hf measurements were conducted using LA-ICPMS at the ARC National Key Centre for Geochemical Evolution and Metallogeny of Continents (GEMOC), via the ARC Centre of Excellence in Core to Crust Fluid Systems (CCFS), based in the Department of Earth and Planetary Sciences at Macquarie University, Australia.

Copy editor: RL Hitchings
Cartography: M Prause, AK Symonds
Desktop publishing: RL Hitchings
Printed by Images on Paper, Perth, Western Australia

Disclaimer

This product was produced using information from various sources. The Department of Mines and Petroleum (DMP) and the State cannot guarantee the accuracy, currency or completeness of the information. DMP and the State accept no responsibility and disclaim all liability for any loss, damage or costs incurred as a result of any use of or reliance whether wholly or in part upon the information provided in this publication or incorporated into it by reference.

Published 2014 by Geological Survey of Western Australia

This Report is published in digital format (PDF), as part of a digital dataset on CD, and is available online at <www.dmp.wa.gov.au/GSWApublications>.

Further details of geological publications and maps produced by the Geological Survey of Western Australia are available from:

Information Centre
Department of Mines and Petroleum | 100 Plain Street | EAST PERTH | WESTERN AUSTRALIA 6004
Telephone: +61 8 9222 3459 Facsimile: +61 8 9222 3444 www.dmp.wa.gov.au/GSWApublications

Cover photograph: Typical outcrop of the Gwynne Creek Gneiss of the Arid Basin along Gwynne Creek, Plumridge Lakes Nature Reserve, northeastern Albany–Fraser Orogen. Photograph by Catherine Spaggiari.

Contents

Abstract	1
Introduction	2
Tectonic synthesis and subdivisions of the Albany–Fraser Orogen	2
Tectonic settings and models	4
The Biranup and Nornalup Zones	5
The Fraser Zone	6
Sedimentary basins of the Albany–Fraser Orogen	8
The Barren Basin	8
Stirling Range Formation	8
Mount Barren Group	8
Lindsay Hill Formation	12
Woodline Formation	12
Unnamed occurrences	12
Fly Dam Formation	14
Synthesis and interpretation of detrital zircon data from the Barren Basin	15
K–S tables	15
Provenance of the Barren Basin	18
The Arid Basin	19
Malcolm Metamorphics	20
Whalehead Rock paragneiss	20
Gwynne Creek Gneiss	20
Snowys Dam Formation	22
Synthesis and interpretation of detrital zircon data from the Arid Basin	22
K–S tables	22
Provenance of the Arid Basin	22
The Ragged Basin	26
Potential source regions of the detritus	27
Loongana oceanic magmatic-arc, Madura Province	27
Hf isotope fingerprints of detrital zircons	32
Methodology	32
Barren Basin	32
Arid Basin	33
Basin evolution and tectonic setting	35
Barren Basin	35
Significance of the basin fill	36
Barren Basin evolution	36
Factors affecting basin evolution	36
Initiation of basin evolution	37
Tectonic model for the Barren Basin	38
Arid Basin	40
Significance of the basin fill	40
Arid Basin evolution	41
Factors affecting basin evolution	41
Tectonic model for the Arid Basin	41
Implications for Stage I of the Albany–Fraser Orogeny	45
The role and significance of large-scale structures	45
Concluding summary	46
References	46

Appendices

Appendix 1	51
Appendix 2	52
Appendix 3	59
Appendix 4	63

Figures

1.	Simplified, pre-Mesozoic interpreted bedrock geology of the Albany–Fraser Orogen and tectonic subdivisions of the Yilgarn Craton showing locations and units discussed in the text.....	3
2.	Probability density diagram and histograms of mean U–Pb zircon magmatic crystallization ages from magmatic rocks from the Northern Foreland	5
3.	Probability density diagram and histograms of mean U–Pb zircon magmatic crystallization ages and metamorphic ages from the Biranup and eastern Nornalup Zones	6
4.	Probability density diagram and histograms of mean U–Pb zircon magmatic crystallization ages and metamorphic ages from the Recherche Supersuite and Fraser Zone	7
5.	Photographs of Barren Basin rocks	9
6.	Probability plot of SHRIMP U–Pb detrital zircon dates from the Stirling Range Formation	12
7a.	Normalized probability density diagram of detrital zircon dates from samples of the Barren Basin	13
7b.	Probability density diagram and histogram for detrital zircon data (individual analyses) from the Barren Basin	14
8.	Photographs of Arid Basin rocks	21
9a.	Normalized probability density diagram of detrital zircon dates from the Arid Basin	25
9b.	Probability density diagram and histogram for all detrital zircon data from the Arid Basin	26
10.	Probability density diagram and histogram of detrital zircon data from all Mount Ragged Formation samples	28
11.	Reduced-to-pole aeromagnetic image over the east Albany–Fraser Orogen and Eucla basement, showing major tectonic units and structures, and the locations of drillhole sites discussed in the text	28
12.	Photographs of drillcore from the Loongana and Haig prospects	30
13.	Log plot of Th/Yb vs Nb/Yb from Loongana gabbros	31
14.	Plot of V (ppm) vs Ti (ppm) distinguishing low Ti/V mafic rocks	31
15.	Plot of SiO ₂ vs K ₂ O showing the distinct compositional differences between Madura Province plagiogranites and Albany–Fraser Orogen granites	31
16.	Nd-isotopic evolution diagram comparing the isotopic evolution of magmatic components of the Albany–Fraser Orogen with those from the Musgrave and Madura Provinces	31
17.	Hf evolution diagram for detrital zircons from the Barren Basin	32
18.	Initial Hf evolution plot for Group 3 analyses in the Big Red paragneiss	33
19.	Histograms of T _{DM} ² model ages from components of the Barren Basin and potential cratonic or lithotectonic sources.....	34
20.	Hf evolution diagram for detrital zircons from the Arid Basin	34
21.	Histograms of T _{DM} ² model ages from components of the Arid Basin.....	35
22.	Tectonic evolution of the Barren Basin	39
23.	Tectonic evolution of the Arid Basin	43

Tables

1.	Summary of tectono-thermal events in the Albany–Fraser Orogen	4
2.	Summary of age and depositional relationships of the Barren Basin	10
3.	K–S analysis comparing samples from the Barren Basin	16
4.	Summary of age and depositional relationships of the Arid Basin	23
5.	K–S analysis comparing samples from the Arid Basin	24

Tectonic links between Proterozoic sedimentary cycles, basin formation and magmatism in the Albany–Fraser Orogen, Western Australia

by

CV Spaggiari, CL Kirkland, RH Smithies, and MTD Wingate

Abstract

Preserved in the Albany–Fraser Orogen are the remnants of two, regionally extensive basin systems — the c. 1815 to 1600 Ma Barren Basin and the c. 1600 to 1305 Ma Arid Basin. An extensive U–Pb zircon geochronology dataset is used to demonstrate that the two regional basins record two cycles of sedimentation related to major tectonic events in the Albany–Fraser Orogen. The first cycle (Cycle 1) filled the Barren Basin with dominantly Neoproterozoic zircon detritus derived from the Archean Yilgarn Craton. Coeval voluminous, dominantly felsic magmatism modified the southern and southeastern Yilgarn Craton crust from 1815 to 1800 Ma, 1780 to 1760 Ma, and during the 1710–1650 Ma Biranup Orogeny, providing a second important detrital zircon source into the Barren Basin. The abundance of locally derived sediment deposited onto a reworked Archean Yilgarn Craton substrate indicates a largely extensional tectonic setting, consistent with a broad continental rift basin or alternatively, a long-lived back-arc basin system along the craton margin. However, if the Barren Basin formed in a back-arc setting, the associated subduction zone and magmatic arc must have been a substantial distance outboard of the Yilgarn Craton margin, as there is no evidence of a magmatic arc within the Albany–Fraser Orogen.

The relatively quiescent period and apparent lack of magmatic activity from c.1600 to 1455 Ma indicates a change from active, rift-related extension, to a proto-oceanic rift, through to a passive-margin and adjoining marginal basin. This marked the onset of the second depositional cycle (Cycle 2), and initial formation of the Arid Basin. In contrast to the Barren Basin, the Arid Basin is dominated by c. 1455 to 1375 Ma detritus that does not correspond to any known source within the Albany–Fraser Orogen, signifying an external, but proximal, new source. This new source is interpreted to be an oceanic magmatic-arc — the c. 1410 Ma Loongana arc — within the Madura Province to the east of the Albany–Fraser Orogen. Soft collision and accretion of the Loongana oceanic magmatic-arc at c. 1330 Ma took place after closure of the initial marginal basin via east-dipping subduction. In response to this accretion, Cycle 2 detritus from the oceanic magmatic-arc and its environs was fed into a foreland basin system that developed above a craton-vergent fold and thrust belt, producing a second phase of Arid Basin development. The accretion of the Loongana oceanic magmatic-arc is interpreted to have triggered the earliest magmatism of Stage I of the Albany–Fraser Orogeny at c. 1330 Ma. Detritus sourced from the Paleoproterozoic Biranup and Nornalup Zones, which constitutes the second-most abundant age component in the Arid Basin, was mixed with the younger foreland basin sediments. Thus, the Arid Basin evolved from a marginal ocean basin to a foreland basin, before it was intruded by granites of the widespread 1330–1280 Ma Recherche Supersuite and gabbros of the 1305–1290 Ma Fraser Zone. The two basin systems reflect a distinct change in tectonic regime from Paleoproterozoic rifting of the Yilgarn Craton, to the formation of a marginal basin that was subsequently closed during the Mesoproterozoic. The extensional structures produced during basin formation were inverted during orogen-wide, craton-vergent thrusting, which dominates the present-day crustal architecture.

KEYWORDS: basin analysis, geochronology, provenance, tectonics

Introduction

Sedimentary basins preserve information about tectonic history and setting, crustal architecture and paleotopography, and evidence of eroded tectonic elements in their detritus (Rahl et al., 2003; Martin et al., 2008). The analysis of sedimentary basins is particularly beneficial when linked with an understanding of associated magmatic rocks, leading to a more holistic understanding of a region's geodynamic history. For example, magmatic rocks can provide information about heat production, which in turn affects the mechanical properties of the crust during basin formation (Allen and Allen, 2005; McLaren et al., 2005). Magmatic rocks can also provide independent constraints on the tectonic setting of related basins, leading to a greater understanding of the evolution of poorly exposed regions, such as the Albany–Fraser Orogen in Western Australia (Fig. 1).

Basin analysis includes recognizing the critical factors of a basin's history, understanding the fundamental mechanisms of its evolution, and attempting to classify a basin according to an established scheme (e.g. Allen and Allen, 2005, and references therein). Identifying the pre-existing type and condition of the crustal substrate on which a basin formed is essential to resolve the type of basin setting, e.g. rift basin, foreland basin. Knowledge of the depositional sequences (basin fill), the basin-forming tectonic mechanisms that control where basins form, and basin-modifying tectonic processes such as ongoing deformation and magmatism are all important factors for determining a basin's setting and history. Fundamental mechanisms that influence basin formation include: 1) lithospheric flexure, causing bending and subsidence or rebound due to sediment loading or unloading, and torque; 2) isostatic effects from changes in lithospheric thicknesses, such as stretching or subsidence, formation of crustal roots, or long-wavelength buckling; and 3) dynamic effects such as mantle flow or underplating causing dynamic topography (Ingersoll and Busby, 1995; Allen and Allen, 2005). Basin classification helps to determine the tectonic setting because it includes defining features such as the type of lithospheric substrate, proximity to a plate boundary (plate margin or interior), and the type of plate motion (divergent, convergent, transform, intraplate) (Kingston et al., 1983; Ingersoll and Busby, 1995; Allen and Allen, 2005).

Until recently, the regional extent and tectonic significance of the sedimentary successions of the Albany–Fraser Orogen have not been fully documented and considered, nor has any potential genetic link to regional magmatic events been explored. We present a statistical analysis of an extensive ion microprobe (SHRIMP) detrital zircon U–Pb geochronology dataset to define the extents of the individual formations and their parent basins (now inverted within thrust sheets) (Fig. 1). This analysis is applied in conjunction with isotopic dating of magmatic and metamorphic rocks to determine potential provenance links from the hinterland, the basin substrates, possible coeval magmatic sources, distal or unexposed sources, or exotic sources. In addition, we present Lu–Hf analyses

from dated detrital zircons, which reveal information on the crustal source of the zircon-bearing magma. We also use whole-rock geochemical data from magmatic rocks from the adjacent Madura Province to help constrain the sources of the basin fill. These results have helped define the tectonic processes and settings of two regional, basin-forming events, and have allowed us to propose tectonic evolution models for the formation of the Albany–Fraser Orogen. Further details on individual Geological Survey of Western Australia (GSWA) geochronology samples compiled in this work are provided in the Geochronology Record series available online at <www.dmp.wa.gov.au/geochron/>. The geochronology samples cited in this report are listed in Appendix 1 — full references for the geochronology records can be found in the References section. Details on detrital zircon U–Pb dating methodology and a list of all samples used in this report can be found in Appendix 2. Geochemical data used in this work are listed in Appendix 3, and are available using the GeoChem Extract at <www.dmp.wa.gov.au/geochem/>.

Tectonic synthesis and subdivisions of the Albany–Fraser Orogen

The Albany–Fraser Orogen extends over a distance of at least 1200 km along the southern margin of the Archean Yilgarn Craton, and is part of the West Australian Craton (Fig. 1). The eastern extent of the orogen is interpreted as the Rodona Shear Zone, which separates the orogen from the Madura Province (Spaggiari et al., 2012). Paleoproterozoic and Mesoproterozoic rocks, which are largely a product of reworking of the southern and southeastern Yilgarn Craton from at least 1815 Ma through to 1140 Ma, dominate the Albany–Fraser Orogen (Nelson et al., 1995; Spaggiari et al., 2011). Paleoproterozoic tectonic events recognized so far include dominantly felsic magmatism during the 1815–1800 Ma Salmon Gums Event, the 1780–1760 Ma Ngadju Event, and the 1710–1650 Ma Biranup Orogeny, which includes the c. 1680 Ma, high-temperature, compressional deformation phase termed the Zanthus Event (Table 1; Kirkland et al., 2011a; Spaggiari et al., 2011, 2014). Mesoproterozoic tectonism is defined as the Albany–Fraser Orogeny, which took place in two stages: 1345–1260 Ma (Stage I) and 1215–1140 Ma (Stage II) (Clark et al., 2000; Bodorkos and Clark, 2004a). Stage I was a long-lived, widespread, coeval felsic and mafic magmatic event accompanied by high-temperature and moderate- to high-pressure metamorphism and deformation (Nelson et al., 1995; Clark, 1999; Clark et al., 2000; Bodorkos and Clark, 2004b; Oorschot, 2011). Stage II was dominated by intense deformation including craton-vergent thrusting, high-temperature and moderate-pressure metamorphism, and mainly felsic magmatism after c. 1200 Ma (Myers, 1995a; Clark et al., 2000; Dawson et al., 2003; Spaggiari et al., 2009, 2011).

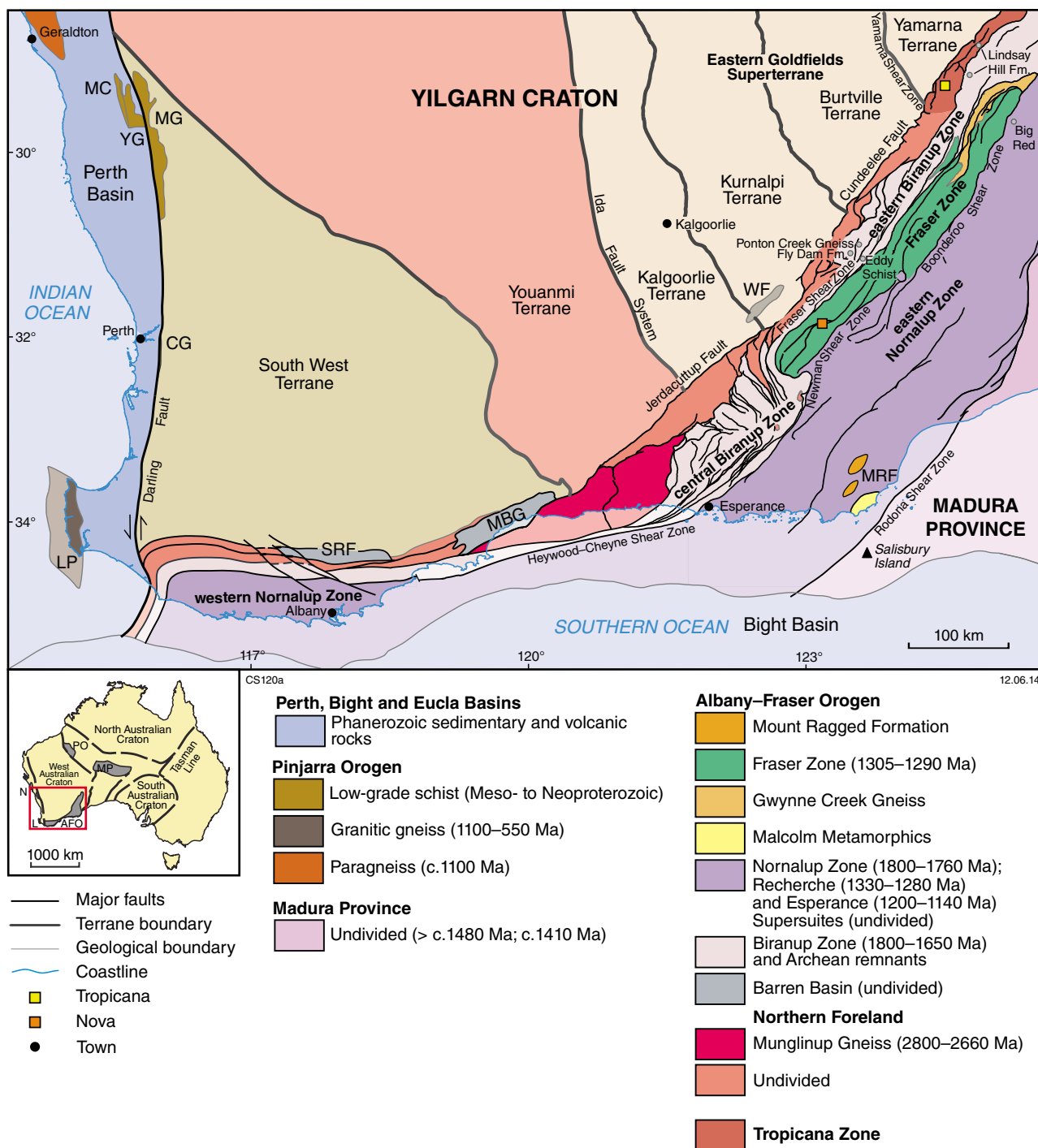


Figure 1. Simplified, pre-Mesozoic interpreted bedrock geology of the Albany–Fraser Orogen and tectonic subdivisions of the Yilgarn Craton showing locations and units discussed in the text (modified from Spaggiari et al., 2009; Spaggiari and Pawley, 2012; Cassidy et al., 2006; Pawley et al., 2012; Tyler and Hocking, 2001). Abbreviations used: SRF = Stirling Range Formation; MBG = Mount Barren Group; WF = Woodline Formation; MRF = Mount Ragged Formation; CG = Cardup Group; LP = Leeuwin Province; MC = Mullingarra Complex; MG = Moora Group. Inset: AFO = Albany–Fraser Orogen; MP = Musgrave Province; PO = Paterson Orogen; L = Leeuwin Province; N = Northampton Province.

Table 1. Summary of tectono-thermal events in the Albany–Fraser Orogen

	Northern Foreland		Kepa Kurl Booya Province			
			Tropicana Zone	Biranup Zone	Fraser Zone	Nornalup Zone
Stage II AFO: 1225–1140 Ma	ES?; D and Met	?		ES; D and Met	ES?; D and Met?	ES; D and Met
Stage I AFO: 1330–1260 Ma	RS; D and Met?	?		RS; D and Met	M, RS; D and Met	RS; D and Met
Biranup Orogeny: 1710–1650 Ma	M; D and Met?			M; D and Met (c. 1680 Ma Zanthus Event)	N/A	M; D and Met?
Ngadju Event: 1780–1760 Ma	M; D and Met?	M; D and Met		M; D and Met?	N/A	M; D and Met?
Salmon Gums Event: 1815–1800 Ma	M; D and Met?	M; D and Met?		M; D and Met?	N/A	M; D and Met?

NOTE: M = magmatism; D = deformation; Met = metamorphism; ES = Esperance Supersuite; RS = Recherche Supersuite

The timing of Stage I initiation at c. 1345 Ma is speculative, as it is based on two c. 1345 Ma inherited zircons from a Recherche Supersuite granitic vein (Clark et al., 2000). The age of these zircons fits with known detrital ages (see Arid Basin section), so may not be representative of local magmatic activity. A more robust age for the initiation of Stage I is provided by the oldest known Recherche Supersuite intrusion dated at 1330 ± 14 Ma (GSWA 83662). Stage II has been previously interpreted to have commenced at c. 1215 Ma (Clark et al., 2000), although older metamorphic dates of c. 1225 Ma in metamonzogranite and quartzite from Plum Pudding Rocks in the central Biranup Zone (Fig. 1; Spaggiari et al., 2009) indicate it commenced at least 10 Ma earlier.

The Albany–Fraser Orogen is divided into two main tectonic components that reflect its relationship to the Yilgarn Craton: the Archean Northern Foreland, and the dominantly younger, Paleo- to Mesoproterozoic Kepa Kurl Booya Province (Table 1; Spaggiari et al., 2009). The Northern Foreland is the portion of the Archean Yilgarn Craton that was intruded by Paleoproterozoic magmatic rocks, and reworked during the Mesoproterozoic Albany–Fraser Orogeny (Myers, 1990; Nelson et al., 1995; Spaggiari et al., 2009, 2011). It consists of greenschist and amphibolite to granulite facies Archean gneisses and granites, remnant greenstones, and younger dolerite dykes (Myers, 1995a; Spaggiari et al., 2009). The Munglinup Gneiss, with protolith ages of 2717–2640 Ma (Fig. 2a), is a major component of the Northern Foreland (Fig. 2b) and is preserved in thrust sheets in the central part of the orogen (Nelson et al., 1995; Spaggiari et al., 2009, 2011). The Kepa Kurl Booya Province is defined as the various, dominantly Proterozoic crustal components affected by, and probably amalgamated by the 1330–1260 Ma Stage I tectonism during the Albany–Fraser Orogeny (Spaggiari et al., 2009). It includes four geographical and structural, fault-bounded zones defined as the Tropicana, Biranup,

Fraser, and Nornalup Zones (Fig. 1, Table 1; Spaggiari et al., 2009, 2011, 2014). In summary, where Yilgarn Craton rocks dominate and are clearly recognizable even through the effects of reworking, they are defined as belonging to the Northern Foreland. Where pre- to syn-Stage I orogenic Proterozoic rocks are dominant, even though they may include Archean Yilgarn Craton remnants, they are defined as belonging to the Kepa Kurl Booya Province. The Tropicana Zone is an exception; although it is dominated by Archean rocks that have an affinity to the Yilgarn Craton, their geological evolution is distinct and cannot be readily correlated with adjacent terranes, such as the adjacent Yamarna Terrane (Kirkland et al., 2014a; Occhipinti et al., 2014).

Supracrustal rocks of the Albany–Fraser Orogen are divided into three major basins: the c. 1815 to 1600 Ma Barren Basin, the c. 1600 to 1305 Ma Arid Basin, and the c. 1280 to 1200 Ma Ragged Basin (Clark et al., 2000; Spaggiari et al., 2011; Waddell, 2014). The southeastern part of the Biranup Zone and most of the Nornalup Zone contain granitic intrusions of the 1330–1280 Ma Recherche Supersuite and the 1200–1140 Ma Esperance Supersuite, marking two major magmatic events that coincided with Stages I and II of the Albany–Fraser Orogeny, respectively (Nelson et al., 1995; Clark, 1999; Clark et al., 2000; Spaggiari et al., 2011).

Tectonic settings and models

Most previous interpretations for the evolution of the Albany–Fraser Orogen have focused on its Mesoproterozoic history and have included models of accretion or collision of exotic terranes, and more specifically, northwest-directed convergence and subsequent collision of the Mawson Craton with the Yilgarn Craton, as part of the larger West Australian Craton (Myers et al., 1996; Clark et al., 2000; Betts and

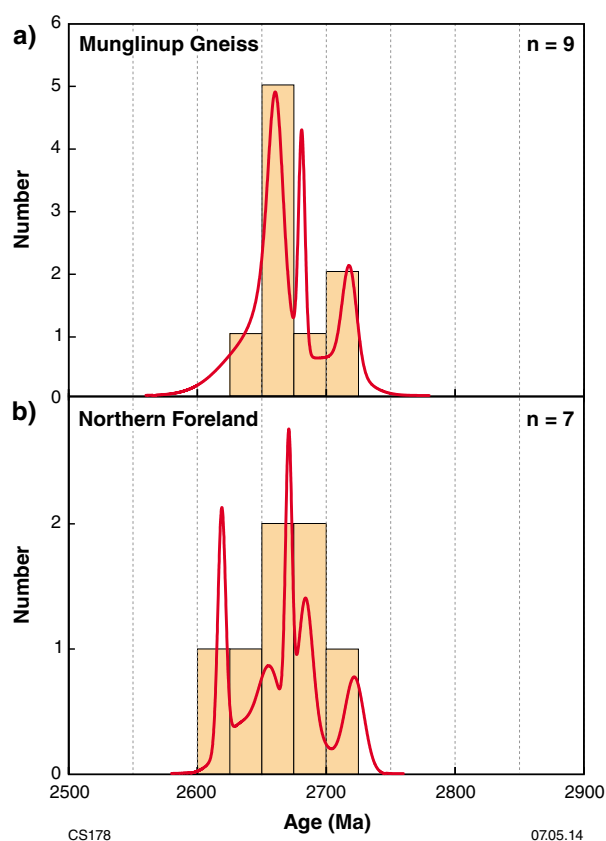


Figure 2. Probability density diagram and histograms of mean U–Pb zircon magmatic crystallization ages from magmatic rocks: a) Munглинup Gneiss; b) the Northern Foreland. The letter n refers to the number of dated samples.

Giles, 2006; Bodorkos and Clark, 2004a; Spaggiari et al., 2009). These models have envisaged the Fraser Zone as a magmatic or oceanic magmatic-arc, as generally related to a southeast-dipping subduction zone (Condie and Myers, 1999; Bodorkos and Clark, 2004a). However, the currently available U–Pb geochronology, whole-rock geochemistry, and Lu–Hf and Sm–Nd isotope data do not support these interpretations — no exotic components, nor Mesoproterozoic magmatic or oceanic magmatic-arcs, have been recognized within the orogen (Kirkland et al., 2011a,b; Spaggiari et al., 2011; Smithies et al., 2013). In addition, recently dated Paleoproterozoic metagranitic rocks within the eastern Nornalup Zone imply a similar substrate to that of the Biranup Zone as far eastwards as the Rodona Shear Zone (Spaggiari et al., 2011). These results have led to suggestions of a continental rift or distal back-arc setting, rather than accretion and collision, for Stage I (Kirkland et al., 2011a; Spaggiari et al., 2011, 2012).

Stage II has been interpreted to reflect intracratonic orogenesis that was ultimately responsible for the preserved crustal architecture, which is dominated by craton-directed, fault-bound thrust slices of largely mid-crustal, high-grade rocks (Myers, 1995a,b; Clark et al., 2000; Spaggiari et al., 2009 and references therein; GSWA, 2007, 2011; Spaggiari and Pawley, 2012).

Until recently, the Paleoproterozoic history of the orogen has received comparatively little attention, although Paleoproterozoic rocks were initially described in Bunting et al. (1976, and references therein), and Paleoproterozoic U–Pb dates were reported by Nelson et al. (1995). These rocks were considered to be exotic to the West Australian Craton (e.g. Myers et al., 1996; Spaggiari et al., 2009). However, whole-rock geochemistry and Lu–Hf data from Biranup Zone Paleoproterozoic granitic gneisses are consistent with modification of Yilgarn-like Archean crust, with increasingly more juvenile magmatism as time progressed (Kirkland et al., 2011a,b). The available data show that magmatic zircons trend towards more radiogenic ϵ_{Hf} values over time, commencing at approximately -12 at 1700 Ma and increasing to +2.6 at 1655 Ma (Kirkland et al., 2011b). Whole-rock chemical evolution, and neodymium and hafnium isotopes all support a model of melt production from mixed sources — an evolved component with crustal residence ages of less than c. 3100 Ma, and an additional, more juvenile component (Kirkland et al., 2011b). The strong connection of Biranup Zone magmatism to the Yilgarn Craton is demonstrated by the presence of Yilgarn-like Archean metagranite within the eastern Biranup Zone, and Biranup Zone intrusions into Northern Foreland rocks in the central part of the orogen, and into the Archean rocks of the Tropicana Zone (Kirkland et al., 2011a, 2014; Spaggiari et al., 2011, 2014). In summary, the available data indicate that the Biranup, Fraser, and Nornalup Zones are neither exotic nor oceanic magmatic-arc-related, and evolved on modified Archean Yilgarn Craton crust.

The Biranup and Nornalup Zones

The Biranup Zone is dominated by strongly deformed orthogneiss, with lesser amounts of metagabbroic and hybrid rocks that range in age from 1815 to 1625 Ma. These flank the entire southern and southeastern margin of the Yilgarn Craton (Figs. 1 and 3a; Nelson et al., 1995; Spaggiari et al., 2009; Kirkland et al., 2011a). The magmatic rocks intrude metasedimentary rocks of the Barren Basin. The Nornalup Zone is the southern- and easternmost unit of the Albany–Fraser Orogen and also spans its entire length, although much of the original basement appears to be masked by intrusions of the 1330–1140 Ma Recherche and Esperance Supersuites (Myers, 1995a,b; Nelson et al., 1995). In the east Albany–Fraser Orogen, the Nornalup Zone is separated from the Biranup and Fraser Zones by the Newman and Boonderoo Shear Zones, and from the Madura Province by the Rodona Shear Zone (Fig. 1; Spaggiari and Pawley, 2012).

The oldest dated Paleoproterozoic magmatic rocks within the Albany–Fraser Orogen are 1815–1800 Ma granitic gneisses that occur in the Biranup and Nornalup Zones (the Salmon Gums Event). In the central Biranup Zone, two diamond drillcores from south of Salmon Gums intersected layered mafic and felsic granitic gneiss that yielded U–Pb zircon dates of 1806 ± 6 Ma and 1804 ± 6 Ma, interpreted to reflect magmatic crystallization (hole SGD001, GSWA 192502; hole SGD002, GSWA 192504, respectively). Two occurrences of c. 1815 Ma metagranite occur in the 1815–1800 Ma

Black Dragon Gneiss in the far northeast of the orogen, adjacent to the Tropicana Zone (Blenkinsop and Doyle, 2014; Occhipinti et al., 2014). In the eastern Nornalup Zone, migmatitic monzogranitic gneiss containing angular mafic inclusions is exposed about 12 km east of Boingaring Rocks, and has yielded a magmatic crystallization age of 1809 ± 8 Ma (Fig. 3b; GSWA 194785). Zircon rims from the same sample yielded a date of 1198 ± 11 Ma, interpreted as the age of metamorphism and migmatization, corresponding to Stage II of the Albany–Fraser Orogeny. Importantly, these granites contain evidence of a mantle component in the form of mafic enclaves and layers.

The 1815–1800 Ma magmatic event was followed by a second phase of magmatic activity between 1780 and 1760 Ma, recorded in both the Biranup and Nornalup Zones, and in the Tropicana Zone (the Ngadju Event; Fig. 1). The similarity in ages in the Biranup and Nornalup Zones implies that the same Paleoproterozoic substrate extends beyond the Biranup Zone itself, below the Fraser Zone (Fig. 1). In the central Biranup Zone, diamond drillcore from south of Salmon Gums intersected granitic gneiss that yielded a magmatic crystallization age of 1779 ± 7 Ma (preliminary data, hole SGD003, GSWA 192505). In the eastern Nornalup Zone, strongly deformed metamonzogranite in the Newman Shear Zone yielded a magmatic crystallization age of 1763 ± 11 Ma, and also recorded a high-temperature metamorphic overprint at 1305 ± 15 Ma (GSWA 194784). In the Tropicana Zone, northeast of the Tropicana gold deposit (Fig. 1), c. 1760 Ma magmatism is recorded in the McKay Creek Metasyenogranite, which yielded a magmatic crystallization age of 1761 ± 10 Ma (GSWA 182424). Mingling of this syenogranite with gabbroic rocks has produced dioritic hybrid rocks (Spaggiari et al., 2011). Dacitic rocks of the Voodoo Child Formation, which also includes mafic to ultramafic rocks, provide evidence of Paleoproterozoic volcanism in the Tropicana Zone (Less, 2013).

The McKay Creek Metasyenogranite is one of several phases of mildly alkaline granite magmatism that produced widespread syenogranitic rocks throughout the eastern Biranup Zone from c. 1760 Ma through to at least 1650 Ma (Spaggiari et al., 2011). Most of the crystallization ages of the metasyenogranites fall within the range of c. 1690 to 1670 Ma, apart from one component of the Eddy Suite and the youngest Biranup Zone granite dated at 1627 ± 4 Ma (GSWA 194736). Other metagranitic rocks of both the central and eastern Biranup Zone include metamonzogranite, metagranodiorite, and rare tonalitic gneiss, with most ages falling in the range 1690–1660 Ma (Nelson et al., 1995; Kirkland et al., 2011a; Spaggiari et al., 2009). The c. 1665 Ma Eddy Suite comprises the most isotopically juvenile magmas of the Biranup Zone (Kirkland et al., 2011b) and ranges from megacrystic metamonzogranite and equigranular metasyenogranitic gneiss, to rapakivi-textured, mingled metagranodiorite and metagabbro (Kirkland et al., 2011a; Spaggiari et al., 2011).

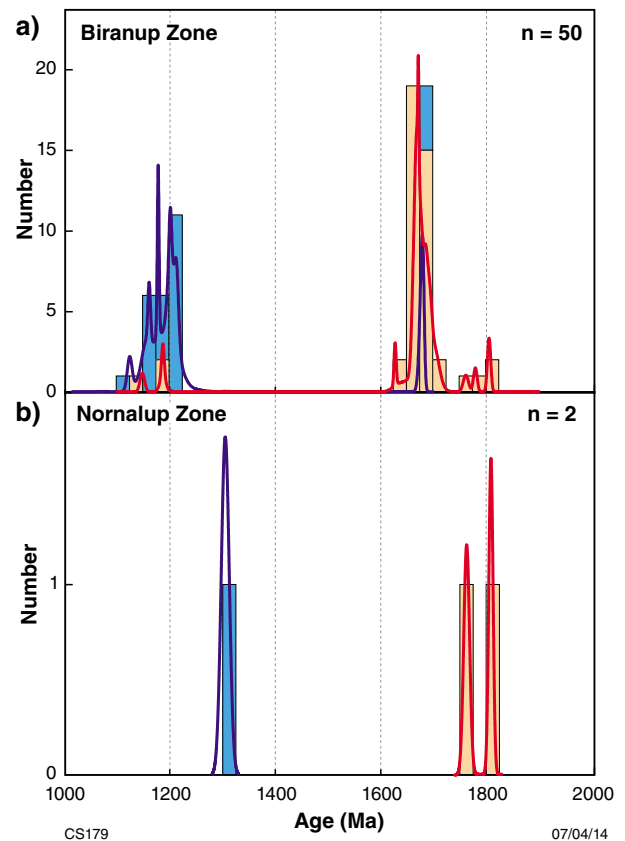


Figure 3. Probability density diagram and histograms of mean U–Pb zircon magmatic crystallization ages (in orange) and metamorphic ages (in blue) from: a) the Biranup Zone; b) eastern Nornalup Zone. The letter n refers to the number of dated samples.

The central and eastern Biranup Zone are dominated by Paleoproterozoic gneisses that contain evidence of partial melting and migmatization, and have therefore undergone upper amphibolite- to granulite-facies metamorphism (Kirkland et al., 2011a; Spaggiari et al., 2011). Most zircon overgrowths in these rocks indicate that high-grade metamorphism occurred during Stage II, from c. 1225 to 1150 Ma (Fig. 3a; Kirkland et al., 2011a; Spaggiari et al., 2011).

The Fraser Zone

The Fraser Zone is bounded by the Fraser Shear Zone along its northwestern edge and southern tip, and by the Newman and Boonderoo Shear Zones along its southeastern edge (Fig. 1; Spaggiari and Pawley, 2012; Spaggiari et al., 2014). It is dominated by high-grade metamorphic rocks that have a strong, distinct geophysical signature in both aeromagnetic and gravity data — the latter reflecting high density attributed to the dominance of metagabbroic rocks. All of the northern part of the

Fraser Zone is overlain by Cretaceous to Cenozoic cover rocks of the Eucla Basin, but the gravity data indicate that it is an approximately 425 km long, northeasterly trending, fault-bounded unit that is up to 50 km wide (Spaggiari and Pawley, 2012). The zone contains the 1305–1290 Ma Fraser Range Metamorphics (Spaggiari et al., 2009), which comprise thin to voluminous sheets of metagabbroic rocks that range in thickness from several centimetres up to several hundred metres. The metagabbroic rocks are interlayered with sheets of metamonzogranitic to metasyenogranitic gneisses and pyroxene-bearing granitic gneiss ranging from cm-scale to 10s metres thickness, as well as hybrid rocks (Spaggiari et al., 2011; Smithies et al., 2013). All are interlayered at various scales with amphibolite to granulite facies, pelitic, semipelitic, and psammitic gneiss, and locally calc-silicate and iron-rich metasedimentary rocks of the Mesoproterozoic Arid Basin (Spaggiari et al., 2011, and references therein). Metagranitic rocks range in composition from metamonzogranite to metasyenogranite. Whole-rock geochemical data for felsic rocks within the Fraser Zone permits these rocks to be subdivided into two broad groups; one compositionally similar to granites representing the majority of the 1330–1280 Ma Recherche Supersuite (Fig. 4a), the other likely reflecting melts derived locally through melting of the metasedimentary components of the Fraser Zone (Smithies et al., 2013).

In the southern portion of the Fraser Zone the gabbroic sheets appear to be thinner in the northwest where they mainly occur as layers within the metasedimentary rocks, and thicker in the southeast, which is volumetrically dominated by metagabbroic rocks. Much of the northwestern side of the Fraser Zone is dominated by tightly to isoclinally folded, strongly foliated to mylonitic rocks, whereas the least deformed and thickest examples of metagabbroic sheets occur in the southeast, reflecting a significant difference in strain before the Newman Shear Zone is reached along the southeastern boundary (Fig.1). Aeromagnetic and gravity data indicate a repetition of this architecture along strike to the northeast, beneath the Eucla Basin.

All isotopic results from the Fraser Zone indicate a short time interval for both mafic and felsic igneous crystallization, predominantly between 1305 and 1290 Ma, and essentially coeval granulite-facies metamorphism (Fig. 4b; Fletcher et al., 1991; Clark et al., 1999; De Waele and Pisarevsky, 2008; Kirkland et al., 2011a; Clark et al., 2014). The close temporal correspondence between mafic to felsic magmatism and the age of granulite-facies metamorphism implies that magmatism provided the thermal impetus for metamorphism (Spaggiari et al., 2011; Clark et al., 2014). All U–Pb zircon geochronology in the Fraser Zone indicates tectono-thermal activity during Stage I of the Albany–Fraser Orogeny, with no evidence of Stage II. The preservation of pre-1250 Ma Rb–Sr cooling ages (Bunting et al., 1976; Fletcher et al., 1991) also indicates a lack of high-temperature Stage II activity, because the Rb–Sr systematics could reasonably be expected to have been disturbed by hydrothermal processes during metamorphism.

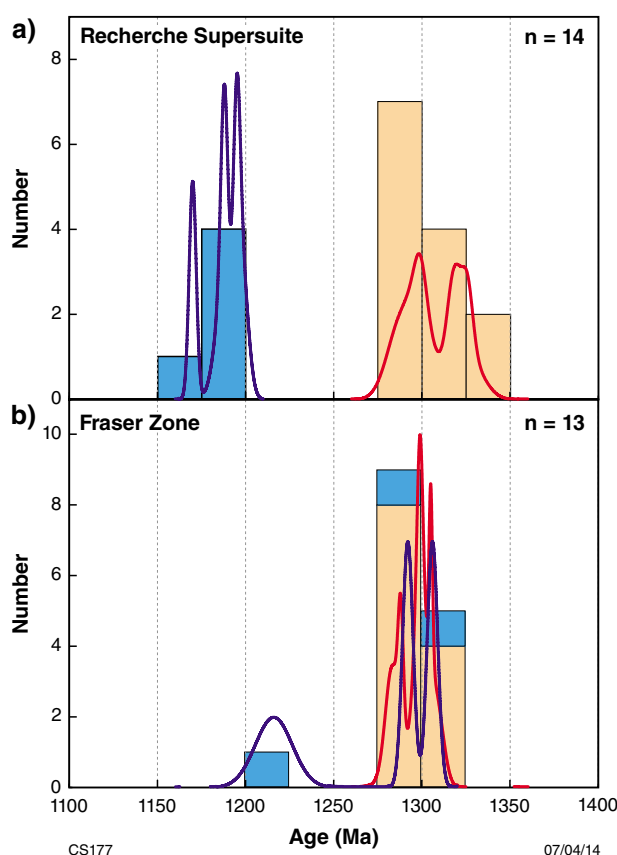


Figure 4. Probability density diagram and histograms of mean U–Pb zircon magmatic crystallization ages (in orange) and metamorphic ages (in blue) from: a) Recherche Supersuite; b) Fraser Zone. The letter n refers to the number of dated samples.

Peak metamorphic temperatures and pressures recorded in the metapelitic rocks reached about 850°C at pressures of 7–9 kbars at c. 1290 Ma, followed by a period of isobaric cooling at pressures of approximately 9 kbars (Oorschot, 2011; Clark et al., 2014). These pressure estimates indicate depths of about 25 km, which may constrain the depth at which the presently exposed gabbros were intruded, and also the minimum thickness of the sedimentary package. However, the peak metamorphic assemblages used to define the P–T estimates grew in early, gneissic, deformation-related fabrics (Clark, 1999; Oorschot, 2011), so could also relate to burial by crustal thickening, or alternatively, to extensional fabrics that formed during intrusion of the magmatic rocks.

Initially, both the metagranitic and metamafic components of the Fraser Zone were interpreted as an exhumed block of lower crust (Doepel, 1975). Subsequently, the mafic rocks of the Fraser Zone were interpreted as part of a large, layered mafic intrusion, with the granitic and metasedimentary rocks representing older basement slivers belonging to the former ‘Biranup Complex’ (Myers, 1985).

Following analysis of trace-element data, it was argued that the mafic magmas were derived from a subduction-related source, and that the former 'Fraser Complex' represented remnants of multiple oceanic magmatic-arcs (Condie and Myers, 1999). More recently, the Fraser Zone has been interpreted as a structurally modified, mid- to deep-crustal 'hot zone', formed by the repeated intrusion of gabbroic magma from a mantle upwelling into quartzofeldspathic country rock, either beneath a continental rift or in a distal back-arc setting (Spaggiari et al., 2011; Smithies et al., 2013; Clark et al., 2014). New whole-rock geochemical data indicate an oceanic magmatic-arc setting, as interpreted by Condie and Myers (1999), is least likely because the enriched crustal component of the gabbroic rocks of the Fraser Zone is better explained by assimilation from an older, felsic basement that included a Sr-depleted component of Archean, or reworked Archean, crust (Smithies et al., 2013). This interpretation is supported by previous and recent Nd- and Hf-isotope data (Fletcher et al., 1991; Kirkland et al., 2011b), and the presence of Paleoproterozoic basement rocks in the eastern Nornalup Zone.

Sedimentary basins of the Albany–Fraser Orogen

The Barren Basin

The Barren Basin comprises Paleoproterozoic metasedimentary rocks belonging to the Stirling Range Formation, Mount Barren Group, Lindsay Hill Formation, Woodline Formation (Woodline Sub-basin), the Fly Dam Formation, and unnamed occurrences of psammitic to semipelitic schist and gneiss (Fig. 1, Table 2; Spaggiari and Pawley, 2012). These units overlie the Yilgarn Craton, Northern Foreland, and the Biranup and Nornalup Zones (Muhling and Brakel, 1985; Thom et al., 1977, 1984a; Hall et al., 2008; Spaggiari et al., 2009, 2011).

Stirling Range Formation

The Stirling Range Formation is exposed in the western Albany–Fraser Orogen (Fig. 1) and consists of sub-greenschist to lower greenschist facies quartzite, shale, slate, and phyllite (Fig. 5a; Muhling and Brakel, 1985) deposited in a tide-dominated, shallow-marine setting (Cruse, 1991; Cruse and Harris, 1994). It has a minimum age of 1800 ± 14 Ma, based on dating of authigenic xenotime of probable diagenetic origin (Table 2; Rasmussen et al., 2004). Detrital zircon and xenotime grains from the Stirling Range Formation indicate a maximum depositional age of 2016 ± 6 Ma (Rasmussen et al., 2002, 2004). The detrital zircons yield dates as old as 3464 ± 17 Ma (1σ), and have significant age components at c. 2748, 2709, 2656, 2246, and 2034 Ma, with the 2034 Ma age component being the most dominant (Fig. 6; Rasmussen et al., 2002; Hall et al., 2008, figure 11). A date of 1215 ± 20 Ma for monazite overgrowths from interbedded sandstone and shale is interpreted to reflect metamorphic growth, consistent with previous Rb–Sr dating (Rasmussen et al., 2002, and references therein).

The dating indicates that metamorphism of the Stirling Range Formation occurred during Stage II of the Albany–Fraser Orogeny.

Discoidal and trace-like fossils discovered in sandstones of the Stirling Range Formation were initially thought to be of Ediacaran affinity, and therefore the formation was interpreted to be Neoproterozoic (Cruse and Harris, 1994). However, the geochronological data are not consistent with this interpretation. Significantly, the 1800 ± 14 Ma authigenic xenotime date is now considered to provide a minimum age for these purported fossils (Rasmussen et al., 2004).

Mount Barren Group

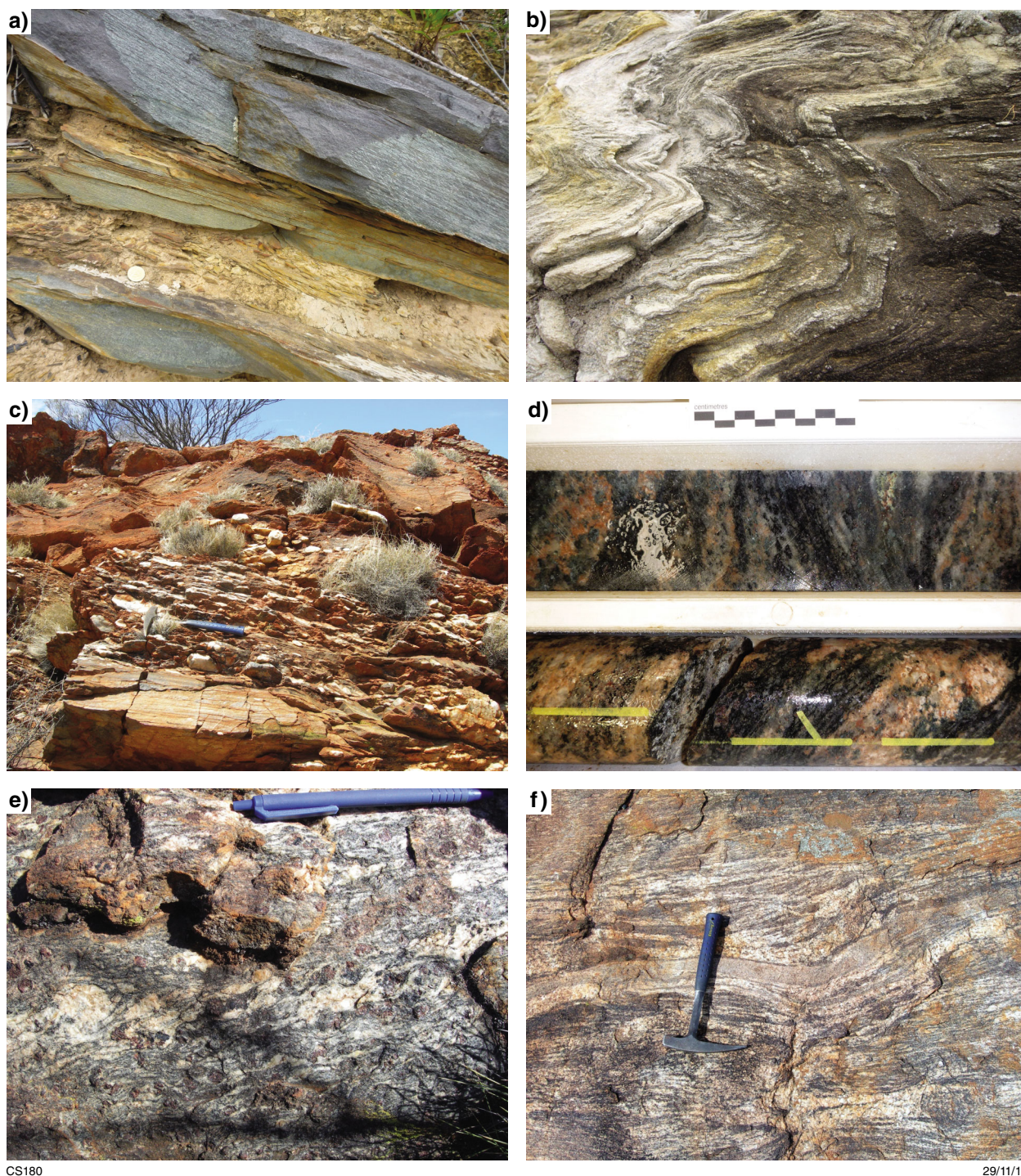
The Mount Barren Group is exposed in the central Albany–Fraser Orogen and consists of lower greenschist to upper amphibolite facies metasedimentary rocks, which overlie the southern edge of the Yilgarn Craton (mostly Northern Foreland rocks) and the northern edge of the Biranup Zone along a strike length of about 120 km (Fig. 1; Thom et al., 1977, 1984b; Witt, 1997). The group is divided into the Steere Formation, the Kundip Quartzite, and the Kybulup Schist (Table 2; Thom and Chin, 1984; Thom et al., 1984a).

The Steere Formation is the lowermost unit and consists of a thin basal conglomerate with clasts of quartzite, chert, banded iron-formation, and felsic volcanic rocks, overlain by several metres of pebbly sandstone and 4 m of dolomitic limestone (Thom et al., 1977, 1984a; Witt, 1997). At its type locality in the Western Steere River, the Steere Formation non-conformably overlies the Archean Manyutup Tonalite of the Yilgarn Craton (Sofoulis, 1958; Thom et al., 1977, 1984a).

The Kundip Quartzite consists predominantly of thickly bedded pure quartzite, which is interbedded with mica- and magnetite-bearing quartzite and mudstone, and minor thin lenses of metaconglomerate dominated by quartzite clasts (Thom et al., 1984a; Witt, 1997; Vallini et al., 2005). Sedimentary structures, such as cross-bedding and ripple marks, are common (Witt, 1997) and suggest deposition under shallow, near-shore marine to tidal-sandflat conditions.

An approximately 300 m-thick mafic intrusion, the Cowerdup Sill, intrudes the Kundip Quartzite (Witt, 1997). It is described as a mafic granophyre with a typical assemblage of quartz–plagioclase–calcic amphibole–chlorite(–K-feldspar–relict clinopyroxene), although pyroxenite is reported to occur near the base of the sill locally (Witt, 1997). The age of the intrusion is unknown and although it is thought to be broadly conformable, it is also reported to crosscut the stratigraphy on a regional scale (Witt, 1997).

The Kybulup Schist is the uppermost unit and is dominated by thinly bedded pelitic and psammitic rocks of variable metamorphic grade. In the northwest, the unit is dominated by slate and phyllite, plus low-grade, mudstone-dominant rhythmite and shale that coarsens upwards into siltstone (Fig. 5b), whereas amphibolite



CS180

29/11/13

Figure 5. Photographs of Barren Basin rocks: a) Cross-bedded sandstone of the Stirling Range Formation, base of Bluff Knoll; b) folded pelitic layers of the Kybulup Schist, Mount Barren Group, Gairdner River (base of photograph is approximately 1 m; photograph courtesy of Suzanne Dowsett); c) interbedded metasandstone and metaconglomerate of the Lindsay Hill Formation, southeast of Bartlett Bluff, from where GSWA 182416 was collected; d) metasedimentary gneiss representative of GSWA 182475, from the Big Red prospect, drill core BRDDH1; e) semipelitic, garnet-rich gneiss with migmatitic leucosomes, Fly Dam Formation; f) strong foliation in migmatitic semipelitic gneiss, Fly Dam Formation.

Table 2. Summary of age and depositional relationships of the Barren Basin

Unit; GSWA sample numbers	Metamorphic facies	Maximum depositional age: youngest single analysis (Ma); youngest group (Ma)	Minimum age	Inferred depositional substrate	Type of basin fill	Depositional setting	Present-day substrate	Estimated true thickness
Fly Dam Formation: 194742, 194743	Amphibolite to granulite	1535 ± 26; c. 1640, 1598 ± 9; c. 1617	1196 ± 13 Ma and 1154 ± 35 Ma metamorphism	Eastern Biranup Zone	Interbedded sandstone and mudstone (turbidites?)	Deep marine?	Eastern Biranup Zone	Unknown; 100 m minimum
Ponton Creek psammitic gneiss; 194731	Amphibolite to granulite	1689 ± 6 (unimodal population)	1666 ± 12 Ma intrusive monzogranite	Eastern Biranup Zone	Sand- and grit-dominated	Moderate energy, shallow-marine? Proximal volcanics?	Eastern Biranup Zone	Unknown
Big Red paragneiss: 182475, 182473	Amphibolite to granulite	1685 ± 11; c. 1773, 1729 ± 27; c. 1763	1326 ± 6 Ma intrusive granitic gneiss	Eastern Normalup Zone	Siltstone and mudstone?	Moderate to low energy, intermediate to deep marine?	Eastern Normalup Zone	Unknown; 50 m minimum
Lindsay Hill Formation: 182416, 182405	Upper greenschist to amphibolite	1752 ± 19 c. 1798, 1990 ± 15; c. 2641	Not constrained	Yilgarn Craton / Eastern Biranup Zone	Cross-bedded quartz-rich sandstone, pebbly conglomerate, and siltstone	Distal fluvial to tidal sandflat? Delta?	Yilgarn Craton / eastern Biranup Zone	Unknown
Coramup Gneiss (Plum Pudding Rocks); 184122	Amphibolite to granulite	1757 ± 39; c. 2031	^(a) 1688 ± 12 Ma intrusive granite	Eastern Biranup Zone	Interbedded sandstone and mudstone	Deep marine?	Eastern Biranup Zone	Unknown
Woodline Formation	Greenschist	^(b) 1651 ± 26; c. 1696	Stage I and/or Stage II deformation ^(c)	Yilgarn Craton ^(c)	Quartz-rich sandstone, pebbly conglomerate, siltstone ^{(c)(d)}	Distal fluvial to marine-dominated ^(c)	Yilgarn Craton	Unknown; 250 m minimum ^(c)
Mount Barren Group; Kybulup Schist	Greenschist to amphibolite	^{(e)(f)} 1751 ± 19; c. 1789	^(f) 1693 ± 4 Ma (deposition)	Yilgarn Craton, and pre-1700 Ma Biranup Zone crust?	Mudstone, siltstone (upwards coarsening), rare carbonates ^{(g)(h)}	Carbonate banks surrounded by deeper-water sediments; lower delta-front ^{(e)(f)(h)}	Yilgarn Craton / Biranup Zone	Minimum of 35 m ^{(g)(h)}
Mount Barren Group; Kundip Quartzite	Greenschist to amphibolite	^{(e)(f)} 1692 ± 12; c. 1766	Stage II metamorphism and deformation ^(e)	Yilgarn Craton, and pre-1700 Ma Biranup Zone crust?	Quartz-rich sandstone, thin mudstone, thin conglomerate ^{(f)(g)(h)}	Shallow, near-shore marine to tidal-sandflat conditions; delta-plain or upper delta-front ^(h)	Yilgarn Craton / Biranup Zone	Minimum of 13 m ^{(g)(h)}

Table 2. continued

Unit; GSWA sample numbers	Metamorphic facies	Maximum depositional age: youngest single analysis (Ma); youngest group (Ma)	Minimum age	Inferred depositional substrate	Type of basin fill	Depositional setting	Present-day substrate	Estimated true thickness
Mount Barren Group; Steere Formation	Greenschist	^(e) 1990 ± 16; c. 2016	Stage II metamorphism and deformation ^(e)	Yilgarn Craton, and pre-1700 Ma Biranup Zone crust?	Basal conglomerate, sandstone, dolomitic limestone ^{(g)(h)}	Fluvial or fluvial-deltaic sediments ^{(e)(f)(h)}	Manyutup Tonalite / Yilgarn Craton ^(g)	Approximately 12 m ^{(g)(h)}
Stirling Range Formation	Lower greenschist ^(k)	⁽ⁱ⁾ 2016 ± 6 (youngest group)	⁽ⁱ⁾ 1800 ± 14 Ma (deposition)	Yilgarn Craton margin?	Quartz-rich sandstone, mudstone, shale ^(k)	Shallow-marine, tide-dominated ^{(i)(j)(m)}	Yilgarn Craton	Minimum of 1600 m ^(k)

SOURCES: (a) GSWA 184125, Bodorkos and Wingate (2008b)
 (d) Asarco Limited (1971)
 (g) Thom et al. (1977, 1984a)
 (j) Rasmussen et al. (2002, 2004)
 (i) Cruse and Harris (1994)

(b) GSWA 177921, Wingate and Bodorkos (2007b)
 (e) Maximum depositional age recalculated; Dawson et al. (2002)
 (h) Witt (1997, 1998)
 (k) Muhling and Brakel (1985)

(c) Hall et al. (2008)
 (f) Vallini et al. (2002, 2005)
 (i) Nelson (1996a,b)
 (k) Cruse (1991)

facies kyanite-, staurolite-, and garnet-bearing schists are found in the southeast (Thom et al., 1984a; Witt, 1997; Fitzsimons and Buchan, 2005; Fitzsimons et al., 2005; Vallini et al., 2005). Rare outcrops of dolostone and calc-silicate schist suggest a depositional setting that included carbonate banks surrounded by deeper water sediments (Witt, 1997).

The Mount Barren Group has been interpreted as a deltaic to shallow-marine sequence, with the Steere Formation recording fluvial or fluvial-deltaic deposition, the Kundip Quartzite a delta-plain or upper delta-front, and the Kybulup Schist lower delta-front deposition, possibly with an upper prograding section (Witt, 1998; Dawson et al., 2002; Vallini et al., 2002, 2005).

A 26 m-thick, low-grade phosphatic unit occurs at the interface between the Kundip Quartzite and the Kybulup Schist (Vallini et al., 2002, 2005). It is thinly bedded and consists of alternating medium- to coarse-grained sandstone and carbonaceous shale, enriched in phosphate minerals. Authigenic xenotime overgrowths on zircons obtained from the phosphatic unit yielded four age components of c. 1693, 1645, 1578, and 1481 Ma (Vallini et al., 2002, 2005). The dating showed no evidence of Stage I or II metamorphism, and the unit was interpreted as a shielded, low-strain envelope due to its low permeability and porosity (Vallini et al., 2005). A paragenetic sequence based on detailed petrography and geochemistry provided a framework for the geochronology (Vallini et al., 2005). The 1693 ± 4 Ma date was interpreted to reflect early diagenesis of unconsolidated sediments, and regarded as closest to the depositional age of the unit. The onset of burial, and a possible change to anaerobic conditions, was interpreted to have commenced prior to c. 1645 Ma. The two younger age components of 1578 ± 10 and 1481 ± 21 Ma were interpreted to reflect periods of hydrothermal xenotime growth that post-dated quartz cementation. Detrital zircon studies of the Mount Barren Group are consistent with this interpretation of the xenotime dating results, yielding a maximum depositional age of c. 1700 Ma. Significant detrital zircon age components of c. 2663, 2645, 2291, 2246, 2018, 1857, 1803, and 1773 Ma have been reported for the Mount Barren Group (Fig. 7a; GSWA 112168 and 112170; Dawson et al., 2002).

Most structural studies of the Mount Barren Group have concluded that it is part of a north- to northwest-vergent fold and thrust belt, although the amount of overall displacement on the thrust faults is unknown (Sofoulis, 1958; Thom et al., 1984a; Myers, 1990; Witt, 1998). Several stages of folding and associated fabrics have been recognized, with the highest degree of complexity in the higher grade rocks to the south and southeast (Witt, 1998; Wetherley, 1998; Dawson et al., 2003). Kyanite-bearing, amphibolite-facies rocks yielded SHRIMP U–Pb dates of 1206 ± 6 and 1194 ± 8 Ma for xenotime and monazite, respectively (Dawson et al., 2003). These dates were interpreted to represent c. 1205 Ma peak thermal metamorphism, statically overprinting the S1 and S2 foliations (Dawson et al., 2003). The dates fall within the bracket of Stage II of the Albany–Fraser Orogeny (Table 1), and imply that formation of the fold and thrust system occurred during that period.

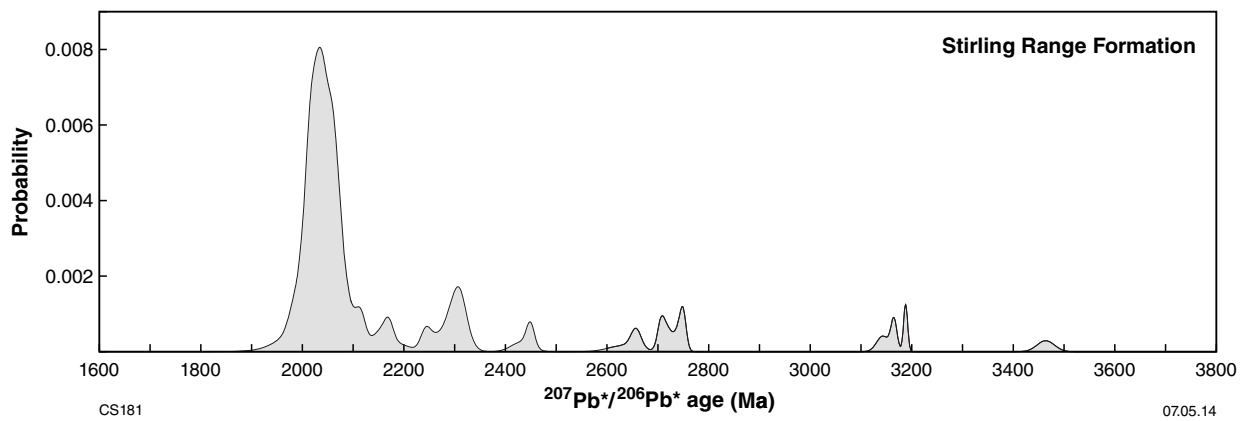


Figure 6. Probability plot of SHRIMP U–Pb detrital zircon dates from the Stirling Range Formation (after Hall et al., 2008; data from Rasmussen et al., 2002).

Lindsay Hill Formation

Isolated ridges and outcrops of metaconglomerate, quartzite and metasandstone occur in the northeastern part of the Albany–Fraser Orogen (Van De Graaff and Bunting, 1975, 1977; Spaggiari et al., 2011; Spaggiari and Pawley, 2012). Collectively, these are named the Lindsay Hill Formation. Quartzite and metasandstone occurrences contain well-developed sedimentary structures, such as cross-bedding and ripple marks, and are folded into northeasterly trending, open to tight folds (Van De Graaff and Bunting, 1975, 1977; Spaggiari et al., 2011). Quartzite from near McKay Creek yields a maximum depositional age of 1990 ± 15 Ma, based on the weighted mean date of two analyses of the youngest zircon (GSWA 182405). A weighted mean date of 2640 ± 3 Ma is indicated for the youngest group of 50 analyses (Table 2).

Northeast of the Tropicana gold deposit (Fig. 1) is a ridge of probable greenschist-grade, quartz-pebble metaconglomerate with a medium-grained, quartz-rich, micaceous matrix, and distinctive iron-rich laminated metasilstone beds throughout (Fig. 5c; Spaggiari et al., 2011). Above this is a pale grey quartzite interbedded with metagritstone and metasandstone. Detrital zircons from this material indicate a maximum depositional age of 1752 ± 19 Ma (1σ) (Table 2), and older detritus of 2835–1794 Ma, including significant age components at c. 2635 and 1807 Ma (GSWA 182416).

Woodline Formation

The Woodline Formation unconformably overlies granite and greenstone of the Eastern Goldfields Superterrane, near its southwestern margin, about 350 km northeast of the Mount Barren Group (Fig. 1; Table 2). The formation consists of weakly deformed, lower greenschist facies, mature sandstone interbedded with thicker horizons of siltstone, and was interpreted as a remnant of a more extensive siliciclastic sequence (Hall et al., 2008). Units immediately above the unconformity are lithologically

variable and range from quartz-rich sandstone to pebbly conglomerate, brown-grey quartzite, and thinly bedded siltstone (Asarco Limited, 1971; Hall et al., 2008). Three quartz-rich sandstone units that include minor amounts of granular to pebbly conglomerates are distributed between layers of thinly bedded siltstone and dark grey quartzite, and locally, thin beds of chert or gritstone that are tens of metres thick. Minor units consist of pebble and cobble conglomerates, and matrix- to clast-supported chert breccias (Asarco Limited, 1971; Hall et al., 2008).

Where best exposed, the Woodline Formation is folded into open, upright, northeasterly trending folds, and contains a weak to moderately developed, axial-planar spaced cleavage (Jones, 2006; Hall et al., 2008). Two dominant sets of paleocurrent directions were recorded, indicating both southeasterly and southwesterly directed flow. These paleocurrent readings have been interpreted either as transverse and axial components in a foreland-basin setting, or as fluvial to deltaic and barrier island sedimentary processes interacting with longshore currents (Hall et al., 2008). The depositional setting of the Woodline Formation is interpreted as changing from a distal fluvial environment to a marine-dominated setting, based on the overall fining upward of the succession from conglomerate, to sandstone and siltstone (Hall et al., 2008). A revised estimate of the maximum depositional age for the Woodline Formation is 1651 ± 26 Ma (1σ), based on the youngest zircon analysis, or more conservatively, c. 1696 Ma, based on the youngest group (Table 2; GSWA 177921).

Unnamed occurrences

A psammitic gneiss in the eastern Biranup Zone, along Ponton Creek, locally contains evidence of anatexis such as thin leucosomes, but also exhibits well-preserved laminations and cross-bedding (Spaggiari et al., 2011). The psammitic gneiss contains K-feldspar (60%) and quartz (35%), and minor garnet and biotite. It yields a unimodal zircon age component of 1689 ± 6 Ma,

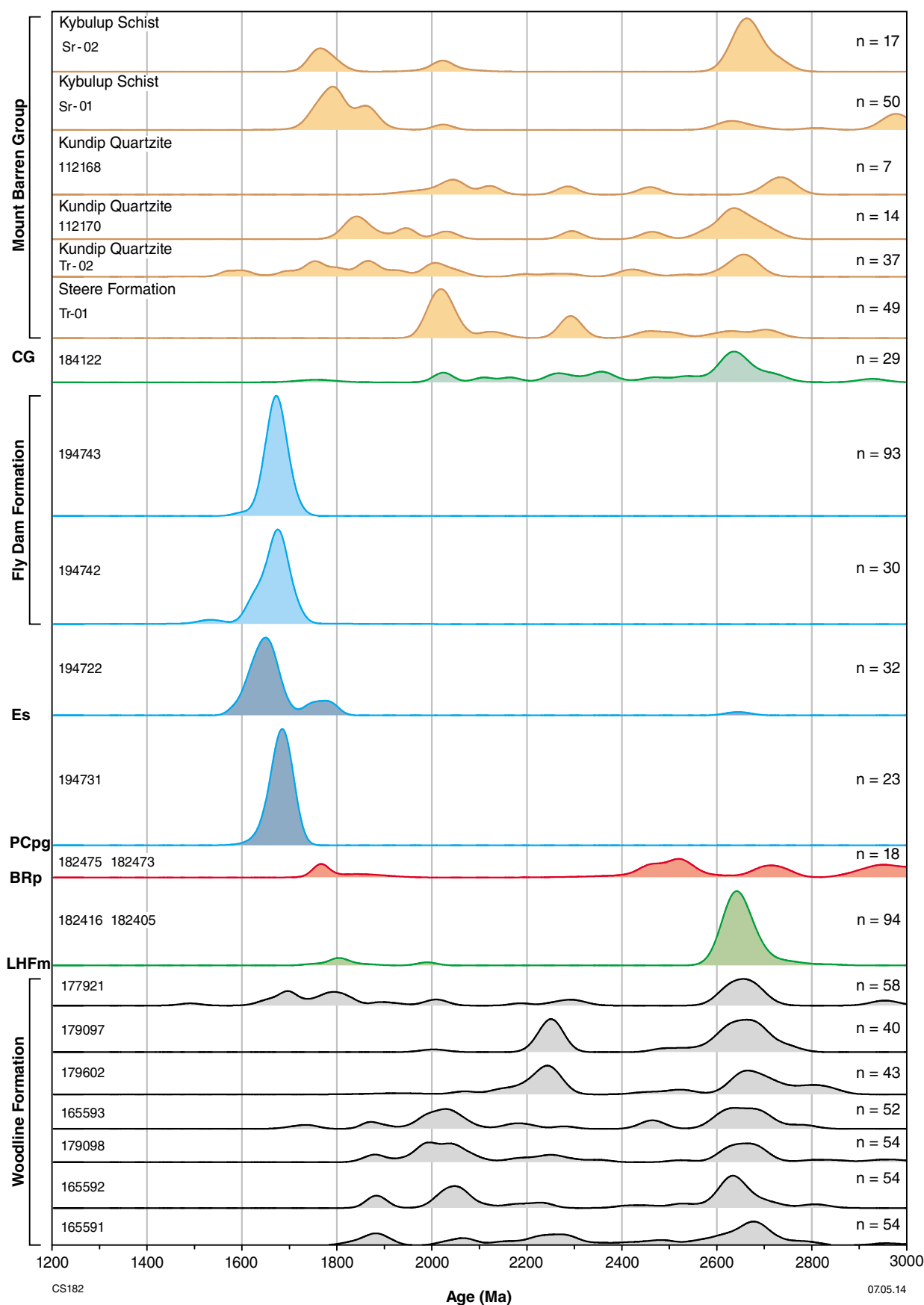


Figure 7a. Normalized probability density diagram of detrital zircon dates from samples of the Barren Basin. Sample numbers are shown on the left, and are listed in Appendix 2. The letter n refers to the number of analyses from each sample. Data are $^{207}\text{Pb}/^{206}\text{Pb}$ ages that are >95% concordant. CG = Coramup Gneiss; Es = Eddy schist; PCpg = Ponton Creek psammitic gneiss; BRp = Big Red paragneiss; LH Fm = Lindsay Hill Formation.

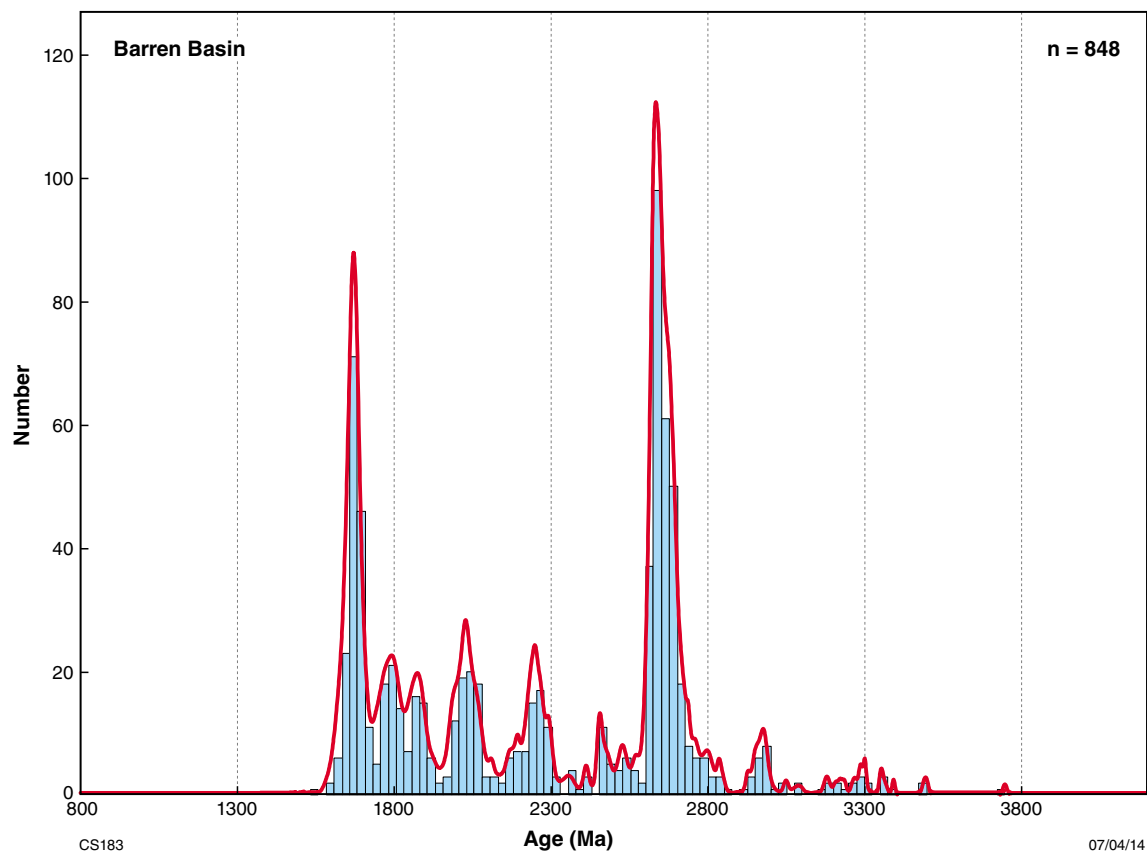


Figure 7b. Probability density diagram and histogram for detrital zircon data (individual analyses) from the Barren Basin. Additional data sources: Nelson, 1996, a,b; Dawson et al., 2002; GSWA data reported in Hall et al., 2008. Data are $^{207}\text{Pb}/^{206}\text{Pb}$ ages that are > 95 % concordant.

interpreted as a maximum depositional age (Table 2; GSWA 194731). A minimum age is constrained by the intrusion of monzogranite at c. 1666 Ma (GSWA 194733). The unimodal age component and high K-feldspar content relative to quartz are both suggestive of a proximal source, which could be interpreted to reflect volcanic activity related to widespread granitic magmatism during the Biranup Orogeny.

Several other occurrences of amphibolite- to granulite-facies metasedimentary rocks, intruded by granitic rocks emplaced during the 1710–1650 Ma Biranup Orogeny, occur throughout the eastern Biranup Zone. Strongly deformed to mylonitic, schistose metasedimentary rock is intruded by magmatic rocks of the c. 1665 Ma Eddy Suite (Kirkland et al., 2011a). Zircons from this schist yielded a maximum depositional age of 1629 ± 9 Ma, and significant detrital zircon age components at c. 2645, 1783, 1745, and 1650 Ma (Fig. 7a; GSWA 194722). The c. 1650 Ma component most likely reflects Eddy Suite pegmatitic or granitic material that was intruded into the metasedimentary rocks, and which subsequently became disaggregated during deformation and metamorphism, forming rounded K-feldspar porphyroclasts (Spaggiari et al., 2011).

Within the eastern Nornalup Zone, drillcore samples of migmatitic paragneiss from the Big Red prospect (Figs 1,5d) yielded a wide range of predominantly Archean detrital ages, and a maximum depositional age of 1685 ± 11 Ma (1σ) (Table 2, Fig. 7a; GSWA 182475; and 182473). Metamorphic zircon rims in these two samples yielded ages of 1193 ± 5 and 1176 ± 10 Ma, indicating that the migmatitic paragneiss from Big Red was metamorphosed under high-temperature conditions during Stage II of the Albany–Fraser Orogeny. The metamorphism is bracketed by the intrusion of Recherche Supersuite granite at 1326 ± 6 Ma (GSWA 182476), and intrusion of Esperance Supersuite granite at 1167 ± 2 Ma (GSWA 182474).

Fly Dam Formation

The Fly Dam Formation has limited exposure, south of the Trans–Australian Railway, in the eastern Biranup Zone of the Albany–Fraser Orogen (Spaggiari and Pawley, 2012). It is a succession of amphibolite- to granulite-facies interlayered psammitic to semipelitic gneisses, interpreted as the metamorphosed equivalents of interbedded sandstones and mudstones. Semipelitic

horizons are layered on the centimetre-scale with alternating quartzofeldspathic and more mafic, biotite-rich material, and also contain abundant garnets ranging from 0.5 to 2 cm in diameter (Fig. 5e,f). The gneisses are mostly migmatitic, and contain isoclinally folded leucosomes as well as leucosomes parallel to the main, axial-planar foliation. Both sets are texturally continuous and locally diatextitic, which indicates they are of a single generation. The formation occurs in large-scale, open to tight, refolded folds that are well defined in aeromagnetic imagery (Spaggiari et al., 2011; Spaggiari and Pawley, 2012).

Detrital zircons from the Fly Dam Formation indicate maximum depositional ages (1σ) of 1535 ± 26 and 1598 ± 9 Ma (analyses of the youngest zircons in two samples, GSWA 194742 and 194743, respectively), or the more conservative estimates of 1640 ± 12 and 1617 ± 26 Ma obtained from the weighted means of the youngest age group in each sample (Table 2; GSWA 194742 and 194743). Significant detrital zircon age components in both samples are at c. 1672 Ma (Fig. 7a). Zircon rims yield metamorphic ages of 1196 ± 13 Ma (GSWA 194743) and a less precise age of 1154 ± 35 Ma (GSWA 194742). These ages are consistent with Stage II of the Albany–Fraser Orogeny.

Synthesis and interpretation of detrital zircon data from the Barren Basin

K–S tables

In many detrital zircon studies, comparisons of age spectra are generally based on visual observations, either as histograms, probability distribution diagrams, or a combination of these graphical means. Some researchers have mathematically described detrital populations (e.g. Gehrels, 2000) and defined the strength of the similarity between populations by statistical techniques (e.g. Sircombe, 2000; Sircombe and Hazelton, 2004). In this Report one such statistical method was used, the Kolmogorov–Smirnov (K–S) test (Press et al., 1986), which has been widely applied to compare the age distributions of detrital zircon populations (e.g. Berry et al., 2001; Kirkland et al., 2011c). The K–S test transposes the datasets into cumulative distribution functions (the sum of the probabilities with increasing age) and tests the probability that the samples were drawn from the same distribution. The value $(1 - p)$ represents the probability that the samples were derived from different distributions. The hypothesis that two samples come from the same source is rejected when the probability (p) drops below 0.05, indicating a level of confidence of 95% that the samples are different. High values, close to 1.0, indicate very similar age spectra and a similar provenance. It does not, however, imply that a specific sediment was deposited at the same time as another, rather that it shared detritus containing zircons of similar ages.

The K–S test incorporates the analytical uncertainties of the data and can be used to compare detrital zircon age data from samples of individual stratigraphic units, and also between stratigraphic units (Table 3). We use

this approach to evaluate whether individual samples and stratigraphic units have statistically similar detrital zircon age spectra, but rely on the geological relationships for a full interpretation. The results of this analysis indicate that many units belonging to the Barren Basin have statistically similar detrital zircon populations. The exceptions to this are the Ponton Creek psammitic gneiss, the Eddy schist, and the Fly Dam Formation, which are dominated by a late Paleoproterozoic peak at 1680–1670 Ma that distinguishes them statistically from the other Barren Basin units.

Samples from the Woodline Formation are statistically similar to each other, with the exception of conglomerate sample GSWA 177921. As is the case for the other Woodline samples, GSWA 177921 contains a significant Neoproterozoic component, but less 2400–1900 Ma detritus, and a greater component of 1900–1690 Ma detritus, probably reflecting a larger, more locally sourced contribution from Biranup Zone granitic rocks (Figs 3a and 7a). This would be consistent with GSWA 177921 being a conglomerate, rather than a sandstone.

Samples from all units of the Mount Barren Group are for the most part statistically similar (Table 3), supporting the interpretation that the units belong to a single group (Thom et al., 1984a). The exception is Kybulup Schist sample Sr-01 (Dawson et al., 2002), which is unlike any other Mount Barren Group sample, but is statistically similar to Big Red paragneiss sample GSWA 182475, shown by a high p -value of 0.812. This sample originated higher in the sequence than any other Mount Barren Group sample (see Dawson et al., 2002, figure 6). The lowermost unit, the Steere Formation (sample Tr-01) is statistically similar to the middle unit, the Kundip Quartzite, but not to the uppermost unit, the Kybulup Schist. This reflects a change in provenance up-sequence. The Kundip Quartzite has a statistically similar detrital population to the Woodline Formation (especially samples GSWA 179098, 165591, 165592, and 165593), the Coramup Gneiss, and the Lindsay Hill Formation. Both samples from the Kybulup Schist (Sr-01 and Sr-02, Dawson et al., 2002) have statistically similar detrital zircon age components to the Big Red paragneiss. Sample Sr-02 also has a similar detrital spectrum to those of the Woodline Formation, the Coramup Gneiss, and the Lindsay Hill Formation, especially metaconglomerate sample GSWA 182416, to which it is nearly identical (p -value > 0.9).

The sample of Coramup Gneiss (GSWA 184122) has a provenance that is statistically similar to most of the Woodline Formation, the Lindsay Hill Formation metaconglomerate (GSWA 182416), the Big Red paragneiss, and samples Sr-02, GSWA 112168 and 112170 from the Mount Barren Group.

Of particular significance is the close correspondence in the ages of detrital zircons between the Big Red paragneiss and the Woodline Formation, the Lindsay Hill Formation, the Coramup Gneiss, and the Mount Barren Group. This implies that some Barren Basin sediments were deposited a substantial distance outboard of the Yilgarn Craton, given that the Big Red paragneiss occurs east of the Fraser Zone (Fig. 1).

Table 3. K-S analysis comparing samples from the Barren Basin

	Woodline Formation										Lindsay Hill Formation	Big Red para-gneiss	Ponton Creek psammitic gneiss
	165591	165592	179098	165593	179602	179097	177921	182405	182416	182473*	182475*	182473*	194731
165591		0.566	0.187	0.312	0.648	0.211	0.024		0.023		0.845	0.175	
165592	0.566		0.764	0.981	0.031	0.006	0.013		0.041		0.750	0.133	
179098	0.187	0.764		0.976	0.004	0.001	0.013		0.007		0.742	0.026	
165593	0.312	0.981	0.976		0.012	0.001	0.047		0.014		0.753	0.088	
179602	0.648	0.031	0.004	0.012		0.766	0.002		0.097		0.539	0.163	
179097	0.211	0.006	0.001	0.001	0.766		0.002	0.002	0.392		0.494	0.149	
177921	0.024	0.013	0.013	0.047	0.002	0.002			0.075		0.909	0.069	
182405									0.316		0.163	0.082	
182416	0.023	0.041	0.007	0.014	0.097	0.539	0.163	0.082			0.658	0.130	
182475*	0.845	0.750	0.742	0.753	0.539	0.494	0.909	0.163	0.658			0.681	0.001
182473*	0.175	0.133	0.026	0.088	0.163	0.149	0.069	0.082	0.130		0.681		
194731											0.001		
194722											0.006		0.030
194742											0.001		0.628
194743													0.499
184122	0.907	0.267	0.085	0.151	0.708	0.866	0.032	0.001	0.213		0.624	0.400	
Ti-01	0.007	0.005	0.051	0.035			0.003				0.483	0.001	
Sr-01							0.007				0.812	0.001	
Ti-02	0.004	0.018	0.042	0.091			0.309		0.001		0.472	0.007	
Sr-02	0.382	0.107	0.188	0.169	0.251	0.189	0.521	0.165	0.991		0.754	0.184	
112170	0.643	0.619	0.682	0.796	0.141	0.122	0.501	0.002	0.143		0.638	0.196	
112168*	0.818	0.909	0.996	0.950	0.267	0.151	0.379	0.004	0.097		0.765	0.142	

Table 3. continued

	Eddy schist	Fly Dam Formation	Coramup Gneiss	Mount Barren Group						
	194722	194742	194743	184122	Ti-01	Sr-01	Ti-02	Sr-02	112170	112168*
165591				0.907	0.007		0.004	0.382	0.643	0.818
165592				0.267	0.005		0.018	0.107	0.619	0.909
179098				0.085	0.051		0.042	0.188	0.682	0.996
165593				0.151	0.035		0.091	0.169	0.796	0.950
179602				0.708			0.000	0.251	0.141	0.267
179097				0.866				0.189	0.122	0.151
177921				0.032	0.003	0.007	0.309	0.521	0.501	0.379
182405				0.001				0.165	0.002	0.004
182416				0.213			0.001	0.991	0.143	0.097
182475*	0.006	0.001		0.624	0.483	0.812	0.472	0.754	0.638	0.765
182473*				0.400	0.001	0.001	0.007	0.184	0.196	0.142
194731	0.030	0.628	0.499							
194722		0.542	0.023							
194742	0.542		0.816							
194743	0.023	0.816								
184122					0.001		0.003	0.485	0.382	0.583
Ti-01				0.001			0.005	0.002	0.168	0.732
Sr-01							0.023	0.013	0.026	0.003
Ti-02				0.003	0.005	0.023		0.070	0.592	0.348
Sr-02				0.485	0.002	0.013	0.070		0.288	0.518
112170				0.382	0.168	0.026	0.592	0.288		0.837
112168*				0.583	0.732	0.003	0.348	0.518	0.837	

NOTES: Numbers in the matrix refer to the probability that the two samples are sourced from the same zircon population and considers the uncertainty in age measurement. Values less than 0.05 indicate the samples are from distinctly different populations (high values indicate similar populations and are in yellow-filled boxes). Blank boxes are values of zero.

Critical values are given in Massey (1951). The table of critical values of D can be found on p. 70.

Results based on $^{207}\text{Pb}/^{206}\text{Pb}$ ages that are > 95 % concordant

* indicates n < 12 analyses

Units that are most dissimilar to the units described above are the Fly Dam Formation (GSWA 194742 and 194743), the Ponton Creek psammitic gneiss (GSWA 194731), and the siliciclastic schist intruded by the c. 1665 Ma Eddy Suite (GSWA 194722). These units do correlate to some degree to each other, especially the Fly Dam Formation and the Ponton Creek psammitic gneiss (Table 3; Fig. 7a). However, the Fly Dam Formation must be substantially younger than the Ponton Creek psammitic gneiss because its maximum depositional age of c. 1617 Ma is considerably younger than the c. 1666 Ma granite that intrudes the Ponton Creek psammitic gneiss (Table 2). Given the young maximum depositional ages, it is feasible that the Fly Dam Formation is not part of the Barren Basin, but instead is part of the younger Arid Basin. However, because of its occurrence within the eastern Biranup Zone, close to where other metasedimentary rocks are intruded by Biranup Zone granites, it is tentatively included in the Barren Basin. One possible explanation for the younger ages could be that they represent inclusions of Biranup Zone granitic veins that intruded the paragneiss, strongly overprinted by migmatization and deformation (Fig. 5f).

Provenance of the Barren Basin

The Barren Basin contains detrital zircons with ages spanning 3000–1600 Ma, with two main peaks at 2650–2625 and 1675–1650 Ma (based on bin widths of 25 Ma, Fig. 7b). Very minor age components are present between 3800 and 3000 Ma. The most dominant age of Barren Basin detritus is Neoproterozoic, mostly spanning the range 2750–2600 Ma (Fig. 7b). For example, quartzite from the Lindsay Hill Formation (GSWA 182405) yielded 58 analyses with dates of 2735–2619 Ma, with a significant age component at c. 2640 Ma. Metaconglomerate of the Lindsay Hill Formation (GSWA 182416) also yielded a significant age component at c. 2635 Ma, as well as one at c. 1807 Ma. Detrital zircons from the Stirling Range Formation indicate significant Neoproterozoic age components at c. 2748, 2709, and 2656 Ma, although these are not as dominant as the Paleoproterozoic age components (Fig. 6; Rasmussen et al., 2002). The 2750–2600 Ma age range occurs in all units except the Fly Dam Formation (GSWA 194742 and 194743), the Ponton Creek psammitic gneiss (GSWA 194731), and the siliciclastic schist intruded by the c. 1665 Ma Eddy Suite (GSWA 194722). The Neoproterozoic ages are consistent with the ages of granites and greenstones of the Yilgarn Craton (Cassidy et al., 2006, and references therein) and, given its close proximity and unconformable contact relationships with some units (Table 2), the Yilgarn Craton is regarded as the most likely source. Smaller, older peaks at c. 3300 and 2950 Ma (Fig. 7a) could also be interpreted as having been derived from the Yilgarn Craton (Nutman et al., 1993; Wang et al., 1996; Witt, 1998).

The Barren Basin also contains several significant detrital zircon age components spanning 2550–1900 Ma that imply sources distal to the Albany–Fraser Orogen, or alternatively, unrecognized or destroyed basement components (Fig. 7b). The dominant age components in the 2550–1900 Ma range occur at c. 2250 and 2035 Ma.

Both are present in samples of the Stirling Range Formation, with the c. 2035 Ma age component the largest of the two (Fig. 6; Rasmussen et al., 2002). The Coramup Gneiss also contains significant age components at c. 2357, 2263, and 2031 Ma (Bodorkos and Wingate, 2008a). In the Woodline Formation, significant age components in the range 2550–1900 Ma occur in individual samples at c. 2292 Ma (GSWA 177921), c. 2042 and 1988 Ma (GSWA 179098). If the Woodline Formation is considered as a single group, the most significant age components in this range are c. 2246 and 2035 Ma (Hall et al., 2008, figure 11), identical to those in the Stirling Range Formation. In the Mount Barren Group, significant age components in this range occur at c. 2291, 2246, and 2018 Ma (Fig. 7a; Hall et al., 2008, figure 11; Nelson, 1996a; Dawson et al., 2002).

In contrast, the Big Red paragneiss yielded significant detrital age components between 2575 and 2450 Ma, with a probability peak at c. 2457 Ma, as well as older components at c. 3177 and 3027 Ma (GSWA 182475 and 182473). The 2575–2450 Ma age range is not as significant in other Barren Basin units, although it does appear in the Woodline Formation, with major age components in individual samples occurring at c. 2532 Ma (GSWA 179602), c. 2486 Ma (GSWA 165591), and c. 2466 Ma (GSWA 165593). Minor age components occur in the Coramup Gneiss at c. 2532 and 2469 Ma (GSWA 184122).

After the Neoproterozoic component, the second largest detrital zircon age component in much of the Barren Basin spans the range 1900–1600 Ma, with the largest probability peak defined between 1700 and 1650 Ma (Fig. 7b). Subsidiary components are defined between 1800 and 1750 Ma, and a smaller peak at c. 1875 Ma. The 1700–1650 Ma range matches that observed from magmatic rocks emplaced during the Biranup Orogeny, and the 1800–1750 Ma range matches known granitic magmatism in the Tropicana, Biranup, and Nornalup Zones (Table 1, Fig. 3; Kirkland et al., 2011a; Spaggiari et al., 2011, 2014). The c. 1875 Ma peak is unknown, and may indicate an as yet unrecognized magmatic event in the Albany–Fraser Orogen, or alternatively, detritus from a distal source.

All Barren Basin units, except the Stirling Range Formation, contain significant age components between 1900 and 1600 Ma, implying a significant geographic extent of the sediment transportation pathways that dispersed zircons from their original sources, or recycled sources, throughout the Albany–Fraser Orogen. It is interesting to note the presence of c. 1770 Ma detritus in the Mount Barren Group (GSWA 112168 and 112170; Dawson et al., 2002), which could imply the presence of crust of that age in the central Albany–Fraser Orogen. Broadly similar age components occur at c. 1826, 1773, and 1763 Ma in the Big Red paragneiss (GSWA 182475 and 182473), at c. 1807 Ma in metaconglomerate from the Lindsay Hill Formation (GSWA 182416), and at c. 1757 Ma in the Coramup Gneiss (GSWA 184122). The Woodline Formation contains significant age components in this range at c. 1886 (summary in Hall et al., 2008), c. 1794 and 1696 Ma (GSWA 177921), and c. 1739 Ma (GSWA

165593). The Mount Barren Group contains significant age components in this range at c. 1857, 1803, and 1773 Ma (GSWA 112168 and 112170; Dawson et al., 2002).

Of note is the abundance of late Paleoproterozoic detritus in the Fly Dam Formation (c. 1829, 1673, 1640, and 1617 Ma; GSWA 194742 and 194743), the Ponton Creek psammitic gneiss (c. 1689 Ma; GSWA 194731), and the siliciclastic schist intruded by the c. 1665 Ma Eddy Suite (c. 1783, 1745, and 1650 Ma; GSWA 194722). The c. 1650 Ma component is interpreted to reflect the age of intrusive pegmatites into the schist, which were subsequently deformed (Spaggiari et al., 2011). These detrital age components suggest derivation from local Biranup Zone sources (Fig. 3a), with little input from elsewhere.

Previous interpretations for the provenance of Barren Basin units have suggested that Paleoproterozoic detritus was far-travelled and sourced from other terranes, e.g. the Mount Barren Group was sourced from the Gawler Craton (Dawson et al., 2002), or the Woodline Formation was sourced from unrecognized or exotic terranes outside the West Australian Craton, and was possibly a lateral equivalent to the Earahedy Group on the northeastern margin of the Yilgarn Craton (Hall et al., 2008). More recently, the ages of magmatism in the Albany–Fraser Orogen have become much better constrained, and correlate well with the dominant ages of Paleoproterozoic detritus (1900–1600 Ma) in the Barren Basin (Fig. 3). This suggests that, in conjunction with the presence of Neoproterozoic detritus, there is no necessity to invoke exotic or distal sources for the majority of detritus in the Barren Basin, with the main exceptions being the less dominant age components in the range 2550–1900 Ma. The significant differences between the age components of the Woodline Formation and the Mount Barren Group (Hall et al., 2008 and references therein) can be explained by the large geographical separation of the units during deposition (Fig. 1), and the more distal original position inferred for the Mount Barren Group, prior to cratonward thrusting. This interpretation would be consistent with the relatively lesser amount of Neoproterozoic material present in the Mount Barren Group, and the significant component of 1810–1760 Ma detritus, which in turn fits with inheritance and granitic protolith ages from the Biranup and Nornalup Zones (Fig. 3). The Woodline Formation is thus regarded as having been deposited during Cycle 1 in a separate sub-basin (the Woodline Sub-basin) from the Mount Barren Group, though it is still part of the more extensive Barren Basin.

The provenance of detritus in the age range 2550–1900 Ma is more difficult to explain, as there are no known local sources of this age (Fig. 3). If such sources were present during deposition of the Barren Basin, they have since been eroded, been tectonically destroyed, or have not as yet been found. However, if the sources are considered as more distal or exotic, there is potential for a zircon crystallization age connection to the Glenburgh Terrane of the Gascoyne Province. Interlayered granitic gneisses of the Halfway Gneiss have igneous crystallization ages between 2555 and 2430 Ma, and are interpreted as reworked basement to the Glenburgh

Terrane (Johnson et al., 2011a,b). This basement was intruded by the 2005–1970 Ma Dalgaringa Supersuite, interpreted as a continental magmatic-arc that formed on the southern margin of the Glenburgh Terrane during the Glenburgh Orogeny, prior to collision with the northern Yilgarn Craton (Sheppard et al., 2004; Johnson et al., 2011a). Lu–Hf isotope data from the Halfway Gneiss indicate that it was exotic to both the Yilgarn and Pilbara Cratons, and was thus part of an external terrane — the Glenburgh Terrane — that subsequently collided with each craton in two distinct, orogenic episodes (Johnson et al., 2011a,b). Halfway Gneiss Lu–Hf signatures cluster at ϵ_{Hf} -5 to +4 (see Hf isotope fingerprints of detrital zircons section). This signature lies within the isotopic gap present in the Big Red paragneiss dataset, which contains 2555–2450 Ma detrital zircons of similar age to the Halfway Gneiss. It is therefore unlikely that the 2555–2450 Ma detrital zircon age component found in the Big Red paragneiss, and possibly also the Woodline Formation and the Coramup Gneiss, was derived from erosion of the Halfway Gneiss.

However, the significant age components that cluster around c. 2250 and 2035 Ma potentially may have been derived from the Gascoyne Province (cf. Hall et al., 2008). The Quartpot Pelite of the Camel Hills Metamorphics was deposited between c. 2000 and 1959 Ma in a fore-arc basin setting, during the Glenburgh Orogeny (Johnson et al., 2011a). It is dominated by detrital zircons in the range 2080–2000 Ma, which, based on their Hf isotope compositions, are interpreted to be derived from early (currently unexposed) Dalgaringa arc magmatism on the southern margin of the Glenburgh Terrane (Johnson et al., 2011a). Unfortunately, no Hf-isotope data from the Stirling Range Formation, Mount Barren Group, or Woodline Formation are available and there are only a few data points from the Coramup Gneiss, so their compositions cannot be robustly compared. However, the source of the Quartpot Pelite described above could explain the origin of the c. 2035 Ma peak in the Barren Basin, potentially recycled through other units or dispersed along the Yilgarn Craton margin. The Quartpot Pelite also contains age components between c. 2300 and 2175 Ma, the origin of which is unknown (Johnson et al., 2011a). Whether this has any relationship to the 2250 Ma peak in the Barren Basin is also unknown.

The Arid Basin

Several successions of metasedimentary rocks have maximum depositional ages younger than the latest Biranup Zone magmatism (c. 1625 Ma), but have been affected by Stage I tectonism. These sedimentary successions belong to the Arid Basin, and include the Malcolm Metamorphics of the eastern Nornalup Zone (formerly the Malcolm Gneiss; Myers, 1995a), the Gwynne Creek Gneiss in the northeastern part of the orogen, and metasedimentary rocks of the Fraser Range Metamorphics, here named the Snowys Dam Formation (Fig. 1; Table 4; Spaggiari et al., 2011). Also included are paragneissic rocks from the western Nornalup Zone such as those found at Whalehead Rock near Albany (Fig. 1; Love, 1999).

Malcolm Metamorphics

The Malcolm Metamorphics are dominated by siliciclastic metasedimentary rocks, but also include layers of mafic amphibolitic schist and less abundant calc-silicate rocks. Locally, the mafic schist and calc-silicates are distinctly interlayered on a several cm-scale, and may represent former volcanic and volcanoclastic horizons (Figs 8a,b). These rocks are in turn variably interlayered with the siliciclastic metasedimentary rocks, indicating primary relationships between all protoliths. The mafic schist contains an assemblage of clinopyroxene–epidote–plagioclase–garnet–titanite (Clark, 1999). The calc-silicates contain aggregates of garnet–plagioclase–clinopyroxene–quartz \pm calcite \pm hornblende \pm wollastonite \pm clinozoisite, locally secondary epidote, and accessories titanite and magnetite (Clark, 1999). The metasedimentary rocks consist dominantly of quartz–K-feldspar–plagioclase–muscovite–biotite psammitic gneiss, interlayered with garnet–biotite–sillimanite pelitic rocks (Clark, 1999; Adams, 2012). Both lithologies are locally migmatitic and contain layer-parallel leucosomes. The siliciclastic metasedimentary rocks, mafic schist, and calc-silicates have all been folded at least twice into east-northeasterly trending, tight to isoclinal folds (see also Adams, 2012). There is at least one early generation of pegmatite that is also folded, and locally boudinaged. Low-pressure, high-temperature metamorphism at 4–5 kbar and 750–800°C is interpreted to relate to formation of the first gneissic fabric (S1, Clark et al., 2000). Small- to medium-scale, dominantly sinistral shears, pegmatite, and fine-grained equigranular granitic veins cut the folds (see also Clark, 1999 and Adams, 2012). The granitic veins trend parallel to the main fabric and are foliated, but not folded. One of these granitic veins was dated at 1313 ± 16 Ma (Clark et al., 2000). Late coarse-grained pegmatite veins cut all phases and structures.

Two samples of upper amphibolite, migmatitic semipelitic schist yielded maximum depositional ages of 1455 ± 16 Ma (upper intercept age in sample PM-11-011) and 1456 ± 21 Ma (upper intercept age in GSWA 194867; Adams, 2012). This shows that these rocks are substantially younger than the previously published maximum depositional age of 1560 ± 40 Ma (GSWA 112128), and also indicates that suggestions of the presence of c. 1450 Ma granitic gneiss in the Point Malcolm area (Myers, 1995) may reflect detrital, rather than intrusive, material. This fits with the lithological character of the quartzofeldspathic gneisses in the Point Malcolm area, which are dominantly psammitic, rather than granitic. Sample GSWA 112128 also yielded a detrital age component at 1807 ± 35 Ma, and single zircons with ages of c. 2734, 2175, and 2033 Ma (Fig. 9a).

Two periods of metamorphic monazite growth have been identified at 1311 ± 4 and 1180 ± 5 Ma, coincident with both Stages I and II of the Albany–Fraser Orogeny (combined mean ages from migmatitic semipelitic schist [PM-11-011 and GSWA 194867] and psammitic schist [GSWA 194869; Adams, 2012]). Monazite from PM-11-011 is interpreted to represent leucosome crystallization at 1313 ± 6 Ma (Adams, 2012). This

probably occurred shortly prior to intrusion of the crosscutting granitic vein dated at 1313 ± 16 Ma (Clark et al., 2000).

Whalehead Rock paragneiss

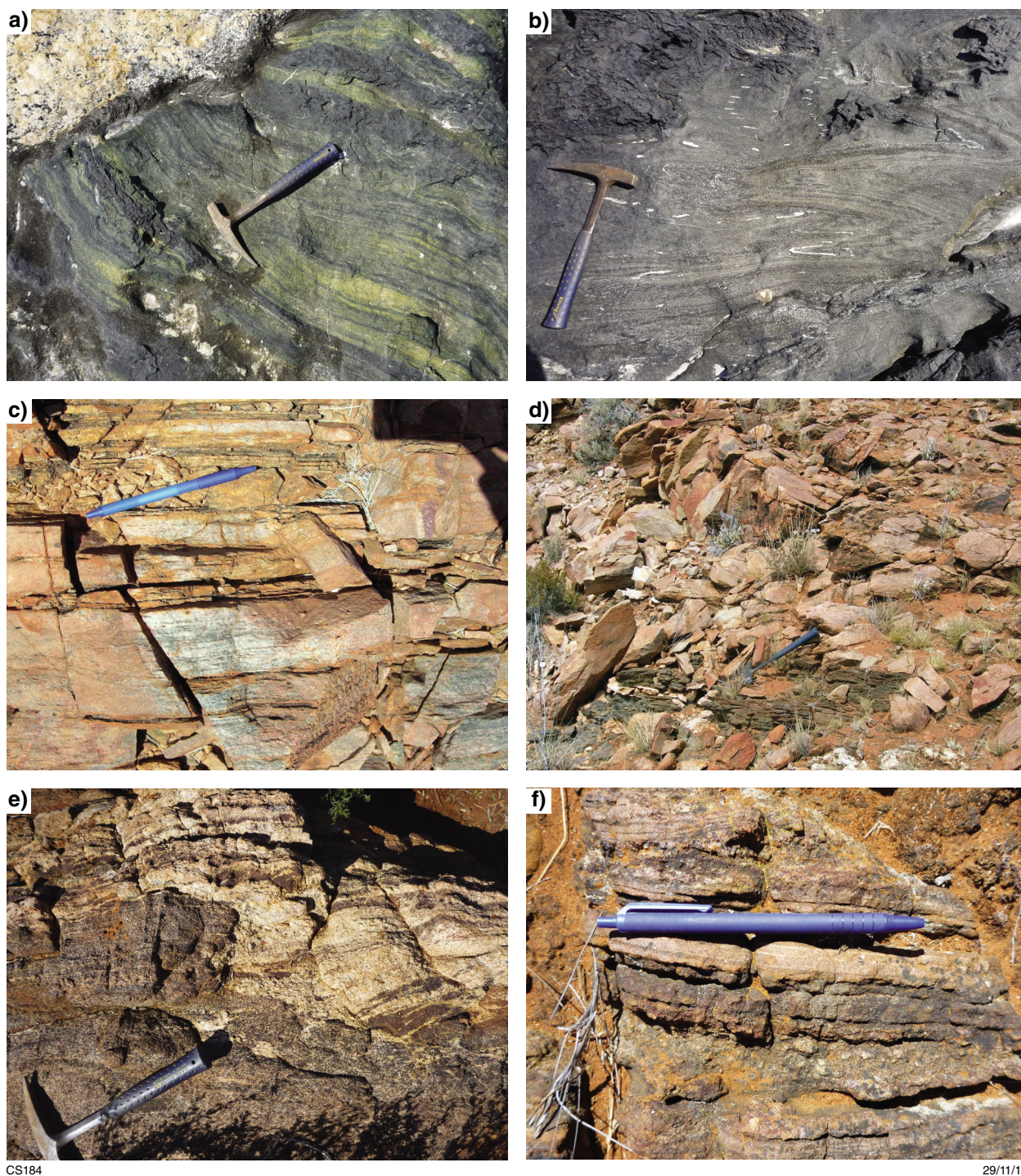
The Whalehead Rock succession in the western Nornalup Zone includes a garnet–cordierite paragneiss that occurs with orthopyroxene-bearing metagranite (enderbitic gneiss) with trains of mafic enclaves, and metatonalite (Fitzsimons and Buchan, 2005). The orthopyroxene-bearing metagranite is dated at 1289 ± 10 Ma (Pidgeon, 1990), and a c. 1300 Ma age was obtained for the metatonalite (Love, 1999), indicating both granitic phases are part of the Recherche Supersuite. The paragneiss is characterized by psammitic gneiss, quartzite, and garnet (–cordierite) and garnet(–sillimanite) migmatite that locally contains boudins of calc-silicate rocks (Clark, 1995; Love, 1999).

The pelitic migmatitic rocks contain detrital zircons with ages of 1750–1720 Ma, have a maximum depositional age of c. 1360 Ma (Whalehead Rock; Love, 1999), and were metamorphosed at 1314 ± 5 Ma (Whalehead Rock; Love, 1999) and 1304 ± 3 Ma (Ledge Point; Clark, 1995). This constrains the depositional age of the Whalehead Rock paragneiss to between c. 1360 and 1310 Ma, and the first episode of metamorphism in these rocks to Stage I (Fitzsimons and Buchan, 2005). Interestingly, the early Stage I metamorphic age of 1314 ± 5 Ma is similar to that recorded in the Malcolm Metamorphics.

Gwynne Creek Gneiss

The Gwynne Creek Gneiss occurs in the northeastern part of the Albany–Fraser Orogen, between the Fraser and Biranup Zones, east of the Tropicana gold deposit (Fig. 1; Spaggiari and Pawley, 2012). The unit is dominated by psammitic and semipelitic gneiss, and also includes layered, finely laminated, quartzofeldspathic gneiss with layer-parallel leucosomes (Fig. 8c; Spaggiari et al., 2011). Minor metagranitic, metamafic, and meta-ultramafic rocks intrude the metasedimentary rocks, and are possibly related to the Fraser Zone intrusions (Fig. 8d). Alternatively, they may represent earlier magmatic activity during deposition of the Arid Basin. The metasedimentary rocks are also intruded by late, coarse to very coarse, K-feldspar-rich pegmatites.

The semipelitic gneiss has a maximum depositional age of 1483 ± 12 Ma (1 σ , based on the youngest analysis), with a more conservative estimate of 1533 ± 11 Ma, based on six analyses (GSWA 182432; Table 4). This sample also includes a significant 1675 Ma detrital zircon age component, and minor components at c. 1739 and 1607 Ma. Garnet–biotite-bearing, quartzofeldspathic migmatitic gneiss (Fig. 9a; GSWA 194735) yielded a concordia age of 1657 ± 5 Ma, interpreted as representing detrital material from a migmatitic precursor, based on the maximum depositional age described above. Two phases of metamorphic overgrowth were recorded in this rock at 1270 ± 11 and 1193 ± 26 Ma (GSWA 194735).



CS184

29/11/13

Figure 8. Photographs of Arid Basin rocks: a) Interlayered mafic schist and calc-silicate of the Malcolm Metamorphics, cut by pegmatite, Point Malcolm; b) folded layering in mafic schist of the Malcolm Metamorphics, Point Malcolm; c) interbedded psammitic and semipelitic gneiss with laminations near the top of the photo, Gwynne Creek Gneiss, Gwynne Creek; d) psammitic gneiss intruded by metamafic rock, Gwynne Creek Gneiss, Gwynne Creek; e) Fraser Zone gabbro intruded into psammitic gneiss of the Snowys Dam Formation, near Yardilla prospect, Fraser Range; f) thinly laminated, alternating dark, magnetite-rich layers with thin quartz-rich layers in metasedimentary rocks of the Snowys Dam Formation, near Mount Malcolm.

Snowys Dam Formation

The Snowys Dam Formation is a new name for the metasedimentary component of the Fraser Range Metamorphics of the Fraser Zone. These metasedimentary rocks are mostly exposed along the northwestern side of the Fraser Zone (Fig. 1), and are typically intercalated with layers of mafic granulite or amphibolite that are interpreted as sills or sheets of the Fraser Zone gabbroic intrusions (Fig. 8e; Spaggiari and Pawley, 2012), although it is possible that some may represent older magmatic activity. The southwestern exposures of the Snowys Dam Formation are predominantly garnet-rich pelitic and semipelitic gneisses, with locally iron-rich metasedimentary rocks, and quartz-rich psammitic gneiss (e.g. the Gnamma Hill and Mount Malcolm areas). The pelitic gneiss at Gnamma Hill is quartz rich and typically contains quartz–K-feldspar–garnet–Fe–Ti oxides–sillimanite–biotite–cordierite \pm plagioclase and foliation-parallel leucosomes (Oorschot, 2011). The iron-rich rocks near Mount Malcolm consist of thinly laminated, alternating dark, magnetite-rich layers with thin quartz-rich layers (Fig. 8f). The iron-rich layers also include abundant garnet, minor pyroxene, and possibly grunerite. These rocks occur with pink, felsic metasedimentary rocks rich in garnet, with plagioclase, perthite, quartz, hypersthene, diopside, and biotite, and locally sillimanite (see petrographic description in GSWA 194778).

Along the northwestern edge of the exposed section of the Fraser Zone, the Snowys Dam Formation is dominated by psammitic to semipelitic gneiss with layers of mafic amphibolite. Locally these rocks are interlayered with metasedimentary rocks that have calc-silicate affinities, and may represent metamorphosed marls, or volcanoclastic protoliths. In some areas these rocks contain layers packed with unusual, orange-coloured, euhedral garnets up to 1 cm, set in a white, sugary matrix dominated by quartz and lesser plagioclase, and variable amounts of titanite, epidote or zoisite, minor hornblende, and magnetite (Spaggiari et al., 2011, figure 12c).

Maximum depositional ages of the Snowys Dam Formation indicate that deposition occurred not long before mafic magmatism (Table 4). Garnet–biotite semipelitic gneiss from near Mount Malcolm yielded the youngest maximum depositional age of 1332 ± 21 Ma (single zircon analysis), or the more conservative estimate of 1363 ± 9 Ma (24 youngest analyses; GSWA 194778). Zircon rims from the same sample yielded a metamorphic age of 1298 ± 12 Ma, identical to that for metamorphic zircons from mafic granulite at the American Quarry (1292 ± 6 Ma; GSWA 194718).

Synthesis and interpretation of detrital zircon data from the Arid Basin

K–S tables

As described in the Barren Basin section, the K–S statistical analysis was used to assist in the evaluation of the similarity of detrital zircon age distributions

from both individual samples and stratigraphic units, in conjunction with the geological relationships. The results of the analysis show that all stratigraphic units grouped as within the Arid Basin are statistically permissible (Table 5; Fig. 9a). Even though the Gwynne Creek Gneiss is exposed over 200 km to the north or northeast of the other two units, it is reasonable to include it in the Arid Basin as it has a minimum (i.e. metamorphic) age of c. 1270 Ma (Table 4), and therefore cannot be younger than the other Arid Basin units. In addition, sample GSWA 182432 is nearly identical to sample GSWA 177910 of the Snowys Dam Formation (p -value > 0.9).

Samples from the Snowys Dam Formation are statistically similar to each other, with the exception of the quartz metasandstone sample GSWA 177910 mentioned above (Table 5). Although this sample has a statistically similar detrital zircon spectrum to pelitic gneiss sample GSWA 112128 of the Malcolm Metamorphics, it is dissimilar to the other two Malcolm Metamorphics samples, which contain much less Paleoproterozoic material and no Archean detritus. Nonetheless, there is a general correlation between the detrital zircon profile in the Snowys Dam Formation and the other two Malcolm Metamorphics samples. However, it should be noted that the zircon U–Pb data for the Malcolm Metamorphics are sparse and affected by radiogenic-Pb loss, which prohibits a thorough analysis of this unit.

Interestingly, quartz metasandstone sample GSWA 177910 from the Snowys Dam Formation is statistically identical to both of the Gwynne Creek Gneiss samples, suggesting some horizons in different units may have similar sources. These samples are from more quartzofeldspathic horizons, which could explain their favourable correlations relative to the other more pelitic or compositionally variable lithologies.

Provenance of the Arid Basin

The Arid Basin contains detrital zircons with ages spanning c. 1325 to 1850 Ma, and very minor occurrences with ages between 2025 and 2750 Ma (Fig. 9b). The peaks of the two main age components occur at 1675–1650 Ma and at 1400–1375 Ma (based on 25 Ma bin widths, Fig. 9b). Detrital zircons with ages between the two main peaks form a continual spread, with a trough at 1550–1525 Ma.

The most dominant age component of Arid Basin zircon detritus is Mesoproterozoic, spanning the range 1425–1375 Ma, with subordinate components in the ranges 1475–1425 Ma and 1375–1325 Ma (Fig. 9b). All three Arid Basin units contain minor age components in the range 1600–1475 Ma (Fig. 9a). The dominant age component of 1425–1375 Ma occurs in the Snowys Dam Formation of the Fraser Zone, although this unit is also where the majority of the data come from (Fig. 9a). The most significant age component in garnet–biotite semipelitic gneiss from the southern part of the Fraser Zone is c. 1401 Ma (GSWA 194778), similar to garnet-rich semipelitic gneiss from nearby, in which the most significant age component is c. 1383 Ma (GSWA 194777).

Table 4. Summary of age and depositional relationships of the Arid Basin

Unit; GSWA sample numbers	Metamorphic facies	Maximum depositional age: youngest single analysis; youngest group	Minimum age	Inferred depositional substrate	Type of basin fill	Depositional setting	Present-day substrate	Estimated true thickness
Snowy Dam Formation: 194714, 177910, 194777, 194778	Amphibolite to granulite	1332 ± 21 Ma; c. 1363 Ma	1304 ± 7 Ma metamorphism	Eastern Biranup Zone and/or Nornalup Zone	Highly variable; interbedded sandstone and mudstone, calcareous rocks or marls, iron-rich horizons, possible volcanoclastics. Intruded by mafic sills	Moderate to low energy marine? Proximal volcanics? Restricted basins?	Fraser Zone	Unknown
Gwynne Creek Gneiss: 182432, 194735	Amphibolite to granulite	1483 ± 12 Ma; c. 1533 Ma	1270 ± 11 Ma metamorphism	Eastern Biranup Zone and/or Nornalup Zone	Interbedded sandstone and lesser mudstone	Shallow marine?	Boundary between Eastern Biranup Zone and Fraser Zone	Unknown
Malcolm Metamorphics: 194869, 194867, 112128	Amphibolite	c. 1455 Ma ^(a)	Intruded by microgranite at 1313 ± 16 Ma ^(b)	Eastern Nornalup Zone	Interbedded sandstone and mudstone with calcareous horizons. Interlayered mafic rocks possibly basaltic flows or sills	Moderate to low energy marine? Proximal volcanics? Restricted basins?	Eastern Nornalup Zone	Unknown

SOURCES: (a) Adams, 2012

(b) Clark et al., 2000

Table 5. K–S analysis comparing samples from the Arid Basin

	Gwynne Creek Gneiss			Snowys Dam Formation			Malcolm Metamorphics		
	194735	182432	177910	194778	194777	194714	112128	194867*	194869*
194735		0.314	0.432				0.003		0.001
182432	0.314		0.987				0.024		0.003
177910	0.432	0.987					0.167		0.003
194778					0.550	0.415		0.992	0.191
194777				0.550		0.236		0.526	0.039
194714				0.415	0.236			0.997	0.493
112128	0.003	0.024	0.167						0.010
194867*				0.992	0.526	0.997			0.511
194869*	0.001	0.003	0.003	0.191	0.039	0.493	0.010	0.511	

NOTES: Numbers in the matrix refer to the probability that the two samples are sourced from the same zircon population and considers the uncertainty in age measurement. Values less than 0.05 (in boxes with no colour fill) indicate the samples are from distinctly different populations. High values indicate similar populations and are in yellow-filled boxes. Blank boxes are values of zero.

Critical values are given in Massey (1951). The table of critical values of D can be found on p. 70.

Results based on $^{207}\text{Pb}/^{206}\text{Pb}$ ages that are > 95 % concordant

* indicates $n < 12$ analyses

The younger Mesoproterozoic age range of 1375–1325 Ma, which approaches the minimum depositional age as constrained by Stage I intrusions and metamorphism (Table 3), also occurs in the Snowys Dam Formation. A significant detrital zircon age component within this range from garnet–biotite semipelitic gneiss in the southern Fraser Zone is indicated at c. 1349 Ma, by 25 detrital analyses (GSWA 194778). The most significant detrital zircon age component in psammitic gneiss in the same region is c. 1374 Ma (GSWA 194714).

The 1475–1425 Ma age range also occurs in detritus of the Snowys Dam Formation, as well as in the Malcolm Metamorphics. In the former, the second largest detrital zircon age component in a garnet-rich semipelitic gneiss is indicated at c. 1457 Ma (GSWA 194777), and minor age components at c. 1444 and 1466 Ma occur in a nearby garnet–biotite semipelitic gneiss (GSWA 194778), and in quartz metasandstone (GSWA 177910), respectively. In the Malcolm Metamorphics, zircon detritus in the range of 1475–1425 Ma is indicated by upper intercept ages of c. 1455 Ma from two samples that have lost radiogenic-Pb (Fig. 9a; Adams, 2012).

The second most dominant detrital age component in the Arid Basin is Paleoproterozoic and spans the range 1700–1650 Ma, with minor components in the ranges 1825–1725 and 1650–1600 Ma (Fig. 9b). The 1700–1650 Ma age range occurs in the Snowys Dam Formation, but is most dominant in the Gwynne Creek Gneiss (Fig. 9a). In the latter, the largest age component from a semipelitic gneiss has a maximum of c. 1677 Ma (GSWA 182432), whereas garnet–biotite quartzofeldspathic gneiss yielded a single, non-metamorphic age component with a weighted mean age of 1657 ± 5 Ma, interpreted as representing detrital material from a migmatitic precursor (GSWA 194735). The second largest age component in the semipelitic gneiss has a maximum of c. 1607 Ma, with this sample being the only representative of the range 1650–1600 Ma. In the Snowys

Dam Formation, smaller components of c. 1640 and 1680 Ma occur in metasandstone (GSWA 177910), and at c. 1671 Ma in psammitic gneiss (GSWA 194714).

Detritus in the range of 1825–1725 Ma occurs in the Snowys Dam Formation as a minor component in garnet-rich semipelitic gneiss at c. 1787 Ma (GSWA 194777), and in the Gwynne Creek Gneiss in semipelitic gneiss, with a maximum of c. 1739 Ma (GSWA 182432). Pelitic gneiss from the Malcolm Metamorphics also contains a minor age component in this range with a weighted mean of 1807 ± 35 Ma (GSWA 112128). Interestingly, the dominant age component in the Mount Ragged Formation is between 1825 and 1750 Ma (Fig. 10), and migmatitic rocks from the western Albany–Fraser Orogen contain detrital zircons with ages of 1750–1720 Ma (Whalehead Rock; Love, 1999). This zircon U–Pb geochronology shows that 1825–1725 Ma detritus is regionally widespread.

The age range of 1600–1475 Ma is evident in all three Arid Basin units (Fig. 9a). In the Snowys Dam Formation garnet-rich semipelitic gneiss has a minor age component with a maximum of c. 1553 Ma (GSWA 194777), whereas psammitic gneiss has an identical minor age component with a maximum at c. 1553 Ma (GSWA 194714). Semipelitic gneiss in the Gwynne Creek Gneiss has a minor age component with a weighted mean of 1533 ± 11 Ma (GSWA 182432), and in the Malcolm Metamorphics pelitic gneiss has a minor age component with a weighted mean of 1560 ± 40 Ma (GSWA 112128).

The least significant age components in all units occur between 2750 and 2600 Ma, 2550 and 2450 Ma, and from 2075 to 2025 Ma (Figs 9a, b). In the Snowys Dam Formation, garnet-rich semipelitic gneiss yielded single zircons dated at c. 2694, 2648, 2518, 2430, and 2072 Ma (GSWA 194777). In the Malcolm Metamorphics, pelitic gneiss yielded single zircons with ages of c. 2734, 2175, and 2033 Ma (GSWA 112128).

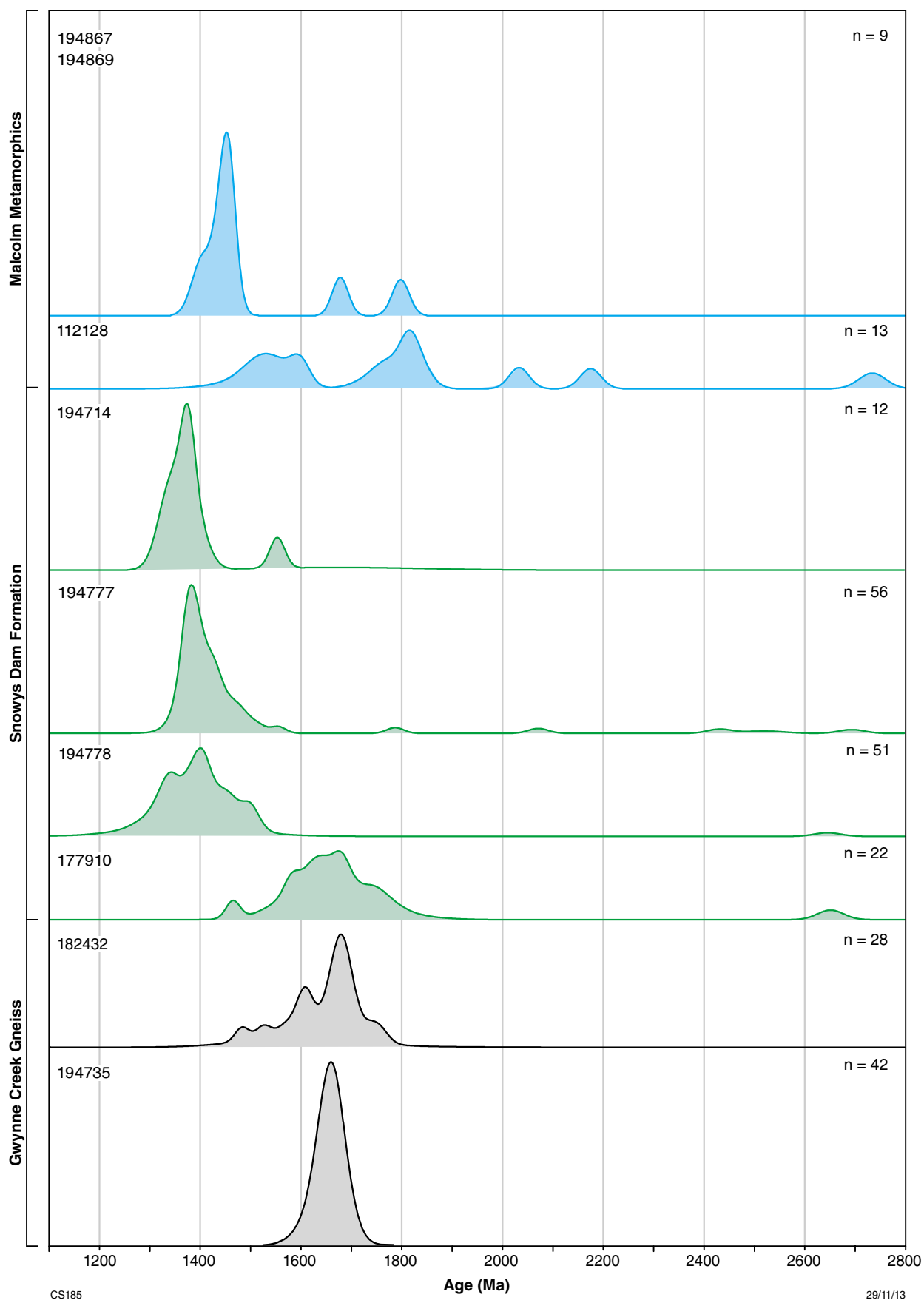


Figure 9a. Normalized probability density diagram of detrital zircon dates from individual samples of the Arid Basin. Sample numbers are shown on the left, and are listed in Appendix 2. The letter n refers to the number of analyses from each sample

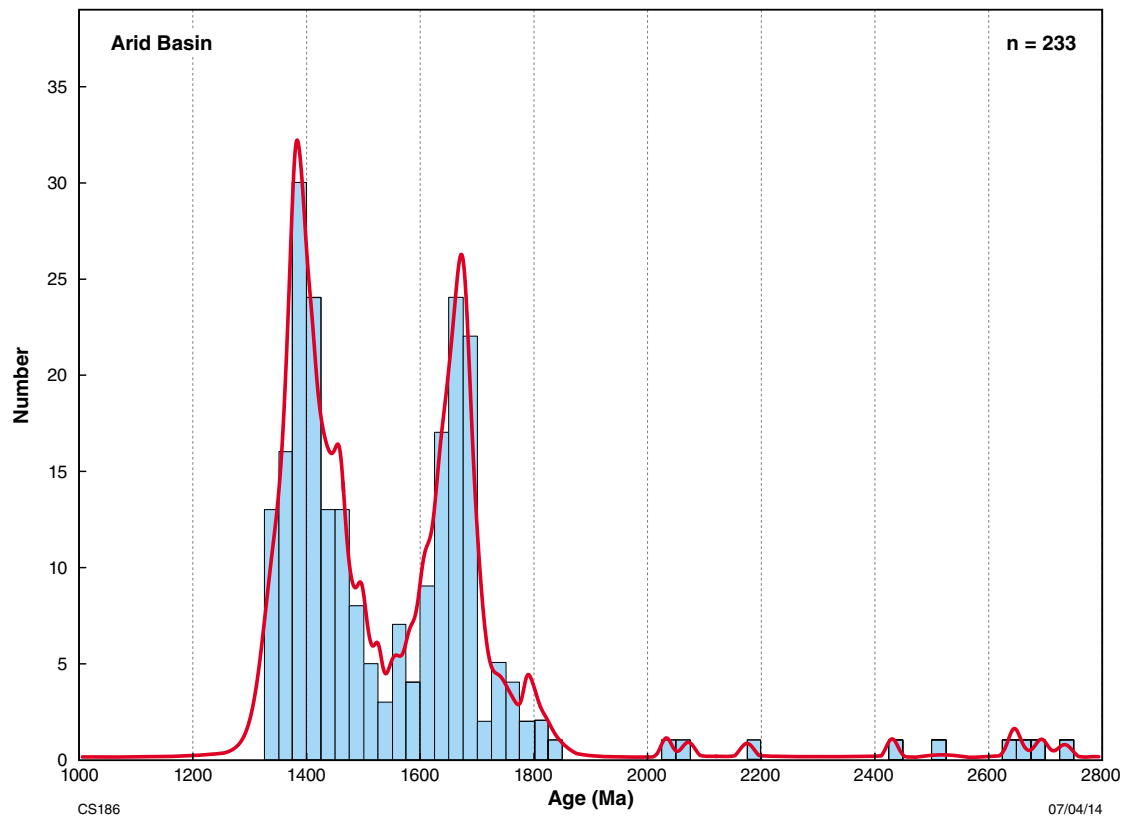


Figure 9b. Probability density diagram and histogram for all detrital zircon data (individual analyses) from the Arid Basin. Additional data source: samples 194867 and 194869 from Adams, 2012. Data are $^{207}\text{Pb}/^{206}\text{Pb}$ ages that are > 95 % concordant.

These results show a striking difference between the provenance of the Barren Basin and that of the Arid Basin. In the Barren Basin, most age components, particularly the dominant ones, can be readily correlated with known sources, such as the Yilgarn Craton and the magmatic rocks of the Biranup and Nornalup Zones. In contrast, the dominant age range of 1425–1375 Ma in the Arid Basin is not recognized at all in the Albany–Fraser Orogen, nor are the flanking age ranges of 1475–1425 Ma and 1375–1325 Ma, with the exception of the oldest known Recherche Supersuite intrusions at c. 1330 Ma (Figs 3, 4, and 9b). From this it is clear that a new source, or sources, had emerged by the time that the Arid Basin was forming.

The second most dominant age range in the Arid Basin of 1700–1650 Ma can be readily correlated with known sources produced by the Biranup Orogeny, which could include both magmatic and metamorphic zircon (e.g. from the migmatitic rocks of the Zanthus Event at c. 1680 Ma; Kirkland et al., 2011a). The flanking age range of 1825–1725 Ma also correlates well with known ages of magmatic rocks of the Tropicana, Biranup, and Nornalup Zones (e.g. granitic rocks dated at 1815–1800 Ma and 1780–1760 Ma; Fig. 3). The Paleoproterozoic detrital zircons may have been sourced directly from these magmatic rocks, indicating they were exposed and eroding at the time, or may also have been recycled from the Barren Basin. However, the most significant detrital zircon age components of the Barren Basin, which are

of Neoproterozoic age ranging from 2750 to 2600 Ma, are the smallest in the Arid Basin, and only occur as single zircons dated at c. 2734, 2694, and 2648 Ma (see earlier in this section). In addition, Paleoproterozoic detrital zircons in the range 2550–1900 Ma constitute a significant component of Barren Basin zircon detritus, but also only occur as single zircons in the Arid Basin (dated at c. 2518, 2430, 2175, 2072, and 2033 Ma). This suggests that recycling of the Barren Basin was minor and, given that the Neoproterozoic zircon detritus in the Barren Basin fits with derivation from the Yilgarn Craton, also shows that input from the adjacent Yilgarn Craton was minimal by this time.

The Ragged Basin

The Ragged Basin represents a restricted sequence of which the only known unit is the Mount Ragged Formation, which is exposed in the eastern Nornalup Zone (Fig. 1). The metasedimentary component of the Salisbury Gneiss, which is exposed on Salisbury Island within the Madura Province (Fig. 1), is regarded as having been deposited at a similar time to the Mount Ragged Formation, between Stages I and II of the Albany–Fraser Orogeny (Clark, 1999; Clark et al., 2000). However, there is little constraint on its depositional age (see below). In addition, the Madura Province and the eastern Nornalup Zone are two distinct tectonic units separated by a major

structure, the Rodona Shear Zone (Fig. 1). Given the above, the Salisbury Gneiss is included in this section, but is not regarded as part of the Ragged Basin.

On Salisbury Island, the Salisbury Gneiss comprises pelitic gneisses and mafic granulite, porphyritic granitic gneiss, and a two-pyroxene metagabbro that is undeformed in its core but deformed and amphibolitic at its margins (Clark, 1999). Outcrops of migmatitic pelitic gneiss contain mesosomes of biotite–sillimanite–garnet–cordierite–feldspar–quartz(–spinel), and leucosomes that are K-feldspar-rich, locally with garnet(–cordierite). These gneisses record granulite-facies metamorphic conditions of approximately 800°C and >5 kbar (Clark, 1999; Clark et al., 2000). Migmatitic leucosome derived from partial melting of the pelitic gneiss yielded dates of 1214 ± 8 Ma (18 core analyses) and 1182 ± 13 Ma (six rim analyses; Clark et al., 2000). The c. 1214 Ma date provides a minimum age of deposition of the pelitic rocks. This date was interpreted as the age of crystallization of the leucosome, whereas the younger date of 1182 ± 13 Ma was interpreted to reflect zircon growth during decompression from peak metamorphic conditions (Clark et al., 2000). A lack of evidence for Stage I metamorphism led Clark (1999) to interpret deposition of the sediments to have occurred after that event.

The Mount Ragged Formation comprises upper-greenschist to lower-amphibolite facies metasedimentary rocks dominated by pale grey, medium-grained, well-sorted, planar cross-bedded quartzite, locally interbedded with pelite or metasilstone (Waddell, 2014; Clark, 1999). Poorly sorted, quartz-pebble conglomerates interbedded with thick layers of well-sorted granular, quartz-dominated gritstones also occur locally (Waddell, 2014). The succession has been interpreted as deposited in a shallow intracratonic basin (Clark et al., 2000), although more recent work has refined this interpretation as a shallow basin fed by a large fluvial system dominated by a shifting complex of sandy braided channels (Waddell, 2014). The sequence is interpreted to gradually coarsen upwards, which implies a distal fluvial environment characterized by channel migration and abandonment evolving to a proximal fluvial environment characterized by rapid periods of sedimentation, producing coarser deposits (Waddell, 2014).

Previously published SHRIMP U–Pb data from the Mount Ragged Formation identified an older detrital zircon component (seven analyses) with a weighted mean age of 1783 ± 12 Ma, a maximum depositional age (12 analyses) of 1321 ± 24 Ma, and a single grain dated at 1261 ± 31 Ma (1 σ) (Clark, 1999; Clark et al., 2000). These data are not sufficient to establish whether the Mount Ragged Formation was distinct from other sedimentary rocks of the Arid Basin. The age of 1321 ± 24 Ma was interpreted as consistent with local derivation from the underlying Recherche Supersuite, and the contact was interpreted as an angular unconformity (Clark et al., 2000). These relationships suggested deposition of the Mount Ragged Formation post-dated Stage I of the Albany–Fraser Orogeny (Clark et al., 2000). Amphibolite-facies metamorphism (4–5 kbar, 550°C) and growth of 1154 ± 15 Ma rutile indicate that these rocks were

buried and metamorphosed during Stage II (Clark et al., 2000). This is further constrained by the undeformed granite intrusion exposed at Scott Rock, recently dated at 1175 ± 12 Ma (preliminary data, GSWA 192586). Aeromagnetic imagery indicates that this granite crosscuts the fold and thrust architecture of the Mount Ragged Formation (Waddell, 2014).

Recently acquired geochronology of detrital zircons from the Ragged Range and The Diamonds Hill nearby support the interpretation that the Mount Ragged Formation is younger than the Arid Basin, and indicate that the maximum depositional age could be as young as 1234 ± 32 Ma (1 σ) (based on a single analysis, preliminary data, GSWA 194875). The same sample yielded the youngest conservative estimate for the maximum age of deposition at 1314 ± 19 Ma (1 σ) (based on 14 analyses). Other samples have also yielded younger, single zircon analyses at 1300 ± 28 and 1290 ± 84 Ma (preliminary data, GSWA 194866 and 194874, respectively). Although sparse, these young single grains appear to occur in all samples, including that of Clark et al. (2000), indicating that deposition took place during the latest part of Stage I of the Albany–Fraser Orogeny, or after it, or both.

The largest detrital zircon age component that includes Stage I ages (1375–1250 Ma in Fig. 10) is dominated by the age range 1350–1325 Ma, coincident with the early part of Stage I. Of note also is the largest detrital zircon age component between 1825 and 1750 Ma, and the scarcity of detrital zircons of both Archean age and Biranup Orogeny age (1710–1650 Ma in Fig. 10). If these sediments were locally sourced from the eastern Nornalup Zone substrate, they suggest that it is dominated by 1750–1825 Ma basement. Alternatively, they could be dominantly recycled zircons from either the Barren or Arid Basin, or both.

Potential source regions of the detritus

Loongana oceanic magmatic-arc, Madura Province

The c. 1400 Ma Loongana intrusion lies to the east of the Albany–Fraser Orogen in the Madura Province (Fig. 11), and is regarded as a potential source of detritus within the Arid Basin. The eastern margin of the Albany–Fraser Orogen is defined by the Rodona Shear Zone, which separates it from the Madura Province. The basement geology of the Madura Province is inferred from geophysical interpretations and sampled only through a small number of exploration drillholes. Interpretations of geochemical data from six diamond drillcores, which are all from an area of roughly 3500 km² located in the central part of the Madura Province (Fig. 11), are discussed below. These include two cores drilled as part of Helix Resources' Loongana Project (LNGD001 and LNGD002; Bunting and McIntyre, 2003) and two cores each at Haig

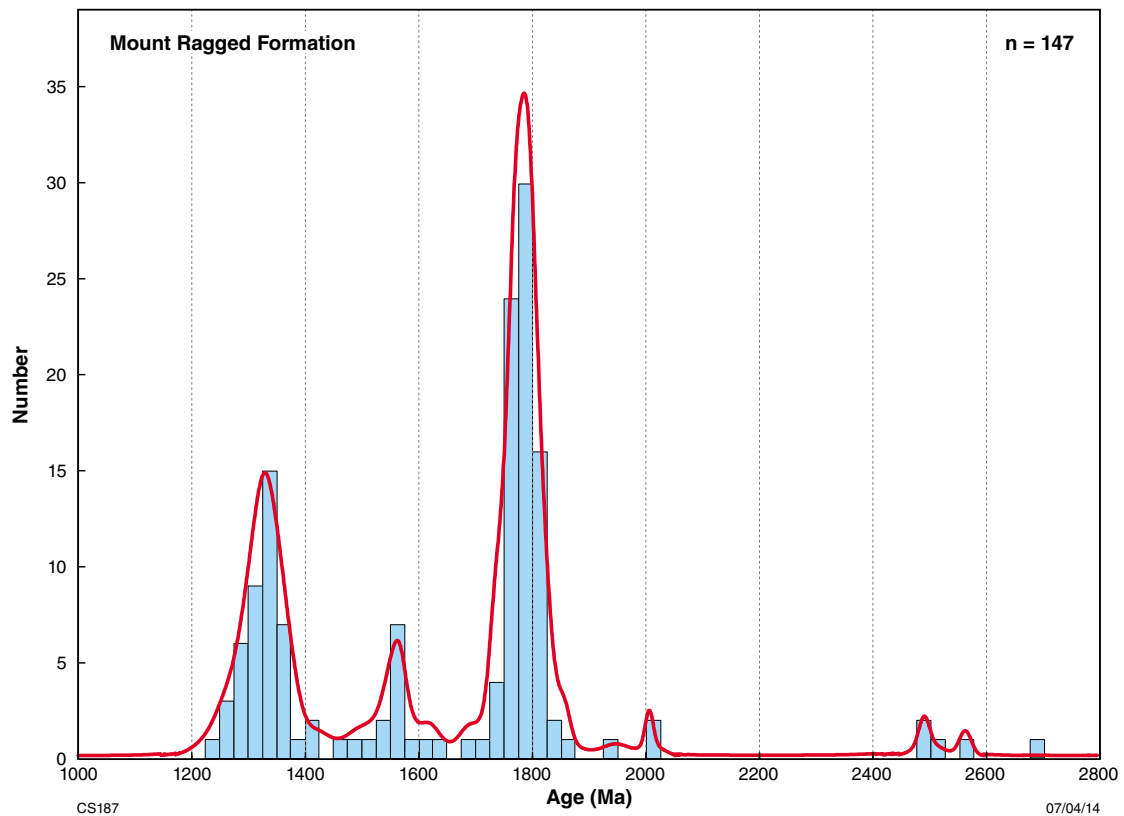


Figure 10. Probability density diagram and histogram of detrital zircon data (individual analyses) from all Mount Ragged Formation samples. Additional data source: sample 9510101 from Clark et al., 2000. Data are $^{207}\text{Pb}/^{206}\text{Pb}$ ages that are > 95 % concordant.

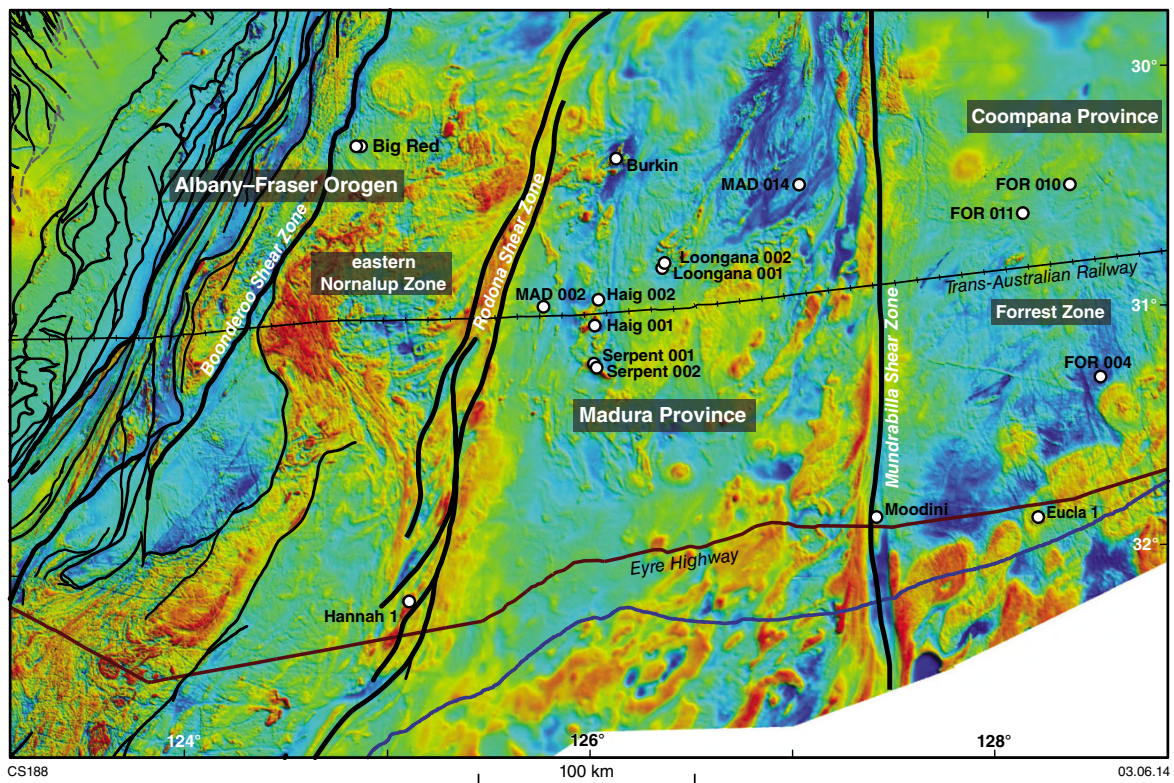


Figure 11. Reduced-to-pole aeromagnetic image over the east Albany–Fraser Orogen and Eucla basement, showing major tectonic units and structures, and the locations of drillhole sites discussed in the text. Note that the Madura Province is not equivalent to the Madura Shelf of the Eucla Basin.

(HDDH001 and HDDH002) and Serpent (SDDH001 and SDDH002), drilled as part of Teck Australia's Eucla Project and co-funded through the Exploration Incentive Scheme (EIS) (Tillick, 2011; Tillick and Hunt, 2010). The interpretations suggest that the Loongana intrusion represents part of an oceanic-arc, which has implications for the way in which sediment may have been derived from such a source. A list of samples used in this analysis can be found in Appendix 3.

Weakly layered, medium-grained, mafic cumulate rocks form the basement lithology at the Serpent prospect. They also greatly dominate the basement geology defined by the two Haig cores, but here are intruded by medium- to coarse-grained trondhjemitic plagiogranite (Figs 12a,b). Each of the drillcores for both Haig and Serpent sample geochemically distinct mafic cumulate rocks, indicating that distinct intrusive chambers were sampled. The two drillcores from Loongana cannot be distinguished from each other on the basis of lithological variation or geochemistry, although relatively few samples were taken from LNGD002. This indicates at least five, geochemically distinct mafic intrusive bodies. In Loongana core LNGD001, the upper portion of the basement component is dominated by weakly layered, medium-grained, mafic cumulate rocks but also includes an approximately 13 m thick interval of medium-grained, peridotitic cumulate rocks (Fig. 12c). The lower part of the basement component is dominated by medium- to coarse-grained trondhjemitic plagiogranite (Fig. 12d), which is also the dominant lithology in LNGD002.

U–Pb zircon dating of plagiogranite and gabbro from the Loongana intrusion indicates the mafic and felsic components were synchronous between c. 1410 and 1400 Ma, which is consistent with observed contact relationships. Fine-grained, equigranular, unfoliated biotite microtonalite from LNGD0001 yielded a magmatic crystallization age of 1408 ± 7 Ma, identical to the igneous crystallization age of 1407 ± 7 Ma obtained for medium- to coarse-grained, foliated biotite tonalite gneiss taken from the same core (GSWA 178071 and 178072). Recently dated tonalitic gneiss from LNGD002 yielded a magmatic crystallization age of 1411 ± 6 Ma (Fig. 12e; GSWA 192558). Metagabbro from the same core yielded a date of 1403 ± 6 Ma, interpreted as the magmatic crystallization age, and although unlikely, the possibility that it represents a metamorphic age cannot be ruled out (Fig. 12f; GSWA 192557). A sample of amphibolite, also from LNGD0002, yielded a magmatic crystallization age of 1415 ± 7 Ma (GSWA 178070). It is unclear whether the material dated represents the mafic or felsic component of that section of core, although mingling textures suggest that the two phases were coeval. Neither the Serpent nor Haig cores have been dated isotopically, but their geochemical affiliations suggest they are part of the same magmatic event, and are therefore likely to be close in age to the Loongana intrusion.

The compositional variation of the mafic to ultramafic cumulate rocks typically involves processes of Fe- and Ti-enrichments, and all of these cumulate bodies are derived from low- to medium-K, tholeiitic parental magmas. Trace-element variations identify two main compositional groups. The processes involved in producing the

distinct compositions can be rationalized within the Th/Yb – Nb/Yb projections described by Pearce (2008). The first group contains a single gabbro body (Haig 1) with low Th/Nb ratios (and low Th/Yb and Nb/Yb) lying close to mid-ocean ridge basalt (MORB) values and reflecting a depleted mantle source (Fig. 13). The second group contains the remaining four gabbro and gabbro-peridotite bodies. On a diagram of Th/Yb versus Nb/Yb these four bodies collectively form a trend that parallels the array for uncontaminated, mantle-derived melts (the mid-ocean ridge basalt–ocean island basalt (MORB–OIB) array; Pearce, 2008), but at Th/Nb ratios significantly higher than those expected of uncontaminated mantle-derived melts (Fig. 13). The MORB–OIB array-parallel trends individually shown by, for example, the gabbro from Loongana, most likely reflect mineralogical variations alone, at constant Th/Nb ratios, as these bodies comprise generally cumulate mineralogies. However, there is no indication that the overall trend collectively shown by the bodies has been influenced by interaction with continental crustal material, which produces trends to significantly elevated Th/Nb ratios (Fig. 13). Thus, this trend is best interpreted in terms of individual magma batches derived via different degrees of partial melting of a subduction-enriched mantle source with a narrow range of Th/Nb ratios. The difference between the two groups is also seen on a plot of V versus Ti (Fig. 14), which can be used to distinguish V-enriched basalts of (oceanic) arcs from non-subduction related basalts (e.g. Shervais, 1982). Thus, in terms of their ranges in Th/Nb and V/Ti ratios, it can be suggested that the Group 1 gabbro (Haig 1) was derived from a depleted mantle source with little or no prior subduction enrichment, whereas the magmas forming the other gabbro-peridotite bodies were most likely derived from a subduction enriched mantle source. The spatial and temporal association of basalts from such diverging mantle source regions is not uncommon in arc environments (e.g. Pearce, 2008).

Plagiogranites are associated with gabbros at Loongana and Haig. They have high SiO₂ (66–77 wt%), Na₂O (3.1 – 4.8 wt%) and CaO (2.1 – 6.4 wt%) and very low K₂O (generally < 1 wt%) (Fig. 15). Their composition is typical of felsic magmas associated with the formation of oceanic magmatic-arcs (e.g. Leat et al., 2006) and this is consistent with their very juvenile Hf- and Nd-isotopic compositions (ϵ_{Hf} values in zircon of -2.5 to +11.5, with a median of +7.8 at 1400 Ma [see Hf isotope fingerprints of detrital zircons section]; whole-rock ϵ_{Nd} of +1.3 to 1.9 at 1400 Ma). This lends strong support to a suggestion that the small amount of material so far sampled from the Madura Province most likely formed between c. 1410 and 1400 Ma in an oceanic magmatic-arc setting, with little contribution from continental material. The validity of these isotopic and whole-rock geochemistry interpretations, and the extent of the oceanic magmatic-arc in the Madura Province, remains to be tested.

Interestingly, the available Nd-isotopic data from both gabbroic and plagiogranitic rocks of the Madura Province show a crustal evolution trend that strongly contrasts with that of the Albany–Fraser Orogen, but overlaps the main basement evolution trend for the Musgrave Province to the northeast (Fig. 16).



Figure 12. Photographs of drillcore from the Loongana and Haig prospects showing: a) weakly layered medium- to coarse-grained gabbro from Haig (HDDH001); b) fine- to medium-grained gabbro from Haig (HDDH001); c) medium-grained gabbro, including a layer of cumulate-textured olivine-rich gabbro (brown-stained rock), from Loongana (LNGD001); d) plagiogranite intrusions within fine- to medium-grained gabbro from Loongana (LNGD001); e) dated tonalitic gneiss sample GSWA 192558 in Loongana core (LNGD002); f) dated metagabbro sample GSWA 192557 in Loongana core (LNGD002).

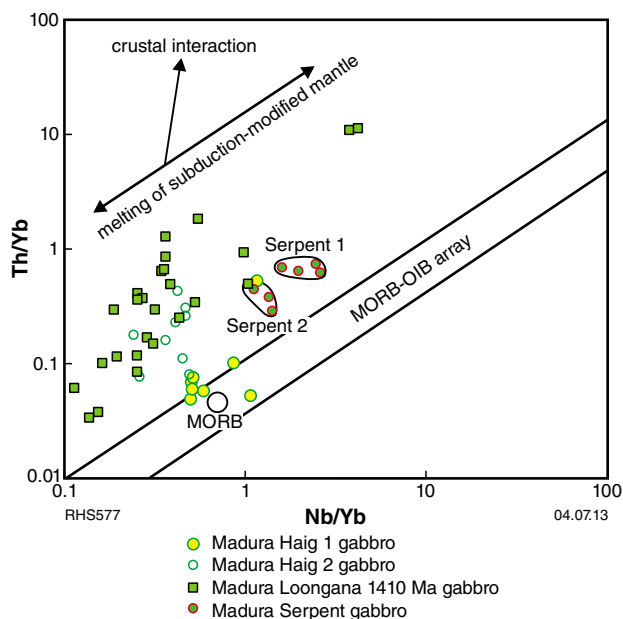


Figure 13. Log plot of Th/Yb vs Nb/Yb (after Pearce, 2008). MORB–OIB array defines the field for uncontaminated sources or magmas of mantle origin. Serpent 1 = SDDH001 core; Serpent 2 = SDDH002 core; Haig 1 = DDH001 core; Haig 2 = DDH002 core. Loongana gabbro data is from both Loongana cores.

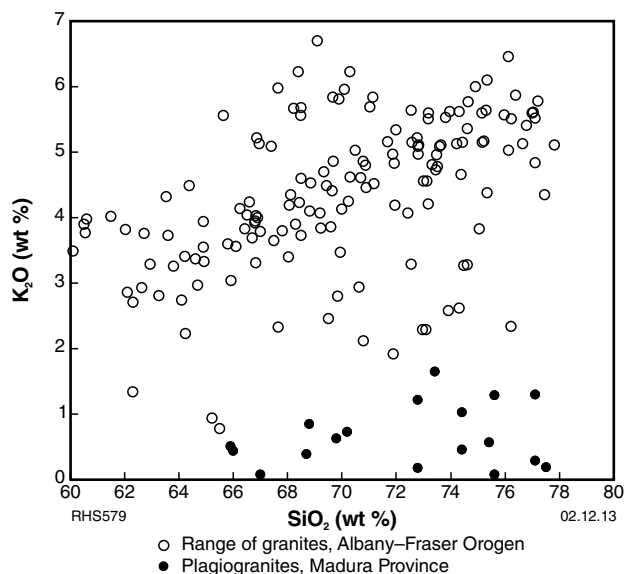


Figure 15. Plot of SiO₂ vs K₂O showing the distinct compositional differences between the ‘oceanic’ plagiogranites of the Madura Province and (for example) the range of granites of varying age from the Albany–Fraser Orogen.

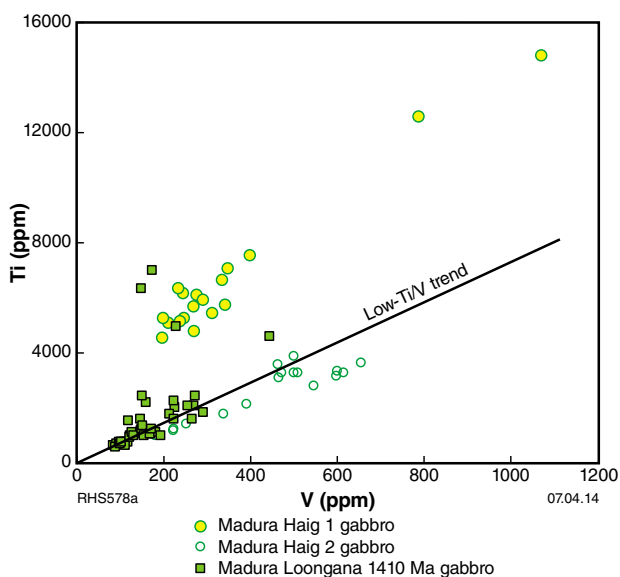


Figure 14. Plot of V (ppm) vs Ti (ppm) distinguishing low Ti/V mafic rocks crystallized from magmas of probable subduction-zone origin from those derived from a mantle source not modified through subduction processes.

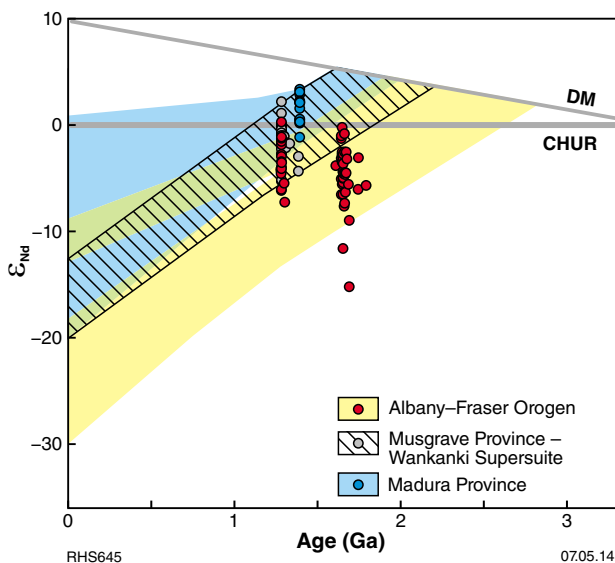


Figure 16. Nd-isotopic evolution diagram comparing the isotopic evolution of magmatic components of the Albany–Fraser Orogen with those of equivalent aged igneous rocks from the Musgrave and Madura Provinces.

Based on these trends, the suggestion that the Musgrave Province and the Albany–Fraser Orogen evolved over a common basement (Smits et al., 2014) is untenable. However, it is plausible that the Musgrave Province formed on Madura Province basement.

Hf isotope fingerprints of detrital zircons

Methodology

Most sedimentary provenance investigations are based on similarities in detrital zircon age components, which are used to draw interpretations on palaeogeographic settings (e.g. Fedo et al., 2003). This approach is effective, yet it has some limitations because zircon growth events may not be distinctive to specific terranes and, importantly, zircon growth events do not necessarily correspond to the time of crust formation, which may form a unique signature of a particular crustal block. These limitations can, to some extent, be circumvented by using additional isotope data, such as Lu–Hf, that provide information on the crustal evolution of the source region (Howard et al., 2009).

The crystallization of zircon in any geological environment results in extreme fractionation of Lu/Hf between zircon and other coprecipitating minerals. The fractionation of Lu/Hf, such as through extraction from the mantle into the crust, is the basis of model-age calculations. Depleted mantle model (T_{DM}^2) ages, calculated using the measured $^{176}\text{Lu}/^{177}\text{Hf}$ of the zircon, provide only the minimum age for the source material of the magma from which the zircon crystallized. Therefore, the model ages described below are two-stage model ages (T_{DM}^2), which are a better estimate of the source age. The use of T_{DM}^2 assumes that a zircon grain's parental magma was produced from a volume of average continental crust ($^{176}\text{Lu}/^{177}\text{Hf} = 0.015$) that itself was originally derived from the depleted mantle (e.g. Griffin et al., 2004; Kirkland et al., 2012j). See Appendix 4 for details of Lu–Hf analytical methods.

Barren Basin

The Fly Dam Formation contains detrital zircons with crystallization ages averaging c. 1660 Ma, with a relatively restricted array of ϵHf values ranging from -5 to +6, corresponding to model ages (T_{DM}^2) of 2.0–2.7 Ga (Fig. 17). Both the age and isotope signature of this formation are identical to those of the magmatic rocks of the Biranup Zone, overlapping the field of most frequently observed values in this lithotectonic unit.

The psammitic gneiss from Ponton Creek has a unimodal zircon age component of c. 1690 Ma and indicates an ϵHf array of -6 to 0, with a single outlier at -12, corresponding to model ages (T_{DM}^2) of 2.4–2.8 Ga (and an outlier at 3.2 Ga) (Fig. 17). Both the age and Hf isotope signature of these detrital zircons are closely similar to magmatic crystallization ages and Hf isotope compositions in the Biranup Zone, and also in detrital zircons of the Fly Dam Formation.

The Lindsay Hill Formation yielded mainly Neoproterozoic zircons, in the range 2750–2600 Ma. These zircons indicated a relatively small range in Hf isotope composition with an ϵHf range of approximately -5 to +4, and model ages (T_{DM}^2) averaging 3.1 Ga (Fig. 17). Both the age and Hf isotope signature of this Archean component is closely similar to that from the Yilgarn Craton and more specifically, they overlap in age and Hf composition with many intrusive rocks from the Kalgoorlie Terrane (Fig. 17), as well as with Archean inherited components in Biranup Zone magmatic rocks. The c. 1800 Ma detrital component in GSWA 182416 yields an array that ranges from Hf isotope compositions similar to the Biranup Zone to more evolved values similar to compositions recognized in the Big Red paragneiss.

The Big Red paragneiss samples (GSWA 182475 and 182473) contain a significant proportion of Archean detrital zircons. The Hf isotope signatures of these samples can be conveniently considered in terms of three age groups (Groups 1, 2, and 3; Fig. 17). The first group consists of zircons with ages > 2700 Ma that define an evolution array corresponding to a $^{176}\text{Lu}/^{177}\text{Hf}$ ratio of 0.011 and a mantle extraction age (assuming it does not reflect a mixture of sources) of 3.5 Ga (Fig. 18).

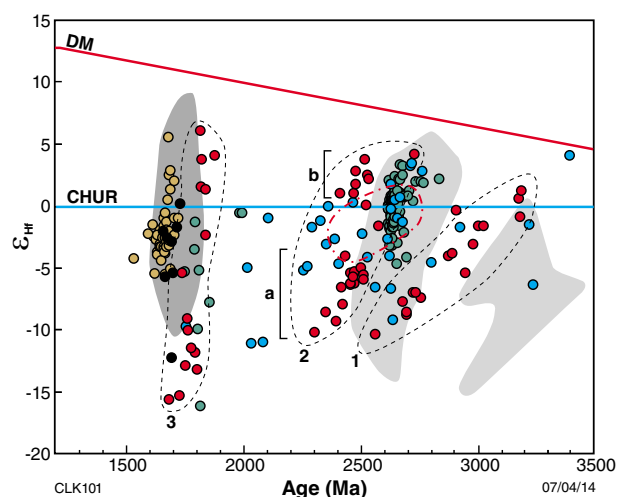


Figure 17. Hf evolution diagram for detrital zircons from the Barren Basin. Light grey fields denote the age and isotopic composition of magmatic zircons in the Yilgarn Craton (Wyche et al., 2012). Dark grey field denotes the age and isotopic composition of magmatic zircons in the Biranup Zone (Kirkland et al., 2011b; 2012j). Red dash-dot field denotes the age and isotopic composition of the Halfway Gneiss (Johnson et al., 2011b). Blue symbols indicate the Coramup Gneiss (GSWA 184122). Red symbols indicate the Big Red paragneiss (GSWA 182473 and 182475). Green symbols indicate Lindsay Hill Formation metaconglomerate (GSWA 182416) and quartzite (GSWA 182405). Black symbols indicate Ponton Creek psammitic gneiss (GSWA 194731). Brown symbols indicate psammitic gneiss and leucosome (GSWA 194742) and semipelitic gneiss (GSWA 194743) of the Fly Dam Formation. DM indicates model depleted mantle. CHUR indicates model bulk silicate earth. See text for further explanation.

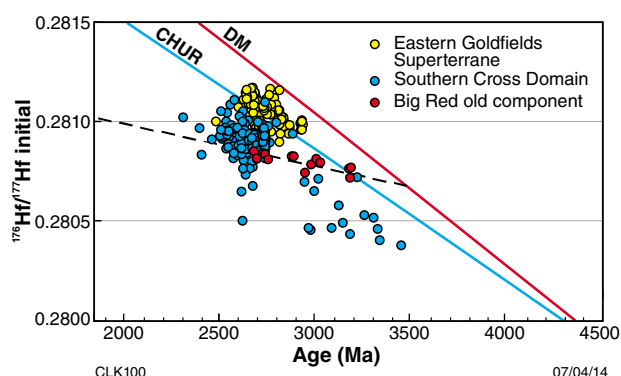


Figure 18. Initial Hf evolution plot for Group 3 analyses in the Big Red paragneiss (GSWA 182473 and 182475, red symbols). The age and isotopic composition of Yilgarn Craton components are indicated. A reference isotopic evolution line corresponding to a $^{176}\text{Lu}/^{177}\text{Hf}$ ratio of 0.011 is shown (dashed line), which is defined by >2700 Ma detrital zircon grains in the Big Red paragneiss. The red line is model depleted mantle (DM) and the blue line is CHUR.

This array is somewhat more radiogenic than an old evolved array within the Southern Cross Domain of the Yilgarn Craton. It may reflect a recycled Archean crustal source distinct from the Yilgarn Craton, or alternatively, an unrecognized younger, deep basement source from the eastern part of the Eastern Goldfields Superterrane. The $^{176}\text{Lu}/^{177}\text{Hf}$ ratio is consistent with the development of continental crust at 3.5 Ga in the source region of this detritus. Similar ages of crust formation are recognized in the Gawler Craton and interpreted to indicate that the earliest period of crustal growth in this region occurred during the Paleoproterozoic (Nebel et al., 2007; Belousova et al., 2009).

The second detrital zircon age group in these samples, c. 2600 to 2300 Ma, yields a scattered isotope array of ϵHf values of -10 to +4 (Fig. 17), which can be characterized by two isotope signatures (Groups 2a and 2b; Fig. 17). An evolved component in this age group clusters around a crustal residence age of c. 3.2 Ga (Group 2a), and could have formed from reworking of crust with an Hf isotope composition similar to that of the Southern Cross Domain of the Yilgarn Craton (Fig. 17). A more radiogenic component in this age group lies around an isotope evolution line of c. 2.8 Ga crust (Group 2b). Similar sources are recognized within the Eastern Goldfields Superterrane of the Yilgarn Craton, which could imply crustal reworking of this source at 2.5 – 2.4 Ga. Magmatic zircon ages similar to the detrital ages within the Big Red paragneiss have been recognized within the Halfway Gneiss of the Glenburgh Terrane, whose igneous protoliths have crystallization ages between 2555 and 2430 Ma (Johnson et al., 2011b). The Halfway Gneiss has ϵHf values that define a broad group between -5 and +4. This signature lies within a distinct gap in isotope compositions for the Big Red paragneiss. This observation suggests that the zircons of the Halfway Gneiss, although of similar age, did not contribute to the detrital population of Big

Red paragneiss.

The third detrital age component is characterized by ϵHf values of +6 to -16 at 1800–1700 Ma. The radiogenic end of this array overlaps with the age and isotope composition of magmatic rocks of the Biranup Zone. The evolved end of this array lies on a normal crustal evolution line from the most radiogenic component recognized in the second age group (Group 2b) from this migmatitic paragneiss, that is, a component with a 2.8 Ga crustal residence age. This could indicate that a 2.8 Ga piece of crust was reworked at c. 2.5 Ga, and then again at c. 1.8 Ga.

Coramup Gneiss sample GSWA 184122 contains significant age components at c. 2357, 2263, and 2031 Ma, and is characterized by a very wide range of detrital zircon ages and isotope values (Fig. 17). The most evolved zircons have an age of c. 2040 Ma and an ϵHf value of -11, whereas the most radiogenic zircons have an age of c. 3390 Ma and an ϵHf value of +4, which is close to depleted mantle values (Fig. 17). The wide range in age and isotopic character for this sample indicates a heterogeneous source, possibly in the hinterland, or multiple reworking of various crustal blocks. The mode for model ages (T_{DM}^2) is c. 3.0 Ga, with other significant model-age components between 3.5 and 3.1 Ga. The majority of results can be explained by reworking of Yilgarn-like source material at various times.

In addition to the comparison of detrital zircon ages in the Barren Basin we compare their model-age distributions (Fig. 19). The model-age (T_{DM}^2) distributions reflect not only the time of crust formation, but also include mixed ages that stem from the process of source-component mixing within magmatic systems (e.g. Smithies et al., 2011). Nonetheless, similar pieces of crust could reasonably be expected to share some degree of similarity in their model-age distributions (e.g. Johnson et al., 2011b). Excluding samples from the Big Red paragneiss (GSWA 182475 and 182473), all other samples indicate model-age modes at c. 3.1 Ga and 2.6 Ga, which can be readily linked to corresponding model-age modes recognized within magmatic zircons of the Eastern Goldfields Superterrane and the Biranup Zone, respectively.

Arid Basin

The 1305–1290 Ma Fraser Range Metamorphics contain pelitic, semipelitic, and psammitic metasedimentary rocks of the Mesoproterozoic Snowys Dam Formation, assigned to the Arid Basin. The Hf isotope values from the samples analysed (GSWA 177910, 194777 and 194714) define three distinct source-component arrays. The first array includes ϵHf values of -10 at 1300 Ma and extends back to ϵHf -2 at c. 1800 Ma (Fig. 20, area 1). This is consistent with reworking of a Biranup Zone source during several melting events during the Proterozoic. The second array includes ϵHf values of +12 to -2 between c. 1300 and 1600 Ma, and reflects a vertical mixing trend between highly radiogenic and CHUR-like components (Fig. 20, area 2). This mixing array encompasses the age and isotope composition of magmatic rocks in the c. 1410 Ma Loongana intrusion (see Loongana oceanic magmatic-arc, Madura Province section), and is consistent

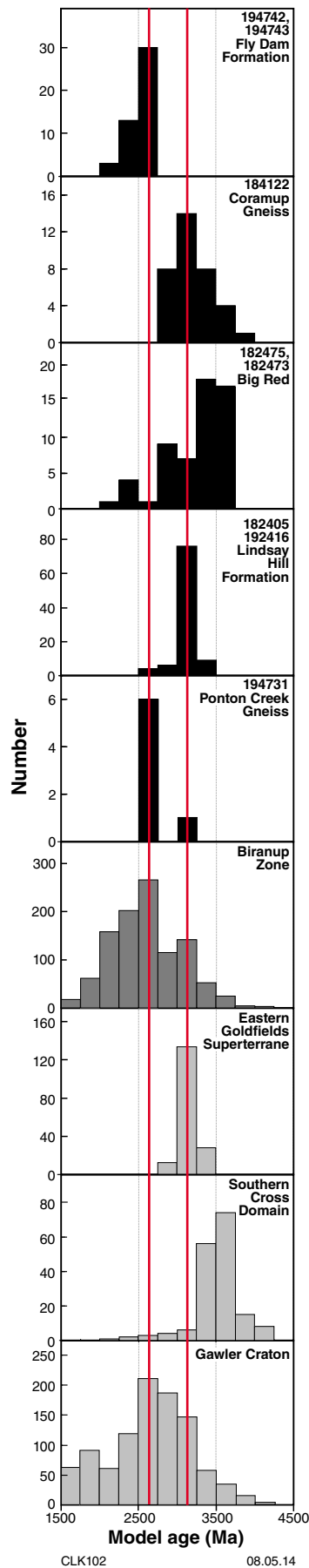


Figure 19. (left) Histograms of T_{DM}^2 model ages from components of the Barren Basin and potential cratonic or lithotectonic sources. Yilgarn Craton components are from Wyche et al. (2012), Biranup Zone from Kirkland et al. (2011b; 2012j); Gawler Craton from Belousova et al. (2009). Red vertical lines denote model-age peaks which are likely to correlate between source and basin, and may reflect real crust formation episodes (see text for more details). GSWA sample numbers are shown where relevant.

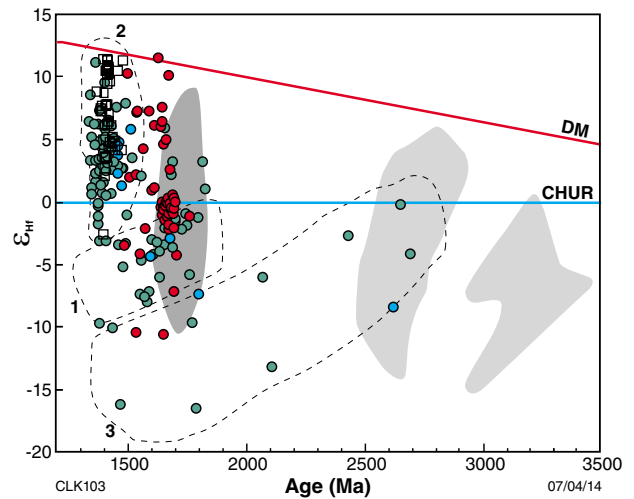


Figure 20. Hf evolution diagram for detrital zircons from the Arid Basin. Light grey fields denote the age and isotopic composition of magmatic zircons in the Yilgarn Craton (Wyche et al., 2012). Dark grey field denotes the age and isotopic composition of magmatic zircons in the Biranup Zone (Kirkland et al., 2011b; 2012j). Green symbols indicate the Snowys Dam Formation (GSWA 177910, 194777, and 194714). Red symbols indicate the Gwynne Creek Gneiss (GSWA 182431, 182432, and 194735). Blue symbols indicate the Malcom Metamorphics (GSWA 194867, 194869, and PM1 [Adams, 2012]). Unfilled squares indicate the Loongana intrusion, Madura Province (GSWA 178070, 178071, and 178072). DM indicates model depleted mantle. CHUR indicates model bulk silicate earth. See text for further explanation.

with a significant detrital component being derived from this material. The third array includes ϵ_{Hf} values of -16 at 1465 Ma and extends back to CHUR-like values at c. 2700 Ma (Fig. 20, area 3). This evolution array is consistent with reworking of Archean Yilgarn-like rocks.

Hf isotope values for samples of the Gwynne Creek Gneiss (GSWA 182431 [preliminary data], 182432 and 194735) range from $\epsilon_{Hf} +11$ at 1626 Ma to -10 at 1650 Ma, with a mode of CHUR-like values at 1700 Ma (Fig. 20). Zircons from Gwynne Creek Gneiss sample GSWA 182431 are mainly metamict and show no catholuminescence (CL) response. Analyses of these zircons yield variable $^{207}\text{Pb}^*/^{206}\text{Pb}^*$ dates of c. 1700 to 1400 Ma, and indicate high uranium contents and low calculated grain densities.

The U–Pb data from GSWA 182431 define a discordia with an upper intercept of 1683 ± 89 Ma and a lower intercept of 1450 ± 76 Ma, interpreted to reflect variable ancient Pb-loss from a c. 1683 Ma protolith, consistent with the metamict nature of these zircons. Nonetheless, the Lu–Hf isotope system is well known to be more robust than the U–Pb system (Scherer et al., 2001) and for all Gwynne Creek Gneiss samples yields Hf isotope compositions consistent with the primary source being Biranup Zone material or its remelted equivalents. Only two analyses from the Gwynne Creek Gneiss sample indicate values less radiogenic than Biranup Zone magmas. This implies minimal influence of the unmodified Archean hinterland in the source of this detritus.

Siliciclastic metasedimentary rocks of the Malcolm Metamorphics contain detrital zircons strongly influenced by metamorphism, causing new zircon growth and radiogenic-Pb loss. Due to the pervasive overprinting, robust ages of detrital material in these samples are few. Nonetheless, a limited number of analyses interpreted to reflect detrital zircon ages yields ϵ_{Hf} values of +4.5 at 1455 Ma to -8 at 2622 Ma (Fig. 20). This scattered dataset includes components which lie well within the fields of the three crustal sources previously defined by the Snowys Dam Formation, indicating a similar provenance for the Malcolm Metamorphics.

The Arid Basin samples indicate model-age modes at c. 2.5 Ga and 2.0 Ga (Fig. 21), which can be readily linked to corresponding model-age (T_{DM}^2) modes recognized within magmatic zircons of the Biranup Zone and the Loongana oceanic magmatic-arc of the Madura Province.

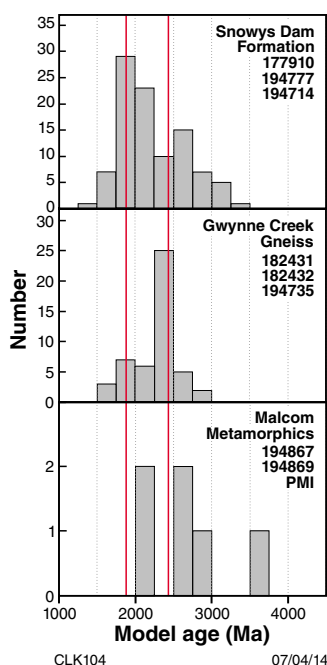


Figure 21. Histograms of T_{DM}^2 model ages from components of the Arid Basin. Red lines reflect the model age median in the Loongana intrusion in the Madura Province at c. 1.7 Ga (GSWA 178070, 178071, and 178072) and in the Biranup Zone at c. 2.5 Ga.

Basin evolution and tectonic setting

Barren Basin

In conjunction with the geochronology data from the Stirling Range Formation (Rasmussen et al., 2002), the extensive geochronology dataset investigated here (Table 2; Fig. 7a,b) implies that the Barren Basin had substantial lateral and outboard extent. Regarding all units as part of the same basin system, albeit one that evolved over a period of more than 200 million years (1815–1600 Ma), the implication is that the Barren Basin spanned at least 1000 km along the southern and southeastern Yilgarn Craton margin. The presence of the Big Red paragneiss, which is located over 100 km southeast of the bounding fault to the Yilgarn Craton (the Cundeelee Fault), suggests the Barren Basin was at least 50 km wide, based on removing the younger Fraser Zone, but not accounting for any shortening effects. The units of the Barren Basin are therefore interpreted to be the structural and erosional remnants of a much larger basin system that evolved along, and in the distal reaches of, the southern and southeastern Yilgarn Craton margin during the late Paleoproterozoic.

At least three main depositional phases are recognized, each closely following magmatic events (Fig. 3). The first commenced prior to c. 1800 Ma with deposition of the Stirling Range Formation, followed by deposition of the Mount Barren Group by 1693 ± 4 Ma (Vallini et al., 2005), and deposition of the sedimentary precursors of the Coramup Gneiss, the Ponton Creek psammitic gneiss, Big Red paragneiss, and the Lindsay Hill Formation between 1710 and 1650 Ma, coincident with the Biranup Orogeny (Table 2). This was followed shortly afterwards by deposition of the Woodline and Fly Dam Formations, possibly in the late stages of, or shortly after, the Biranup Orogeny. The magmatic episodes appear to have provided substantial amounts of detritus to the basin system, much of which was mixed with detritus sourced from the Yilgarn Craton. Collectively, these depositional phases are termed Cycle 1, corresponding with the first recognized significant period of basin formation in the Albany–Fraser Orogen. There appears to have been a close link in the timing between depositional phases and pulses of magmatism, potentially indicative of relatively rapid, cyclical uplift and erosion releasing detritus into the evolving basin system. Although not well constrained regionally, coeval volcanism (e.g. the Voodoo Child Formation in the Tropicana Zone) may also have supplied detritus to the basin.

Understanding the evolution of a Paleoproterozoic basin system, such as the Barren Basin, is problematic because exposure is limited due to younger cover and regolith, and because the basin units are mostly preserved as structural remnants in Mesoproterozoic thrust sheets. This makes it difficult to reconstruct the basin architecture through time. However, it is possible to suggest a framework and model that can be tested by making an assessment of which basin features can be identified. These include the type of basin

fill and the sequence over time, sediment provenance (including recognition of any exotic sources), distinction of depositional substrates, and knowledge of coeval magmatic products and their potential for providing heat to the substrate. It is also important to recognize that there is considerable overlap between different basin features from different tectonic settings, and that the final basin architecture will depend on many tectonic factors, such as the state of stress of the crust over time, changes in crustal thickness, thermal effects, and the potential for dynamic topography related to mantle upwelling or lithospheric underplating (Allen and Allen, 2005; Rosenbaum et al., 2008).

Significance of the basin fill

The majority of sedimentary units of the Barren Basin comprise quartz-rich lithologies including cross-bedded sandstones, pure sandstones (now quartzites), pebbly sandstones, and siltstones (Table 2). For the most part, the preserved units indicate moderate to high energy, fluvial to shallow marine (tidal or deltaic) conditions, indicative of broad, relatively shallow basins. However, a potential bias may exist due to the dominance of units sampled on, or adjacent to, the Yilgarn Craton. The Big Red paragneiss, the farthest outboard Barren Basin unit, is interlayered with metamorphosed iron-rich layers, perhaps indicative of a deeper marine setting. However, the degree of metamorphic overprint and limited occurrence of this unit in drillcore makes such an interpretation difficult. The interbedded sandstone and mudstone protoliths of the Fly Dam Formation were potentially deposited as turbidite flows, which would also be indicative of a deeper marine setting. There is no indication of deposition of this unit onto the Yilgarn Craton substrate (Table 2), so the Fly Dam Formation may also have been deposited farther outboard and carried towards the craton within thrust sheets. The relationships suggest on- or near-craton fluvial to shallow marine deposition, with the basin system gradually deepening away from the craton as time progressed (from c. 1727 Ma, based on the conservative estimate of the maximum depositional age of the Big Red paragneiss). It is difficult to assess whether coeval volcanism made a large contribution to the basin fill, with the only known example being the dacitic rocks of the Voodoo Child Formation (Less, 2013). In addition, the Ponton Creek psammitic gneiss may also have a volcanic protolith, based on its c. 1690 Ma unimodal detrital zircon population (GSWA 194731).

One of the best preserved, most studied, and more informative units is the Mount Barren Group (see Mount Barren Group section). The type of fill, interpreted depositional settings, and overall fining-upward sequence is consistent with a continental rift basin. At the initiation of rifting, sedimentation is typically non-marine, arkosic, fluvial, lacustrine, and eolian (Allen and Allen, 2005, p. 328). The lithology of the lowermost unit, the Steere Formation, which is a basal conglomerate overlain by pebbly sandstone and dolomitic limestone, supports this interpretation (Thom et al., 1977, 1984a). Overlying this is the Kundip Quartzite, which contains sedimentary

structures such as cross-bedding and ripple marks indicative of deposition in shallow, near-shore marine to tidal-sandflat conditions (Vallini et al., 2002; Witt, 1997). The change in setting is consistent with an evolving rift basin which began to deepen, allowing marine incursions due to fault-controlled subsidence to occur at a greater rate than sedimentation (e.g. Allen and Allen, 2005, p. 328). The Kundip Quartzite is overlain by a 26 m thick, thinly bedded, medium- to coarse-grained sandstone and carbonaceous shale (Vallini et al., 2002, 2005), which is overlain by thinly bedded pelitic and psammitic rocks of the Kybulup Schist (Thom et al., 1977, 1984a). Sparse outcrops of dolostone and calc-silicate schist suggest the presence of carbonate banks surrounded by deeper-water sediments (Witt, 1997), consistent with the continuation of deepening in an evolving rift basin setting. Although unconstrained in age, it is feasible that the Cowerdip Sill represents mafic to intermediate magmatism related to crustal thinning of the basin substrate onto which the Mount Barren Group was deposited.

Fining upward is the opposite pattern to what would generally be expected in a foreland basin, where the early sequences are commonly deeper water, fine-grained sediments or turbidites (e.g. flysch deposits), possibly with shallow-water carbonates near the flexural forebulge. These are overlain by coarser grained, continent-derived sediments supplied by the orogenic front or mountain chain as it evolves (e.g. molasse deposits, Allen and Allen, 2005, p. 341). The overall maturity of the Barren Basin fill, and the lack of significant quantities of exotic material, are inconsistent with the presence of a magmatic arc, so a fore-arc basin is also considered unlikely. Equally, the lack of any exotic material, or evidence of another terrane, does not favour a collisional setting. Although it is clear that many factors affect basin fill, and that it cannot solely define tectonic setting, the indications are that the Barren Basin fill is most consistent with a continental rift basin, or perhaps a back-arc basin that was a significant distance from the plate margin and subduction zone.

Barren Basin evolution

Factors affecting basin evolution

Understanding basin formation and setting is dependent on constraining several critical factors, such as type of substrate, proximity to a plate margin, type of plate motion, type of basin fill, basin-forming tectonic mechanisms that control basin locations, and basin-modifying tectonic processes such as ongoing deformation and magmatism.

Based on the field relationships (see the Barren Basin section; Table 2), and the age and isotope signature of the detritus, it is clear that the substrate to the Barren Basin was a combination of Yilgarn Craton and Biranup and Nornalup Zone crust. This is also supported by the strong link between the Paleoproterozoic magmatic history and the interpreted provenance of the detritus. These factors imply a continental crustal substrate to the Barren Basin, linked to the Yilgarn Craton. The distance to a plate margin is more difficult to assess, but given the maturity

of the detritus, and the fact that only small components of the detritus cannot be readily explained by known local sources, the indications are that no exotic crustal elements were in the vicinity, and hence the plate boundary was some distance away. However, if a convergent margin setting is applicable, one could argue that any exotic fill could be blocked by the subduction zone trench.

The type of plate motion is equally challenging to assess, particularly as it is difficult to recognize any plate boundary, and because Paleoproterozoic structures are strongly overprinted by high-temperature Mesoproterozoic fabrics in most areas. An exception is the folding produced during the c. 1680 Ma Zanthus Event, which indicate a short period of northeast-southwest shortening (present-day orientation; Kirkland et al., 2011a). The regional extent of this event is unknown, but it most likely occurred during a short time span, signifying a period of compression within an overall, larger scale extensional system. The long-time interval of basin formation, spanning 1815–1600 Ma, is more indicative of a dominantly extensional regime, at least in the upper crust. This may have been linked to plate divergence, although extension may also have occurred in an overall convergent setting, such as in a back-arc linked to a retreating subduction zone (e.g. Schellart and Rawlinson, 2010).

One of the major factors to have clearly affected the formation of the Barren Basin is magmatism, which was dominantly felsic in character and persisted during much of the basin history (Fig. 3). Given the long time span of basin formation, the effect of contributions from radiogenic heat production from the felsic intrusions on the crustal thermal regime should be assessed. Radiogenic heat production has been inferred as an additional driver of tectonism due to the additional heat component leading to substantial weakening of the crust (McLaren et al., 2005). This in turn makes the crust considerably more susceptible to far-field stresses (McLaren et al., 2005), complicating interpretations of tectonic settings with respect to determining distance to any plate boundary. However, preliminary analysis of radiogenic heat-producing elements (U, Th, and K) in Biranup Zone granites shows that they have relatively low concentrations compared to high heat-producing Australian Proterozoic granites described in McLaren et al. (2005). This is consistent with the interpretation that the Biranup Zone granites were produced by melting Archean crust with relatively low concentrations of U, Th, and K, and suggests that radiogenic heat production was not a major contributing factor to crustal melting. In any case, heat transfer is likely to have occurred because there is a strong link between crustal melting and a mantle input, as shown by the presence of mafic enclaves in the Biranup Zone granites (Spaggiari et al., 2011; Kirkland et al., 2011a). Therefore, the pulses of magmatism would have thermally softened and weakened the lower crust, which, assuming a conducive stress field, would have helped drive extension in the upper crust, which in turn would also contribute to crustal thinning and heat transfer.

The field evidence shows that some Biranup Zone granitic rocks intruded Barren Basin sediments, indicating that some of the granitic magmatism was transferred to upper

crustal levels. This magmatism would have enhanced ductility at upper crustal levels, leading to the formation of one or more extensional detachments, further widening the Barren Basin. The most likely scenario would be asymmetric extension of the basin substrate away from the more robust craton margin, or a core-complex mode of extension (Rosenbaum et al., 2008, and references therein). An additional effect related to magmatism would be the formation of dynamic topography, assuming that magmatism was voluminous enough to produce upwelling and underplating. This is likely to have been the case during the Biranup Orogeny when magmatism was most voluminous, the component of mafic input was potentially more substantial and the degree of influence from the mantle greater (e.g. the c. 1665 Ma Eddy Suite).

Initiation of basin evolution

Although the oldest recognized basin-forming event took place at c. 1800 Ma (denoted by the Stirling Range Formation, Table 2), it is possible that other tectonic events preceded this. The present-day surface expression of the transition from Yilgarn Craton crust unaffected by events recognized in the Albany–Fraser Orogen, to reworked crust, is relatively sharp and marked by southeast-dipping, Mesoproterozoic thrust faults at high angles to the dominant, northwest-trending structural grain of the Yilgarn Craton (Fig. 1). Crosscutting the grain of the Yilgarn Craton are large, east-trending, mafic to ultramafic dykes of the c. 2410 Ma Widgiemooltha Dyke Suite (see Wingate, 2007; and Summary in Spaggiari et al., 2011). These dykes are enigmatic, in that there is no recognized associated tectonic event in the Yilgarn Craton at that time, yet some of the dykes are several hundreds of kilometres long, and cross large portions of the craton (e.g. the Jimberlana and Binneringie Dykes). It is feasible that the Widgiemooltha Dyke Suite represents an early period of extension, potentially related to the late stages of the event that produced the 2500–2450 Ma detritus recorded in the Barren Basin. Rocks of this age are unknown in the Yilgarn Craton, and while they could represent a different terrane, they may also be indicative of the first reworking of the southern Yilgarn Craton, resulting in extension and rifting of the craton between c. 2500 to 2450 Ma. This interpretation could explain the Group 2 and 3 Lu–Hf isotope arrays seen in the Big Red paragneiss that suggest reworking of c. 2.8 Ga Yilgarn-like crust at c. 2.5 Ga (see Hf isotope fingerprints of detrital zircons section). The extensional event would have been followed by intrusion of the Widgiemooltha Dyke Suite at c. 2410 Ma, whose magmatic centre would be located in the rifted portion of the craton. This hypothesis would fit with the observation that the farthest outboard Barren Basin unit, the Big Red paragneiss, is dominated by 2500–2450 Ma detritus, and contains less Neoarchean, Yilgarn Craton-derived detritus.

Another possible connection, although slightly older, could be the c. 2560 to 2500 Ma Sleaford and Mulgathing Complexes in the Gawler Craton, which are inferred to represent a single belt of late Archean rocks (Swain et al., 2005). The complexes include metasedimentary rocks and generally coeval felsic and mafic to ultramafic volcanics, interpreted to have formed by interaction

of a convergent margin and mantle plume, with the sedimentary component deposited in a back-arc or arc-rift basin setting (Swain et al., 2005). These rocks were intruded by felsic to intermediate magmas between c. 2520 and 2500 Ma, and were deformed and metamorphosed under greenschist to granulite facies conditions during the 2480–2420 Ma Sleafordian Orogeny (Hand et al., 2007, and references therein). This was followed by about 400 million years of tectonic quiescence, which has been interpreted as leading to cratonization (Swain et al., 2005; Hand et al., 2007). Although there is no clear direct relationship with the Yilgarn Craton, it is feasible that the tectonic event that produced the Sleaford and Mulgathing Complexes may also have affected the now rifted southern portion of the Yilgarn Craton, with the Widgiemooltha Dyke Suite being the only distal record of this event preserved in the remaining portion of the craton.

Tectonic model for the Barren Basin

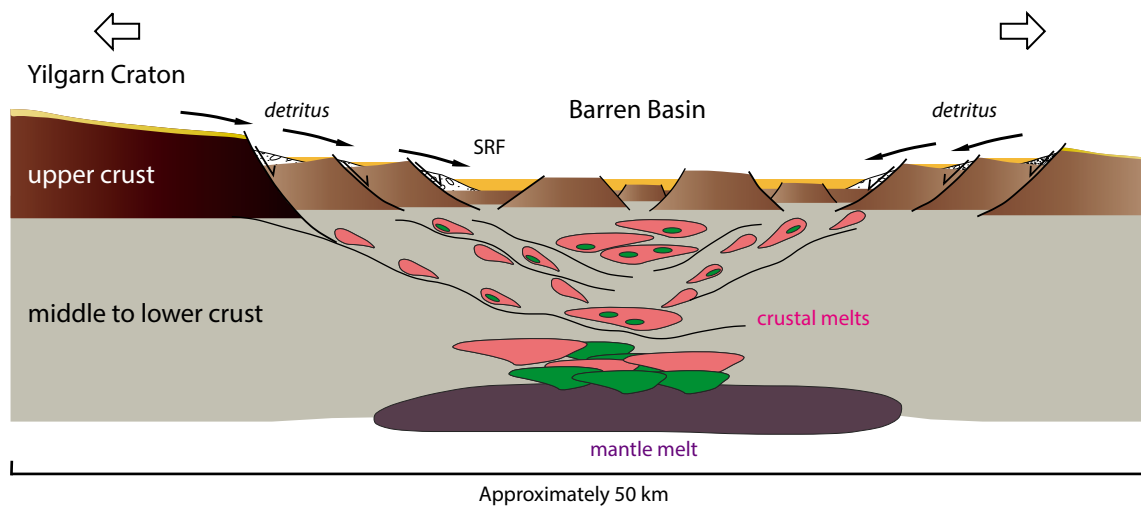
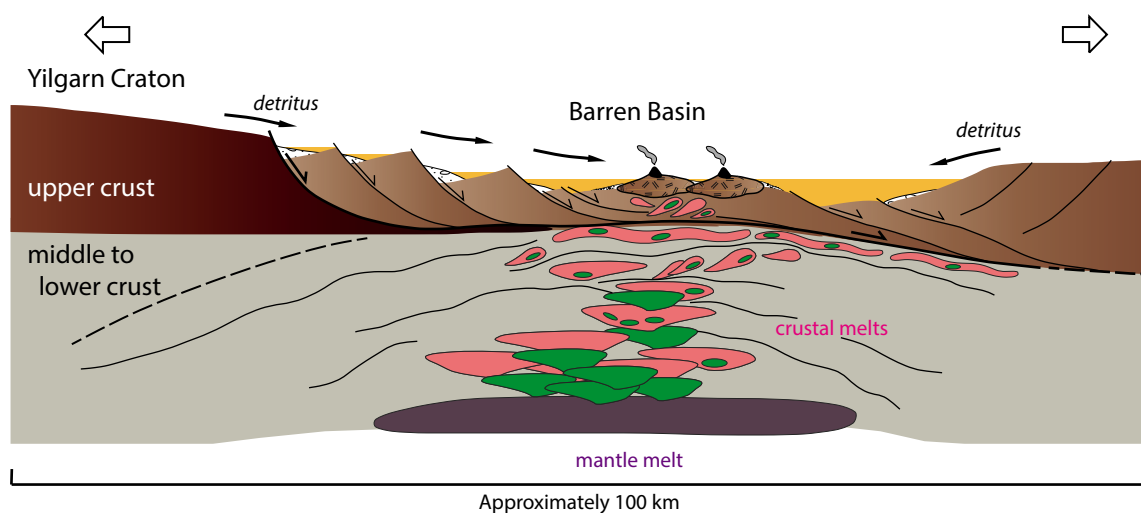
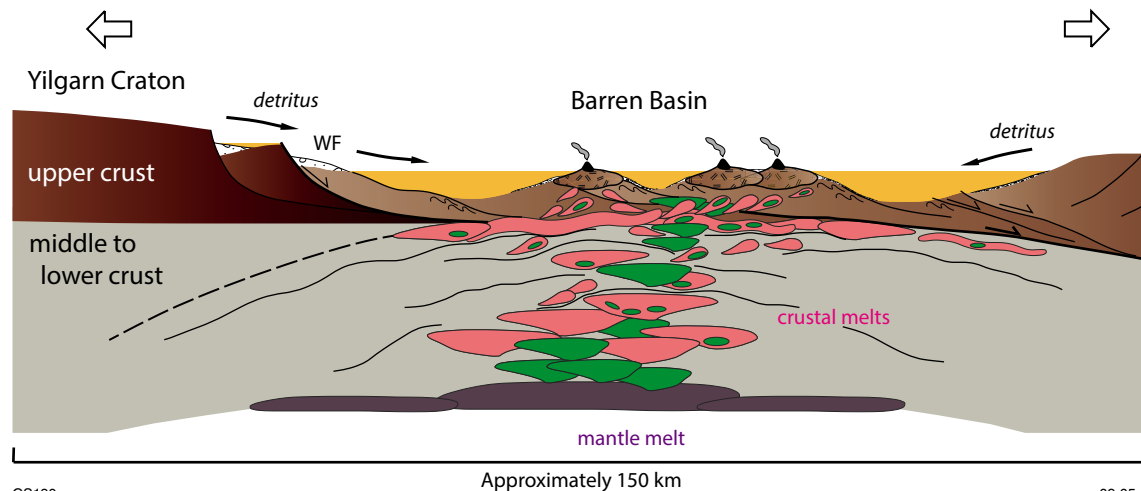
Using the rationale and constraints described above, a model for the formation of the Barren Basin and its related geodynamic history can be proposed. The purpose of proposing such a model is to provide a synthesis of the data and interpretations derived from it, to form hypotheses that can be tested. It should be noted that due to the difficulty in recognizing Paleoproterozoic structures, no account is made for any potential large-scale transpressional or transtensional displacements. In any case, no offset of stratigraphic units is recognizable, and there is no evidence to indicate any substantial strike-slip motion during this period.

At c. 1800 Ma, extension of the southern and southeastern Yilgarn Craton was underway, forming a horst and graben architecture exposing basement highs, presumably oriented in a similar way to the current trend of the orogen (Fig. 22a). The elevated rift margin topography and the basement highs provided detritus, in part from the Yilgarn Craton hinterland. Detrital material with ages of 2575–1900 Ma may have been sourced from reworked Yilgarn Craton crust, or other more distal or recycled sources such as the Gascoyne Province (see Provenance of the Barren Basin section). Detritus from the craton margin and these other sources were fed into dominantly fluvial to deltaic, or shallow marine systems, producing the Stirling Range Formation, and potentially even the lowermost unit of the Mount Barren Group, the Steere Formation, whose detrital pattern is similar to that of the Stirling Range Formation (compare Tr-01 in Fig. 7a with Fig. 6). This is consistent with significant detrital zircon age components in the Stirling Range Formation at c. 2656, 2246, and 2034 Ma, and its maximum depositional age of c. 2016 Ma (Rasmussen et al., 2002). Paleoproterozoic detritus may also have blanketed parts of the Yilgarn Craton at this time, thus providing a significant component of c. 2034 Ma detritus, potentially shed from the Gascoyne Province during the Glenburgh Orogeny. The first recognized period of magmatism resulted in crustal melting, most likely triggered by lower crustal intrusion and intraplating of mafic magmas leading to the production of the c. 1800 Ma granites, which contain mafic layers (the Salmon Gums Event). Injection of mantle

heat and the generation of crustal partial melts started the process of thermally weakening the lower crust.

By c. 1780 Ma, a second pulse of magmatism (the Ngadju Event) had begun producing crustal melts, potentially on a broader scale as c. 1780 to 1760 Ma detritus is widespread and recognized from the western through to the eastern parts of the Albany–Fraser Orogen. Granites of this age, which include mingled, co-magmatic gabbroic rocks, are also known from the Tropicana Zone in the far northeastern part of the orogen, as well as the eastern Biranup Zone and western edge of the Nornalup Zone (Spaggiari et al., 2011, 2014). The effect of this magmatism was to further thermally weaken the crust, leading to greater ductility at shallower crustal levels, and hence the formation of an asymmetric, melt-lubricated detachment away from the craton (Fig. 22b). This potentially increased the rate of extension and crustal thinning, widening the basin. Although volumetrically minor, the gabbroic rocks indicate an ongoing link to the mantle as the crust thinned. Concurrently, the effects of magmatic activity, and perhaps underplating or magma ponding, may have led to dynamic uplift and exposure of more of the substrate, now including the c. 1800 Ma granites, potentially leading to doming and a core-complex mode of extension (e.g. Rosenbaum et al., 2008, and references therein). The effect would be to shed more detritus into the Barren Basin, including c. 1800 Ma detritus, into the Barren Basin, to eventually form units such as the Mount Barren Group, Coramup Gneiss, Lindsay Hill Formation, Woodline Formation, and the Big Red paragneiss. These units show a greater input of Neoproterozoic detritus than that deposited prior to c. 1800 Ma (Stirling Range Formation), suggesting the Paleoproterozoic ‘blanket’ had eroded away, and a greater portion of the Yilgarn Craton was uplifted and eroding.

Figure 22. (facing) Tectonic evolution of the Barren Basin: a) Extension of the southern Yilgarn Craton by c. 1805 Ma formed a horst and graben architecture exposing basement highs. Detritus was sourced from the Yilgarn Craton hinterland, the basement highs, and potentially external sources. The c. 2575 to 2450 Ma, c. 2246, 2034 and 2016 Ma detritus was potentially sourced from reworked Yilgarn Craton crust (denoted by paler brown), or external sources. Mantle melting produced lower crustal melts and granitic intrusions along middle crustal shear zones; b) extension and magmatism was again prevalent between 1780 and 1760 Ma, producing an asymmetric, melt-lubricated detachment leading to doming and a core-complex mode of extension, and basin widening. Volcanism is inferred; c) during the 1710–1650 Ma Biranup Orogeny increased magmatism led to thermal subsidence and deepening of the basin, an increased sediment load, and formation of deeper depositional centres flanked by topographic highs. Volcanism is inferred. The folds are interpreted as formed during the c. 1680 Ma Zanthus Event. Green indicates mafic/mantle component; pink indicates crustal melt/granitic component. SRF = Stirling Range Formation; WF = Woodline Formation. Large arrows indicate approximate stress field orientation.

a) c. 1805 Ma**b) c. 1770 Ma****c) c. 1670 Ma**

This is also indicated in the Mount Barren Group where the lowermost units (Steere Formation, Kundip Quartzite) show an upward increase in the amount of Neoproterozoic detritus, and a corresponding decrease in 2450–2000 Ma Paleoproterozoic detritus, especially the c. 2034 Ma peak. By the time the Kybulup Schist was deposited, much of the detritus of this age was missing, and there was a much larger, younger Paleoproterozoic peak of c. 1800 to 1760 Ma (Fig. 7a).

During the 1710–1650 Ma Biranup Orogeny, magmatism had increased volumetrically and by 1665 Ma included a greater input of more isotopically juvenile mantle material, forming mingled granitic and gabbroic intrusions such as those defined by the Eddy Suite (Kirkland et al., 2011a,b). This would have added heat to the lower crust as it became more refractory. Heat transfer to the upper crust may have contributed to thermal subsidence and deepening of the basin, leading to a thicker sediment pile, which would have increased sediment loading. This perhaps led to flexure of the crustal substrate, although this may have been in part counteracted by dynamic topography, potentially producing a ‘hummocky’ surface with deeper depositional centres flanked by topographic highs (Fig. 22c). If volcanic activity occurred during the Biranup Orogeny, it appears to have been minor, although this is difficult to assess.

The compressional c. 1680 Ma Zanthus Event may reflect a brief period of basin inversion, perhaps releasing the first detritus of Biranup Orogeny age into the Barren Basin, feeding units such as the Fly Dam Formation and to a lesser extent, the Woodline Formation. The Fly Dam Formation, which has a maximum depositional age of c. 1617 Ma (Table 2), may represent the last stage of basin formation, which may have been due to thermal subsidence following the Biranup Orogeny. The end of magmatism associated with the Biranup Orogeny is marked by the youngest known granitic intrusion dated at c. 1627 Ma (GSWA 194736).

It is clear that a regional mantle heat source was present at least periodically, and for a significant interval of time, leading to partial melting of the lower crust and the production of granitic intrusions with a mantle component. In turn, these intrusions redistributed heat in the upper crust, helping drive tectonism. Given this, it is feasible that a simple, dominantly extensional stress field would have been sufficient to drive the tectonism required for basin formation. The proposed tectonic model is suggested to have occurred in a continental rift setting, for reasons outlined above. Alternatively, a convergent margin setting, such as a back-arc basin, may also be applicable, but there is no evidence to indicate the presence of any magmatic-arc or subduction zone in close proximity, so if this model is correct, the subduction zone was distal and to the east. An explanation for the distinct period of quiescence between 1600 and 1455 Ma, shown by the provenance in both the Barren and Arid Basins, and the magmatic history of the Albany–Fraser Orogen, is that the continental rift (or back-arc) evolved into a marginal ocean basin, forming an ocean–continent transition (OCT) and passive margin. If a convergent margin setting is invoked, the quiescent period would indicate substantial retreat of the accompanying subduction zone. This marginal basin marks the initial setting of the Arid Basin.

Arid Basin

Zircon U–Pb geochronology implies that the Arid Basin was regionally extensive, from the Gwynne Creek Gneiss in the far northeastern part of the orogen, through to the paragneiss of the western Albany–Fraser Orogen near Albany (Fig. 1). It is difficult to constrain when this basin system began to form, but if the model for formation of a marginal basin from c. 1600 Ma is correct, then the sedimentary pile associated with that basin would mark the first phase of Arid Basin evolution. A second phase of basin formation was probably underway by c. 1455 Ma, at least in the more outboard, easternmost regions, denoted by the presence of c. 1455 Ma detritus in the Malcolm Metamorphics (Adams, 2012), which most likely represents interlayered synvolcanic material. Deposition continued, although not necessarily without interruption, until at least c. 1332 Ma (Table 4), corresponding to the early part of Stage I of the Albany–Fraser Orogeny. This second significant period of sediment dispersal in the Albany–Fraser Orogen is termed Cycle 2 (Spaggiari et al., 2011).

Significance of the basin fill

The Arid Basin contrasts markedly with the Barren Basin in several ways, indicating some significant differences in tectonic regime. Firstly, the type of basin fill in the Arid Basin is highly variable and includes interbedded sandstone and mudstone, calcareous rocks or marls, iron-rich horizons, and probable volcanoclastic or volcanic successions (compare Tables 2 and 4). Secondly, there is no evidence of fluvial deposits, and the sequences appear to be generally finer grained, less quartz-rich and less mature. Another factor that contrasts with the Barren Basin stratigraphy is the presence of subparallel layers of mafic and calc-silicate rocks in the Malcolm Metamorphics that are interpreted to be derived from synmagmatic activity that produced basaltic flows or high-level sills, and potentially, volcanoclastic debris.

From the detrital zircon analysis it is clear that the Snowys Dam Formation and the Malcolm Metamorphics have an unusual provenance, and that the dominant age range of detritus from c. 1455 Ma through to 1375 Ma does not correspond with any known sources from the Albany–Fraser Orogen (Figs 3 and 4). Furthermore, zircons of this age have the most juvenile Lu–Hf isotope signatures recorded in the Albany–Fraser Orogen, pointing to an exotic source with a different crustal character. Hence, during deposition of these units, sediment was being fed into the Arid Basin in substantial quantities from an unknown source, which must have either been proximal to the Albany–Fraser Orogen, or was recycled from that source. The most likely candidate for the source is the Madura Province, which lies to the east under the Eucla Basin, and which contains c. 1410 Ma oceanic magmatic-arc rocks of the Loongana intrusion (see Loongana oceanic magmatic-arc, Madura Province section). This interpretation is consistent with the matching Lu–Hf isotope signature of the detritus with the Loongana oceanic magmatic-arc (Fig. 20). The c. 1455 to 1375 Ma sediments were mixed with detritus from the Paleoproterozoic Biranup and Nornalup Zones, which

constitute the second-most dominant source of detritus. This detritus is likely to have shed from uplifted portions of these zones, or from the earlier deposition or recycling of these sediments into the marginal ocean basin that formed after the Biranup Orogeny.

Arid Basin evolution

Factors affecting basin evolution

In the east Albany–Fraser Orogen the substrate to both the Snowys Dam Formation and Gwynne Creek Gneiss appears to be either the eastern Biranup Zone or the eastern Nornalup Zone (Table 4). This implies a continental substrate defined by crust of Paleoproterozoic age with a large reworked Archean crustal component. This is consistent with the geochemical and isotope signatures of the Fraser Zone gabbroic rocks that intrude the Snowys Dam Formation, which indicate contamination from older, quartzofeldspathic crust (see Fraser Zone section; Smithies et al., 2013). The substrate that the Malcolm Metamorphics was deposited on is less clear, and although the Malcolm Metamorphics are presently included in the eastern Nornalup Zone, their base is not exposed. In addition, the Malcolm Metamorphics occur in a fault-bounded slice that links to the Rodona Shear Zone, a major structure that marks the eastern edge of the orogen (Fig. 1; Spaggiari and Pawley, 2012; Spaggiari et al., 2014). In the western Albany–Fraser Orogen the substrate to the Arid Basin sediments was likely to have been the western Nornalup Zone. However, that substrate is undefined. Given the large volume of Paleoproterozoic detritus, and minimal Archean component, direct input from the Yilgarn Craton appears to have been minimal suggesting that it was not a topographic high during formation of the Arid Basin, or that it was distal, given the current inverted crustal architecture. The lack of Archean detritus mixed with Paleoproterozoic detritus also suggests that either there was not a significant number of large remnants of Yilgarn Craton crust preserved in the Biranup and Nornalup Zone crust (i.e. similar to that exposed at Mt Andrew, Spaggiari et al., 2011; Kirkland et al., 2011a), or that such remnants were deeply buried. It is also interesting to note that the lack of Neoproterozoic detritus, which constitutes the largest portion of Barren Basin detritus, suggests recycling from that basin was minimal. In addition, there is virtually no record of the less dominant, unrecognized age components of the Barren Basin spanning the range 2550–1900 Ma. This in turn suggests that the sources for that detritus were either exotic, or were less extensive basement components largely consumed during Paleoproterozoic crustal melting.

In contrast with the analysis of the Barren Basin, the presence of the Loongana oceanic magmatic-arc makes distance to a plate margin easier to estimate, suggesting that a plate margin was indeed relatively proximal by at least 1410 Ma. Given that the Loongana magmatism was most likely part of an oceanic magmatic-arc, and not part of a spreading ridge or oceanic transform, the type of plate motion would have been convergent. This would allow for a variety of basin settings such as back-arc, intra-arc, fore-arc, retro-arc or peripheral foreland, or transform.

Initially, the Arid Basin sediments may simply have been deposited onto the inferred pre-existing passive margin and marginal ocean basin substrate, until arrival of the Loongana oceanic magmatic-arc. If the subduction zone related to that arc was dipping away from the continent, the marginal basin setting would have continued.

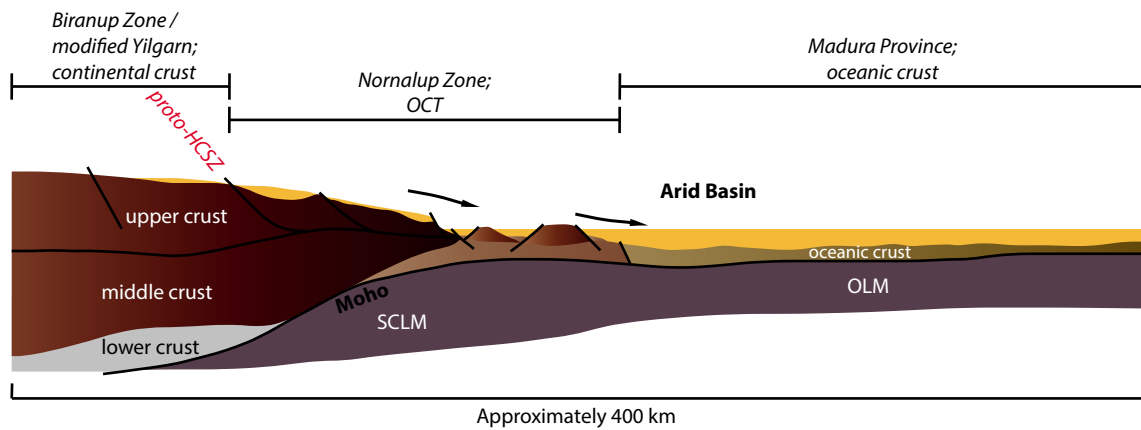
The effects of any thermal influence on basin formation from magmatism are predicted to be minimal, because there is no direct evidence of magma intruding the basin until the late stages of basin formation, i.e. during Stage I of the Albany–Fraser Orogeny. The earliest known intrusion directly into the metasedimentary rocks is the crosscutting granitic vein in the Malcolm Metamorphics, dated at 1313 ± 16 Ma (Clark et al., 2000). However, given the type of basin fill, coeval volcanism is likely to have occurred, at least during deposition of the Malcolm Metamorphics.

Tectonic model for the Arid Basin

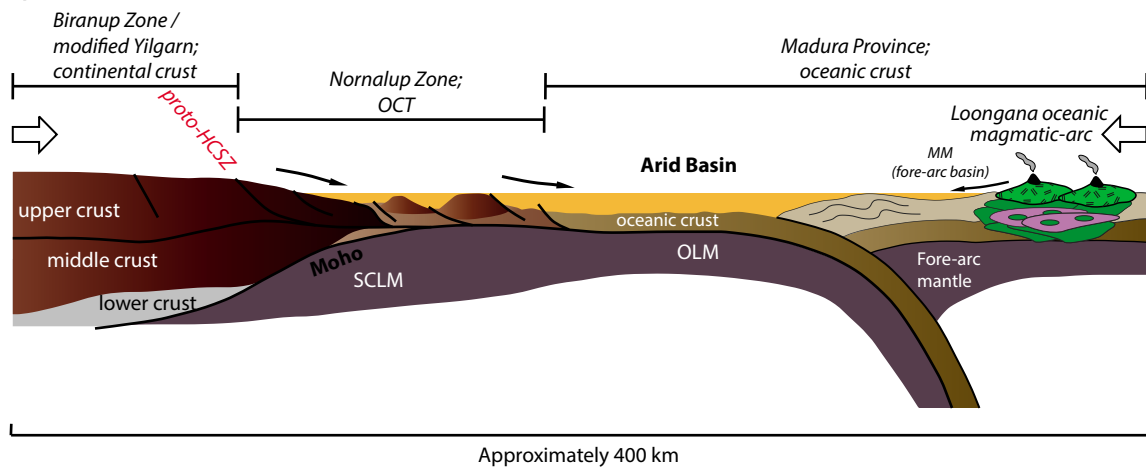
As with the Barren Basin, a tectonic model is proposed to provide a synthesis of the data and interpretations derived from it, to form hypotheses that can be tested. Given the likelihood of a convergent margin setting, three-dimensional complexities over time cannot be underestimated (e.g. Schellart and Rawlinson, 2010), so the model proposed is simplistic and does not take into account lateral differences over time, or the effects of any potential translational movement along strike. These effects are difficult to determine with the current datasets, and as with the Barren Basin, there is nothing to indicate substantial strike-slip displacements.

The earliest Arid Basin sediments are interpreted to have been deposited into the marginal ocean basin that formed after the Biranup Orogeny (see Tectonic model for the Barren Basin section). Therefore, during the period c. 1600 Ma to 1455 Ma, the Arid Basin could be classified as a marginal ocean basin, linked to a passive margin. During this period the sediments were probably derived mainly from the Biranup and Nornalup Zone hinterland (Fig. 23a), and potentially mixed with distal sources by passive margin-parallel sediment routing. Given the tectonic quiescence, sedimentation rates were likely to have been slow and probably not continuous, although over the 150 million-year period a substantial sediment pile may have accumulated. The Nornalup Zone is envisaged as an ocean–continent transition zone that formed as the continental crust was thinned during rifting, and as sea-floor spreading developed, similar to such zones described for the West Iberia passive continental margin (Afilhado et al., 2008; Rosenbaum et al., 2008). For West Iberia, the ocean–continent transition is described as wide and complex, and comprising half-graben basins separated by basement highs above thinned continental crust and exhumed subcontinental lithospheric mantle (Rosenbaum et al., 2008, and references therein). The basins contain both syn- and post-rift sediments, and the basement highs contain both subcontinental lithospheric mantle rocks and E–MORB-type, syn-rift gabbros (Peron-Pinvidic et al., 2007).

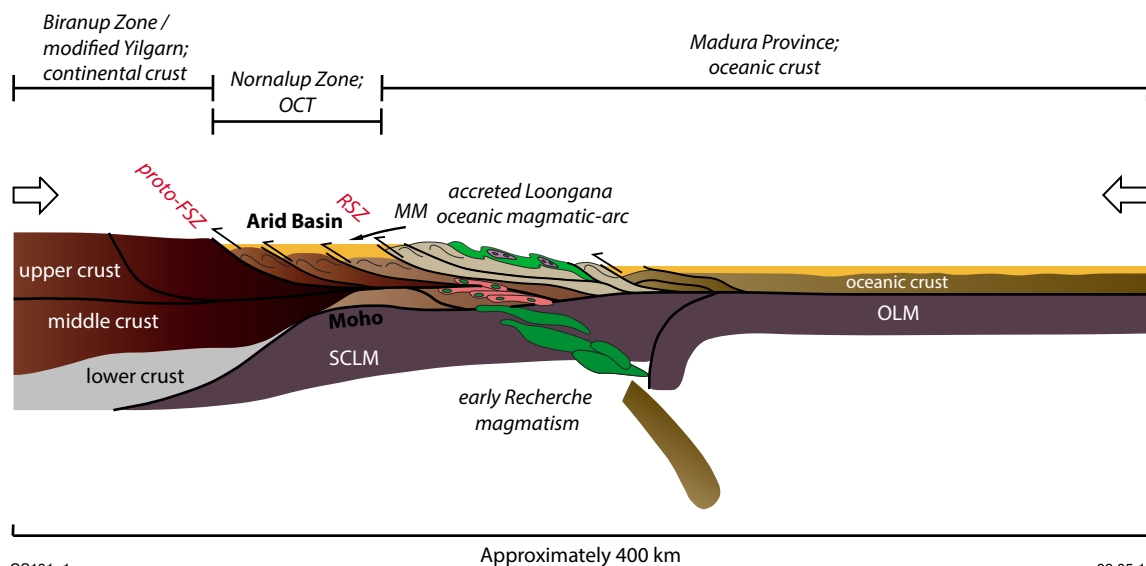
a) c. 1500 Ma



b) c. 1410 Ma



c) c. 1330 Ma



CS191_1

09.05.14

d) c. 1300 Ma

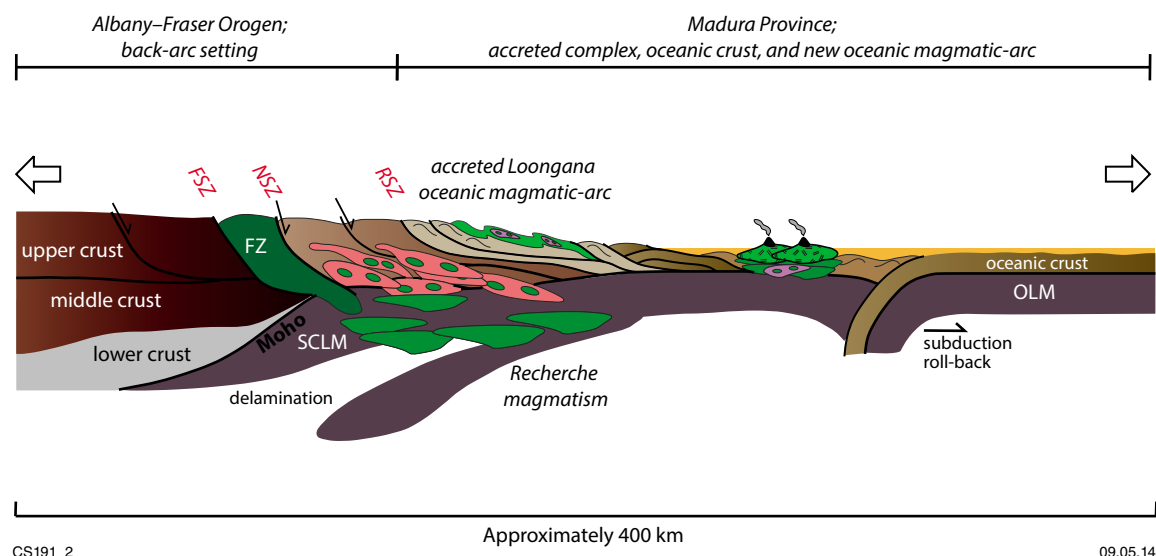


Figure 23. (facing and above) Tectonic evolution of the Arid Basin: a) At c. 1500 Ma the Arid Basin was a marginal basin that lay outboard of the Yilgarn Craton and Biranup Zone, with the Nornalup Zone as an ocean-continent transition (OCT). These zones define a passive margin that provided the bulk of the detritus to the basin at that time (phase 1 of the Arid Basin). The geometry of the margin is modelled on that of the West Iberia passive margin, modified from Afilhado et al. (2008); b) convergent setting and development of the Loongana oceanic magmatic-arc at c. 1410 Ma. The Malcolm Metamorphics are interpreted fore-arc basin sediments, but the bulk of the Arid Basin is still a marginal ocean basin (phase 2 of the Arid Basin); c) closure of the marginal basin, oceanic magmatic-arc accretion and slab detachment triggered the onset of Stage I, and early Recherche Supersuite magmatism. Sediments were transferred from the Loongana oceanic magmatic-arc and its environs to the Arid Basin (phase 3 of the Arid Basin); d) renewed subduction dips west beneath the easternmost extent of the orogen and accreted portion of the Madura Province, forming an oceanic magmatic-arc and adjacent back-arc setting. Roll-back leads to extension of the back-arc and formation of the Fraser Zone. SCLM = sub-continental lithospheric mantle; OLM = oceanic lithospheric mantle; OCT = ocean-continent transition; MM = Malcolm Metamorphics; HCSZ = Heywood-Cheyne Shear Zone; FSZ = Fraser Shear Zone; NSZ = Newman Shear Zone; RSZ = Rodona Shear Zone; FZ = Fraser Zone. Green indicates mafic/mantle component; pink indicates crustal melt/granitic component. Large arrows indicate approximate stress field orientation.

By c. 1455 Ma, the tectonic setting had changed to one of convergence, with east-dipping ocean-ocean subduction occurring outboard. This interpretation is based on the nature of the ensuing c. 1410 Ma Loongana component of this oceanic magmatic-arc, which must have been isolated from any significant mass of continental crust to produce the mafic-ultramafic rocks and low-K plagiogranites. It is also consistent with the lack of any evidence of tectonic activity in the Biranup and Nornalup Zones (the passive-margin hinterland) at this time. It is feasible that at c. 1455 Ma the Malcolm Metamorphics were deposited in either a fore-arc or accretionary prism setting onto an oceanic substrate (cf. Adams, 2012), west of the newly formed oceanic magmatic-arc (Fig. 23b). This is suggested because of the presence of interpreted, synsedimentary volcanic deposits in the Malcolm Metamorphics. If this were the case, the Malcolm Metamorphics would effectively be part of a different basin belonging to the Madura Province, albeit linked to the Arid Basin system. By c. 1410 Ma, the oceanic magmatic-arc had grown, and potentially migrated westwards as convergence continued and the marginal ocean basin was being consumed

(Fig. 23b). Again, there is no record of tectonic activity in the hinterland (Biranup and Nornalup Zones) at this time, which suggests that the oceanic magmatic-arc and subduction zone were still distal to the passive margin, although it is possible that some inversion did occur, producing minor deformation. Any ongoing deposition of the Arid Basin would still have been in a marginal ocean basin setting, with the possible exception of the Malcolm Metamorphics.

It is clear that deposition of the Arid Basin continued until at least 1332 ± 21 Ma (1σ), based on the youngest detrital zircon within GSWA 194778, or more conservatively until 1363 ± 9 Ma (MSWD = 1.09), the mean of the youngest group of 24 analyses whose dates are within 2.5σ of the mean (Table 4). Therefore, sedimentation continued well after formation of the Loongana oceanic magmatic-arc. If we accept that 1425–1375 Ma detrital zircons in the Snowys Dam Formation were sourced from the Loongana oceanic magmatic-arc, which is strongly implied by its isotopic and age characteristics, then a mechanism is required to transport them into the marginal ocean basin.

An east-dipping subduction zone is unlikely because the trench would probably trap and block transportation of most Loongana detritus. West-dipping subduction at c. 1410 Ma, which would put the Arid Basin in a back-arc position, is not favoured because it would be difficult to produce the uncontaminated, juvenile oceanic magmatic-arc magmas in the Loongana arc unless this arc system was a substantial distance from the cratonic passive margin. Equally, west-dipping subduction presents a problem because it would be difficult to consume the substantial length of oceanic crust required to produce the uncontaminated arc magmas without invoking subduction beneath the passive margin, for which there is no evidence. Given that the Snowys Dam Formation is clearly much younger than the Loongana oceanic magmatic-arc, it is likely that any sediment derived from the oceanic magmatic-arc must have either been recycled, or deposited after the oceanic magmatic-arc (and subduction) had changed position. Although it is feasible that the Snowys Dam Formation may contain synsedimentary volcanic deposits, they are unlikely to have been primarily sourced from the Loongana oceanic magmatic-arc, mainly because of the intervening Nornalup Zone. In any case, most of the mafic rocks interlayered with the Snowys Dam Formation appear to be intrusions of the younger Fraser Zone gabbros.

The simplest way to explain deposition of the younger Arid Basin sediments onto the Biranup and Nornalup Zone substrate would be to invoke west-directed, oceanic magmatic-arc soft collision and accretion onto the passive margin (Fig. 23c). The exact timing of this is speculative, but the closure of the marginal ocean basin and termination of ocean–ocean subduction in the Madura Province could be viewed as marking the onset of Stage I of the Albany–Fraser Orogeny. If this is correct, the earliest intrusions of the Recherche Supersuite at c. 1330 Ma may have been caused by this event, through initial crustal thickening producing partial melting of the upper crust, with the addition of a mantle component.

Oceanic magmatic-arc accretion would have produced large-scale compressional structures, forming a suture zone between the Albany–Fraser Orogen (eastern Nornalup Zone) and the Madura Province, marked by the Rodona Shear Zone (RSZ, Fig. 23c). The process of accretion of the Loongana oceanic magmatic-arc is likely to have unroofed and dismembered the arc considerably, leaving a mid-crustal portion preserved in one or more fault slices. This process would also enable the erosional products from the oceanic magmatic-arc, as well as recycled material from the fore-arc and accretionary prism, to be carried towards the hinterland via a craton-vergent fold and thrust belt feeding an evolving foreland basin system during the early part of Stage I (Fig. 23c). Such a system would allow detritus to be rapidly recycled and reach units adjacent to the hinterland, such as the Snowys Dam Formation, marking a third phase of Arid Basin formation. This tectonic process can also explain the mixing of eroded 1700–1600 Ma detritus with the younger detritus, especially adjacent to the hinterland. The development of the fold and thrust system and associated

foreland basin may have led to flexure and buckling of the crust, forming localized, deeper depositional centres. In this context it is interesting to note that the Gwynne Creek Gneiss, which has a maximum depositional age of 1483 ± 12 Ma (Table 3), contains early, well-developed, inclined, craton-vergent folds, which would fit with a fold and thrust evolution related to formation of a foreland basin. If these interpretations are correct, the Arid Basin would have evolved from a marginal ocean basin to a foreland basin.

By c. 1300 Ma it is clear that deposition of the known units of the Arid Basin had ceased, marked by the emplacement of the voluminous Recherche Supersuite intrusions, the 1305–1290 Ma intrusions of the Fraser Zone gabbroic and granitic rocks, and by the earliest phase of metamorphism dated at 1304 ± 7 Ma in the Snowys Dam Formation (GSWA 177910). Similar relationships are observed in the Malcolm Metamorphics, with deformation and metamorphic monazite growth identified at 1311 ± 4 Ma (Adams, 2012), shortly followed by intrusion of a crosscutting granitic vein dated at 1313 ± 16 Ma (Clark et al., 2000). This indicates that these units had a similar history by this time.

Following the accretion of the Loongana oceanic magmatic-arc and closure of the marginal basin, convergence continued and west-dipping subduction was initiated beneath the Albany–Fraser Orogen, accommodating the continued consumption of the Madura Province oceanic crust east of the Loongana oceanic magmatic-arc (Fig. 23d). The extent of this oceanic crust eastwards is speculative, and it is likely that other tectonic elements were on the horizon, for example, those that formed the Forrest Zone of the Coompana Province (Fig. 11), and eventually, the Mawson Craton. Roll-back of the renewed subduction zone produced an extensional regime, placing the Albany–Fraser Orogen into a back-arc setting that accommodated the main pulse of magmatism that produced the remainder of the Recherche Supersuite and the Fraser Zone gabbros (Fig. 23d; Fig. 4b). The Fraser Zone gabbros have previously been interpreted to have formed in either a continental rift or back-arc setting (Spaggiari et al., 2011; Smithies et al., 2013; Clark et al., 2014). If the interpretations described above up to c. 1330 Ma involving soft collision and accretion are correct, a continental rift at c. 1300 Ma could be discounted, although it is feasible that a simple extensional regime combined with delamination could have produced a marginal rift. Both a back-arc or a continental rift setting for the Fraser Zone can explain the crustal contamination observed in the magmatic rocks (Smithies et al., 2013), and the high-temperature metamorphism and its temporal link to mafic magmatism (Clark et al., 2014). A back-arc setting would be possible if subduction was once again occurring to the east, albeit with a westerly dip, placing the Fraser and Nornalup Zones in a back-arc setting by c. 1300 Ma. That would effectively mean that the Fraser Zone would represent the landward — or craton-adjacent — portion of such a system. It is also feasible that the extensional tectonics at this time led to initiation of the Ragged Basin.

The presence of west-dipping subduction at this time is highly speculative, and any evidence for this would now be buried beneath the Eucla Basin, east of the Loongana oceanic magmatic-arc. Given that at some stage the Mawson Craton must have joined with the West Australian Craton, it is feasible that west-dipping subduction allowed closure of the remaining ocean basin, and that the suture zone, however cryptic, is buried beneath the Eucla Basin somewhere between the Madura Province and the Forrest Zone of the Coompana Province. This would pre-date substantial sinistral displacement inferred to have occurred along the Mundrabilla Shear Zone (Smithies et al., 2014).

Implications for Stage I of the Albany–Fraser Orogeny

The tectonic model proposed for the Arid Basin indicates a relatively complex history, with a marked change from passive-margin quiescence to convergence by c. 1455 Ma. Just what triggered the change to a convergent margin setting is unknown, but the presence of reactivated major shear zones in the western Gawler Craton at this time is intriguing (Fraser and Lyons, 2006). It is feasible that the driver for tectonic activity at this time lay somewhere between the Gawler Craton and the ocean–ocean subduction zone in the Madura Province, with the obvious candidate being the poorly understood Coompana Province that presently lies between these regions (Fig. 11). That driver would fit with the model of rotation of the South Australian Craton via an easterly dipping subduction zone in retreat (Giles et al., 2004), and could also explain the onset of easterly dipping ocean–ocean subduction to accommodate it.

Previous interpretations for the Mesoproterozoic Albany–Fraser Orogeny have focused on models of collision between the West Australian and Mawson Cratons (as discussed above; see Myers et al., 1996; Betts and Giles, 2006; Fitzsimons, 2003; Bodorkos and Clark, 2004a). The collision was inferred to have occurred during Stage I (1345–1260 Ma; Clark et al., 2000), with the Nornalup Zone as part of the Mawson Craton (Bodorkos and Clark, 2004a). This interpretation, and the southeast-dipping polarity of subduction, was based on the record of pre-1313 Ma magmatism, deformation, and metamorphism being restricted to the Nornalup Zone (Clark et al., 2000; Bodorkos and Clark, 2004a). However, the data to constrain this were sparse, and only two pre-1313 Ma dates from Recherche Supersuite metagranites in the eastern Nornalup Zone were available (GSWA 83662 and 83663, Nelson et al., 1995), along with the 1313 ± 16 Ma granitic vein that intruded deformed metasedimentary rocks of the Malcolm Metamorphics (Clark et al., 2000). This granitic vein was also inferred to mark the termination of subduction-related Recherche Supersuite magmatism in the eastern Nornalup Zone (Bodorkos and Clark, 2004a).

Although additional data would be advantageous (Figs 3b and 4b), we now know that the Nornalup Zone contains Paleoproterozoic rocks (Spaggiari et al., 2011) and it

is likely that it represents a continuation of the Biranup Zone, albeit potentially more modified by the effects of rifting and the transition to oceanic crust. In addition, two metagranites of the Recherche Supersuite that could be older than 1313 Ma occur close to the eastern Nornalup and Biranup Zone contact (Fig. 1). These are a 1317 ± 7 Ma metasyenogranite from the western edge of the eastern Nornalup Zone, just east of the Newman Shear Zone (GSWA 194710), and a 1322 ± 11 Ma granitic gneiss from the eastern edge of the Biranup Zone at Observatory Point, just west of the Heywood–Cheyne Shear Zone (GSWA 184125). These data show that the eastern Nornalup Zone and at least the eastern edge of the Biranup Zone were intruded by the Recherche Supersuite during Stage I, but the data are still insufficient to present well-constrained interpretations and models of Recherche Supersuite magmatism and tectonics.

The role and significance of large-scale structures

The proposed tectonic models indicate that several large-scale structures were important through time, including some that were likely to have initiated as basin-forming faults. These large-scale structures are zones of crustal weakness that may have in part controlled where the basins formed, and where magmatic intrusions were emplaced, providing pathways to deeper crustal levels. Understanding the evolution of such structures is critical to an understanding of basin development.

If the model of continental rifting for the Barren Basin is correct, large fault structures, including the basal detachment, would have formed initially as extensional faults that were later reactivated and inverted. These may have included structures such as the Cundeelee and Jerdacuttup Faults, and the Coramup and Heywood–Cheyne Shear Zones and their continuation northeast, defined by the Newman and Fraser Shear Zones (Fig. 1). This fault system is one of the largest in the Albany–Fraser Orogen, separating the Biranup and Nornalup Zones, and intervening Fraser Zone (Fig. 1). It is inferred to have initially marked the main transition from continental crust to the ocean–continent transition, and been later used to accommodate the large Fraser Zone gabbroic intrusion (Fig. 23). These structures are interpreted to have been reactivated during the major compressional tectonics during Stage II of the Albany–Fraser Orogeny, which produced the fold and thrust architecture that is preserved in the upper crust.

Of major significance is the role of the Rodona Shear Zone, which marks a soft collision suture zone of the eastern edge of the Albany–Fraser Orogen with the western edge of the Madura Province (Fig. 11). These tectonic elements clearly have different geological histories and character, consistent with the presence of a suture. The Rodona Shear Zone may have initiated as the eastern edge of the ocean–continent transition linked to the marginal basin oceanic crust during the early stages of Arid Basin formation (Fig. 23a).

It should be noted that although some deep crustal-scale structures may appear as sutures based on their size, this may not necessarily be the case. There are other mechanisms that can form deep crust-penetrating structures, such as long-lived weak zones that localize major changes in geodynamics. The recognition of suture zones requires geochronological, isotopic, and geochemical data to constrain the age, evolution and composition of the crust on both sides of the structure, and hence verify the junction as a suture.

Concluding summary

The remnants of two, regionally extensive basin systems are preserved in the Albany–Fraser Orogen, the Barren and Arid Basins. The Barren Basin evolved over a period of more than 200 million years (1815–1600 Ma) and extended at least 1000 km along the southern Yilgarn Craton margin. Deposition took place during three main phases: prior to c. 1800 Ma, prior to c. 1700 Ma, and between 1710 and 1600 Ma. The Barren Basin is dominated by mature, quartz-rich metasedimentary rocks containing detritus that was shed mostly from the Yilgarn Craton as it underwent extension. This was mixed with locally derived detritus from synmagmatic rocks. The basin was formed in either a continental rift setting or alternatively, a back-arc setting with the subduction zone and magmatic-arc a substantial distance outboard of the Yilgarn Craton margin. After c. 1600 Ma the Barren Basin evolved to a marginal ocean basin, flanked by a passive margin defined by the strongly modified Yilgarn Craton margin.

The Arid Basin sediments were initially deposited into this marginal ocean basin from c. 1600 Ma, extending from the far northeastern part of the orogen to the western Albany–Fraser Orogen. In contrast to the Barren Basin, the Arid Basin contains a greater variety of lithologies and is dominated by c. 1455 Ma through to 1375 Ma detritus that does not correspond with any known sources from the Albany–Fraser Orogen. Furthermore, zircons of this age have the most juvenile Lu–Hf isotope signature recorded in the Albany–Fraser Orogen, pointing to an exotic source with newly formed crust of different character. That source is interpreted to have been the c. 1410 Ma Loongana oceanic magmatic-arc, with which this detritus shares a similar isotope and age signature. By c. 1455 Ma, the tectonic setting changed to one of convergence, and the marginal basin included an east-dipping ocean–ocean subduction zone and the Loongana oceanic magmatic-arc. Basin closure by c. 1330 Ma led to soft collision and accretion of the oceanic magmatic-arc over the eastern edge of the Albany–Fraser Orogen (Rodona Shear Zone), feeding detritus westwards into a foreland basin system, towards the craton and hinterland.

As Stage I of the Albany–Fraser Orogeny progressed, west-dipping subduction was initiated as the remaining Madura Province oceanic crust was consumed, placing the orogen in a back-arc setting. It is proposed that the collision zone with the Mawson Craton lies between the Madura and Coompana Provinces, beneath the Eucla Basin.

References

- Adams, M 2012, Structural and geochronological evolution of the Malcolm Gneiss, Nornalup Zone, Albany–Fraser Orogen, Western Australia: Geological Survey of Western Australia, Record 2012/4, 122p.
- Afilhado, A, Matias, L, Shiobara, H, Hirn, A, Mendes-Victor, L and Shimamura, H 2008, From unthinned continent to ocean: The deep structure of the West Iberia passive continental margin at 38°N: *Tectonophysics*, v. 458, p. 9–50.
- Allen, PA and Allen, JR 2005, *Basin Analysis: principles and applications*, 2nd edition, Blackwell Publishing Ltd, 549p.
- Andersen, T 2005, Detrital zircons as tracers of sedimentary provenance: Limiting conditions from statistics and numerical simulation: *Chemical Geology*, v. 216, p. 249–270.
- Asarco Limited 1971, Project, Final report: Geological Survey of Western Australia statutory mineral exploration report, Item 390, A3146, unpublished.
- Belousova, EA, Reid, AJ, Griffin, WL and O'Reilly, SY, 2009 Rejuvenation vs. recycling of Archean crust in the Gawler Craton, South Australia: Evidence from U–Pb and Hf isotopes in detrital zircon, *Lithos*, v. 113, p. 570–582.
- Berry, RF, Jenner, GA, Meffre, S and Tubrett, MN 2001, A North American provenance for Neoproterozoic to Cambrian sandstones in Tasmania?: *Earth and Planetary Science Letters*, v. 192, p. 207–222.
- Betts, PG and Giles, D 2006, The 1800–1100 Ma tectonic evolution of Australia: *Precambrian Research*, v. 144, p. 92–125.
- Blenkinsop, TG and Doyle, MG 2014, Structural controls on gold mineralisation on the margin of the Yilgarn craton, Albany–Fraser orogen: The Tropicana Deposit, Western Australia: *Journal of Structural Geology*, doi: 10.1016/j.jsg.2014.01.013.
- Blichert-Toft, J and Albarède, F 1997, The Lu–Hf isotope geochemistry of chondrites and the evolution of the mantle-crust system: *Earth and Planetary Science Letters*, v. 148, p. 243–258.
- Bodorkos, S and Clark, DJ 2004a, Evolution of a crustal-scale transpressive shear zone in the Albany Fraser Orogen, SW Australia: 2. Tectonic history of the Coramup Gneiss and a kinematic framework for Mesoproterozoic collision of the West Australian and Mawson cratons: *Journal of Metamorphic Geology*, v. 22, no. 8, p. 713–731, doi:10.1111/j.1525-1314.2004.00544.x.
- Bodorkos, S and Clark, DJ 2004b, Evolution of a crustal-scale transpressive shear zone in the Albany Fraser Orogen, SW Australia: 1. P–T conditions of Mesoproterozoic metamorphism in the Coramup Gneiss: *Journal of Metamorphic Geology*, v. 22, no. 8, p. 691–711, doi:10.1111/j.1525-1314.2004.00543.x.
- Bodorkos, S and Wingate, MTD, 2008a, 184122: metamorphosed quartz sandstone, Plum Pudding Rocks; *Geochronology Record* 701, in *Compilation of geochronology data: Geological Survey of Western Australia*.
- Bodorkos, S and Wingate, MTD, 2008b, 184125: orthopyroxene-bearing dioritic gneiss, Observatory Point; *Geochronology Record* 703, in *Compilation of geochronology data: Geological Survey of Western Australia*.
- Bunting, JA, De Laeter, JR and Libby, WG 1976, Tectonic subdivisions and geochronology of the northeastern part of the Albany–Fraser Province, Western Australia, in *Annual report for the year 1975: Geological Survey of Western Australia*, p. 117–126.
- Bunting, JA and McIntyre, JR 2003, Loongana Project combined annual technical report C150/2001: Exploration Licences 69/1516, 1517, 1718, 1719 and 1720 for the period 11/8/2002 to 10/8/2003, Helix Resources Limited, 29p.
- Cassidy, KF, Champion, DC, Krapez, B, Barley, ME, Brown, SJA, Blewett, RS, Groenewald, PB and Tyler, IM 2006, A revised geological framework for the Yilgarn Craton, Western Australia: *Geological Survey of Western Australia, Record* 2006/8, 8p.

- Clark, C, Kirkland, CL, Spaggiari, CV, Oorschot, C, Wingate, MTD and Taylor, R 2014, Proterozoic granulite formation driven by magmatism: an example from the Fraser Range Metamorphics, Western Australia: *Precambrian Research*, v. 240, p. 1–21.
- Clark, DJ 1999, Thermo-tectonic evolution of the Albany–Fraser Orogen, Western Australia: University of New South Wales, Sydney, PhD thesis (unpublished).
- Clark, DJ, Kinny, PD, Post, NJ and Hensen, BJ 1999, Relationships between magmatism, metamorphism and deformation in the Fraser Complex, Western Australia: constraints from new SHRIMP U–Pb zircon geochronology: *Australian Journal of Earth Sciences*, v. 46, p. 923–932.
- Clark, DJ, Hensen, BJ and Kinny, PD 2000, Geochronological constraints for a two-stage history of the Albany–Fraser Orogen, Western Australia: *Precambrian Research*, v. 102, no. 3, p. 155–183.
- Clark, WC 1995, Granite petrogenesis, metamorphism and geochronology of the western Albany–Fraser Orogen, Albany, Western Australia: Curtin University, Perth, Honours thesis (unpublished).
- Condie, KC and Myers, JS 1999, Mesoproterozoic Fraser Complex: geochemical evidence for multiple subduction-related sources of lower crustal rocks in the Albany–Fraser Orogen, Western Australia: *Australian Journal of Earth Sciences*, v. 46, p. 875–882.
- Cruse, T 1991, The sedimentology, depositional environment and Ediacaran fauna of Mondurup and Barnett Peaks, Stirling Range Formation, Western Australia: University of Western Australia, Perth, BSc Honours thesis (unpublished).
- Cruse, T and Harris, LB 1994, Ediacaran fossils from the Stirling Range Formation, Western Australia: *Precambrian Research*, v. 67, p. 1–10.
- Dawson, GC, Krapež, B, Fletcher, IR, McNaughton, NJ and Rasmussen, B 2002, Did late Palaeoproterozoic assembly of proto-Australia involve collision between the Pilbara, Yilgarn and Gawler Cratons? Geochronological evidence from the Mount Barren Group in the Albany–Fraser Orogen of Western Australia: *Precambrian Research*, v. 118, p. 195–220.
- Dawson, GC, Krapež, B, Fletcher, IR, McNaughton, N and Rasmussen, B 2003, 1.2 Ga thermal metamorphism in the Albany–Fraser Orogen of Western Australia: consequence of collision or regional heating by dyke swarms?: *Journal of the Geological Society London*, v. 160, p. 29–37.
- De Bièvre, P and Taylor, PDP 1993, IUPAC Recommended isotopic abundances: *International Journal of Mass Spectrometry and Ion Physics*, 149p.
- De Waele, B and Pisarevsky, SA 2008, Geochronology, paleomagnetism and magnetic fabric of metamorphic rocks in the northeast Fraser Belt, Western Australia: *Australian Journal of Earth Sciences*, v. 55, p. 605–621.
- Doepel, JGG 1975, Albany–Fraser Province, in *The geology of Western Australia: Geological Survey of Western Australia, Memoir 2*, p. 94–102.
- Fedo, CM, Sircombe, KN and Rainbird, RH 2003, Detrital zircon analysis of the sedimentary record, in *Zircon edited by JM Hanchar and PWO Hoskin*: Mineralogical Society of America, Washington, p. 277–303.
- Fitzsimons, ICW 2003, Proterozoic basement provinces of southern and southwestern Australia and their correlation with Antarctica: *Geological Society of London Special Publication*, v. 206, p. 93–130.
- Fitzsimons, ICW and Buchan, C 2005, Geology of the western Albany–Fraser Orogen, Western Australia — a field guide: *Geological Survey of Western Australia, Record 2005/11*, 32p.
- Fitzsimons, ICW, Kinny, PD, Wetherley, S and Hollingsworth, DA, 2005, Bulk chemical controls on metamorphic monazite growth in pelitic schists and implications for U–Pb age data: *Journal of Metamorphic Geology*, v. 23, p. 261–277.
- Fletcher, IR, Myers, JS and Ahmat, AL 1991, Isotopic evidence on the age and origin of the Fraser Complex, Western Australia: a sample of Mid-Proterozoic lower crust: *Chemical Geology: Isotope Geoscience section*, v. 87, no. 3–4, p. 197–216.
- Fraser, GL and Lyons, P 2006, Timing of Mesoproterozoic tectonic activity in the northwestern Gawler Craton constrained by $^{40}\text{Ar}/^{39}\text{Ar}$ geochronology: *Precambrian Research*, v. 151, p. 160–184.
- Gehrels, GE 2000, Introduction to detrital zircon studies of Paleozoic and Triassic strata in western Nevada and northern California, in *Paleozoic and Triassic Paleogeography and Tectonics of Western Nevada and Northern California edited by MJ Soreghan and GE Gehrels*: Geological Society of America, Special Papers 347, p. 1–17.
- Geological Survey of Western Australia 2007, South Yilgarn geological exploration package: Geological Survey of Western Australia, Record data package 2007/13.
- Geological Survey of Western Australia 2011, East Albany–Fraser and southeast Yilgarn, 2011 update: Geological Survey of Western Australia, Geological Exploration Package.
- Giles, D, Betts, PG and Lister, GS 2004, 1.8 – 1.5 Ga links between the North and South Australian Cratons and the Palaeo- to Mesoproterozoic configuration of Australia: *Tectonophysics*, v. 380, p. 27–41.
- Griffin, WL, Belousova, EA, Shee, SR, Pearson, NJ and O'Reilly, SY 2004, Archean crustal evolution in the northern Yilgarn Craton: U–Pb and Hf-isotope evidence from detrital zircons: *Precambrian Research*, v. 131, p. 231–282.
- Griffin, WL, Pearson, N, Belousova, EA and Saeed, A 2007, Reply to 'Comment to short-communication: Hf-isotope heterogeneity in zircon 91500' by WL Griffin, NJ Pearson, EA Belousova, A Saeed (v. 233 (2006) p. 358–363)' by F Corfu: *Chemical Geology*, v. 244, p. 354–356.
- Griffin, WL, Pearson, NJ, Belousova, EA, Jackson, SE, O'Reilly, SY, van Achenberg, E and Shee, SR 2000, The Hf isotope composition of cratonic mantle: LAM-MC-ICPMS analysis of zircon megacrysts in kimberlites: *Geochimica et Cosmochimica Acta*, v. 64, p. 133–147.
- Hall, CE, Jones, SA and Bodorkos, S 2008, Sedimentology, structure and SHRIMP zircon provenance of the Woodline Formation, Western Australia: implications for the tectonic setting of the West Australian Craton during the Paleoproterozoic: *Precambrian Research*, v. 162, p. 577–598, doi:10.1016/j.precamres.2007.11.001.
- Hand, M, Reid, A and Jagodzinski, L 2007, Tectonic framework and evolution of the Gawler Craton, Southern Australia: *Economic Geology*, v. 102, p. 1377–1395.
- Hawkesworth, CJ and Kemp, AIS 2006, Using hafnium and oxygen isotopes in zircons to unravel the record of crustal evolution: *Chemical Geology*, v. 226, p. 144–162.
- Howard, KE, Hand, M, Barovich, KM, Reid, A, Wade, BJ and Belousova, EA 2009, Detrital zircon ages: Improving interpretation via Nd and Hf isotopic data: *Chemical Geology*, v. 262, p. 277–292.
- Ingersoll, RV and Busby, CJ 1995, Tectonics of sedimentary basins, in *Tectonics of sedimentary basins edited by CJ Busby and RV Ingersoll*: Blackwell Science, Oxford, p. 1–51.
- Johnson, SP, Sheppard, S, Rasmussen, B, Wingate, MTD, Kirkland, CL, Muhling, JR, Fletcher, IR and Belousova, E 2011a, Two collisions, two sutures: Punctuated pre-1950 Ma assembly of the West Australian Craton during the Ophiolitic and Glenburgh Orogenies: *Precambrian Research*, v. 189, p. 239–262.
- Johnson, SP, Sheppard, S, Wingate, MTD, Kirkland, CL and Belousova, EA 2011b, Temporal and hafnium isotopic evolution of the Glenburgh Terrane basement: an exotic crustal fragment in the Capricorn Orogen: *Geological Survey of Western Australia, Report 110*, 27p.
- Jones, SA 2006, Mesoproterozoic Albany–Fraser Orogen-related deformation along the southeastern margin of the Yilgarn Craton: *Australian Journal of Earth Sciences*, v. 53, p. 213–234.

- Kingston DR, Dishroon, CP and Williams, PA 1983, Global basin classification: American Association of Petroleum Geologists, Bulletin 67, p. 2175–2193.
- Kinnaird, TC, Prave AR, Kirkland CL, Horstwood M, Parrish R and Batchelor, RAB 2007, The late Mesoproterozoic–early Neoproterozoic tectonostratigraphic evolution of NW Scotland: the Torridonian revisited: *Journal of the Geological Society*, v. 164, p. 541–551.
- Kirkland, CL, Wingate, MTD, Spaggiari, CV and Pawley, MJ 2010a, 194736: metasyenogranite, Bartlett Bluff; *Geochronology Record* 849: Geological Survey of Western Australia, 4p.
- Kirkland, CL, Wingate, MTD, Spaggiari, CV and Pawley, MJ 2010b, 194731: psammitic gneiss, Ponton Creek; *Geochronology Record* 860: Geological Survey of Western Australia, 4p.
- Kirkland, CL, Wingate, MTD, Spaggiari, CV and Pawley, MJ 2010c, 194733: porphyritic metamonzogranite, Ponton Creek; *Geochronology Record* 854: Geological Survey of Western Australia, 4p.
- Kirkland, CL, Wingate, MTD, Spaggiari, CV and Pawley, MJ 2010d, 194722: siliciclastic schist, Harris Lake; *Geochronology Record* 850: Geological Survey of Western Australia, 6p.
- Kirkland, CL, Wingate, MTD, Spaggiari, CV and Pawley, M 2010e, 194735: quartzofeldspathic gneiss, Gwynne Creek; *Geochronology Record* 867: Geological Survey of Western Australia, 5p.
- Kirkland, CL, Spaggiari, CV, Pawley, MJ, Wingate, MTD, Smithies, RH, Howard, HM, Tyler, IM, Belousova, EA and Poujol, M 2011a, On the edge: U–Pb, Lu–Hf, and Sm–Nd data suggests reworking of the Yilgarn Craton margin during formation of the Albany–Fraser Orogen: *Precambrian Research*, v. 187, p. 223–247.
- Kirkland, CL, Spaggiari, CV, Wingate, MTD, Smithies, RH, Belousova, EA, Murphy, R and Pawley, MJ 2011b, Inferences on crust–mantle interaction from Lu–Hf isotopes: a case study from the Albany–Fraser Orogen: *Geological Survey of Western Australia, Record* 2011/12, 25p.
- Kirkland, CL, Bingen, B, Whitehouse, MJ, Beyer, E and Griffin, WL 2011c, Neoproterozoic palaeogeography in the North Atlantic Region: Inferences from the Akkajaure and Seve Nappes of the Scandinavian Caledonides: *Precambrian Research*, v. 186, no. 1–4, p. 127–146.
- Kirkland, CL, Wingate, MTD and Spaggiari, CV 2011d, 182432: semipelitic gneiss, Gwynne Creek; *Geochronology Record* 937: Geological Survey of Western Australia, 5p.
- Kirkland, CL, Wingate, MTD and Spaggiari, CV 2011e, 194718: mafic granulite, American Granulite Quarry; *Geochronology Record* 993: Geological Survey of Western Australia, 4p.
- Kirkland, CL, Wingate, MTD and Spaggiari, CV 2011f, 194714: psammitic gneiss, Gnama Hill; *Geochronology Record* 999: Geological Survey of Western Australia, 6p.
- Kirkland, CL, Wingate, MTD and Spaggiari, CV 2011g, 194710: metagranite, southwest of Boingaring Rocks; *Geochronology Record* 996: Geological Survey of Western Australia, 4p.
- Kirkland, CL, Wingate, MTD and Spaggiari, CV 2012a, 194784: metamonzogranite, Newman Rock; *Geochronology Record* 1026: Geological Survey of Western Australia, 4p.
- Kirkland, CL, Wingate, MTD, Spaggiari, CV and Pawley, MJ 2012b, 182424: metasyenogranite, McKay Creek; *Geochronology Record* 1017: Geological Survey of Western Australia, 4p.
- Kirkland, CL, Wingate, MTD and Spaggiari, CV 2012c, 182475: migmatitic gneiss, Big Red prospect; *Geochronology Record* 1052: Geological Survey of Western Australia, 7p.
- Kirkland, CL, Wingate, MTD and Spaggiari, CV 2012d, 182473: migmatitic gneiss, Big Red prospect; *Geochronology Record* 1050: Geological Survey of Western Australia, 6p.
- Kirkland, CL, Wingate, MTD and Spaggiari, CV 2012e, 182476: migmatitic gneiss, Big Red prospect; *Geochronology Record* 1053: Geological Survey of Western Australia, 4p.
- Kirkland, CL, Wingate, MTD and Spaggiari, CV 2012f, 182474: granite vein, Big Red prospect; *Geochronology Record* 1051: Geological Survey of Western Australia, 4p.
- Kirkland, CL, Wingate, MTD and Spaggiari, CV 2012g, 194742: psammitic gneiss, Buniningia Soak; *Geochronology Record* 1043: Geological Survey of Western Australia, 5p.
- Kirkland, CL, Wingate, MTD and Spaggiari, CV 2012h, 194743: pelitic gneiss, Buniningia Soak; *Geochronology Record* 1042: Geological Survey of Western Australia, 7p.
- Kirkland, CL, Wingate, MTD and Spaggiari, CV 2012i, 194778: migmatitic garnet–biotite gneiss, Mount Malcolm; *Geochronology Record* 1067: Geological Survey of Western Australia, 6p.
- Kirkland CL, Smithies RH, Woodhouse AJ, Howard HM, Wingate MTD, Belousova EA, Cliff JB, Murphy RC and Spaggiari CV 2012j, Constraints and deception in the isotopic record; the crustal evolution of the west Musgrave Province, central Australia: *Gondwana Research*, v. 23, p. 759–781.
- Kirkland, CL, Wingate, MTD and Spaggiari, CV 2013a, 182405: quartzite, McKay Creek; *Geochronology Record* 1136: Geological Survey of Western Australia, 5p.
- Kirkland, CL, Wingate, MTD and Spaggiari, CV 2013b, 192558: granitic gneiss, Haig Cave; *Geochronology Record* 1089: Geological Survey of Western Australia, 4p.
- Kirkland, CL, Wingate, MTD and Spaggiari, CV 2013c, 192557, metagabbro, Haig Cave; *Geochronology Record* 1140: Geological Survey of Western Australia, 4p.
- Kirkland, CL, Spaggiari, CV, Smithies, RH and Wingate, MTD 2014a, Cryptic progeny of craton margins: *Geochronology and Isotope Geology of the Albany–Fraser Orogen with implications for evolution of the Tropicana Zone*, in Albany–Fraser Orogen seismic and magnetotelluric (MT) workshop 2014: extended abstracts, *compiled by CV Spaggiari and IM Tyler*: Geological Survey of Western Australia, Record 2014/6, p. 81–92.
- Kirkland, CL, Wingate, MTD and Spaggiari, CV 2014b, 182416: metasandstone, Rason Lake Road; *Geochronology Record* 1156: Geological Survey of Western Australia, 4p.
- Kirkland, CL, Wingate, MTD and Spaggiari, CV 2014c, 194777: quartzofeldspathic gneiss, Mount Malcolm; *Geochronology Record* 1160: Geological Survey of Western Australia, 6p.
- Kirkland, CL, Wingate, MTD and Spaggiari, CV 2014d, 194785: metatonalite, east of Boingaring Rocks; *Geochronology Record* 1161: Geological Survey of Western Australia, 4p.
- Kirkland, CL, Wingate, MTD and Spaggiari, CV 2014e, 192502: granitic gneiss, Aloa Downs; *Geochronology Record* 1157: Geological Survey of Western Australia, 4p.
- Kirkland, CL, Wingate, MTD, and Spaggiari, CV 2014f, 192504: granitic gneiss, Bishops Road; *Geochronology Record* 1158: Geological Survey of Western Australia, 4p.
- Leat, PT, Larter, RD, and Millar, IL 2006, Silicic magmas of Protector Shoal, South Sandwich arc: indicators of generation of primitive continental crust in an island arc: *Geological Magazine*, v. 144, p. 179–190.
- Less, T 2013, Newly recognised Paleoproterozoic gold–silver mineralisation in the Albany–Fraser orogeny, in *Future understanding of tectonics, ores, resources, environment and sustainability edited by Z Chang, R Goldfarb, T Blenkinsop, C Palczek, D Cooke, K Camuti and J Carranza*: FUTORES Conference, Economic Geology Research Unit Contribution 68, James Cook University, Townsville, Australia, 2 June 2013, p. 31.
- Love, GJ 1999, A study of wall-rock contamination in a tonalitic gneiss from King Point, near Albany, Western Australia: Curtin University, Perth, Honours thesis (unpublished).

- Love, GJ, Bodorkos, S, Nelson, DR and Wingate, MTD 2006a, 179098: coarse-grained quartz sandstone, Madoonia Downs Homestead; Geochronology Record 646, *in* Compilation of geochronology data, June 2006 update: Geological Survey of Western Australia.
- Love, GJ, Bodorkos, S, Nelson, DR and Wingate, MTD 2006b, 179602: coarse-grained quartz sandstone, Madoonia Downs Homestead; Geochronology Record 648, *in* Compilation of geochronology data, June 2006 update: Geological Survey of Western Australia.
- Love, GJ, Bodorkos, S, Nelson, DR and Wingate, MTD 2006c, 165591: quartz sandstone, Madoonia Downs Homestead; Geochronology Record 618, *in* Compilation of geochronology data, June 2006 update: Geological Survey of Western Australia.
- Love, G J, Bodorkos, S, Nelson, DR and Wingate, MTD 2006d, 165592: quartz sandstone, Madoonia Downs Homestead; Geochronology Record 619, *in* Compilation of geochronology data, March 2006 update: Western Australia Geological Survey.
- Love, GJ, Bodorkos, S, Nelson, DR and Wingate, MTD 2006e, 165593: coarse-grained quartz sandstone, Madoonia Downs Homestead; Geochronology Record 620, *in* Compilation of geochronology data, June 2006 update: Geological Survey of Western Australia.
- Martin, DMcB, Sircombe, KN, Thorne, AM, Cawood, PA and Nemchin, AA 2008, Provenance history of the Bangemall Supergroup and implications for the Mesoproterozoic paleogeography of the West Australian Craton: *Precambrian Research*, v. 166, p. 93–110.
- McLaren, S, Sandiford, M and Powell, R 2005, Contrasting styles of Proterozoic crustal evolution: A hot-plate tectonic model for Australian terranes: *Geology*, v. 33, no. 8, p. 673–676.
- Muhling, PC and Brakel, AT (compilers) 1985, Mount Barker – Albany, Western Australia: Geological Survey of Western Australia, 1:250 000 Geological Series Explanatory Notes, 21p.
- Myers, JS 1985, The Fraser Complex: a major layered intrusion in Western Australia, *in* Professional papers for 1983: Geological Survey of Western Australia, Report 14, p. 57–66.
- Myers, JS 1990, Albany–Fraser Orogen, *in* Geology and mineral resources of Western Australia: Geological Survey of Western Australia, Memoir 3, p. 255–263.
- Myers, JS 1995a, Geology of the Esperance 1:1 000 000 sheet (2nd edition): Geological Survey of Western Australia, 1:1 000 000 Geological Series Explanatory Notes, 10p.
- Myers, JS 1995b, Geology of the Albany 1:1 000 000 sheet: Geological Survey of Western Australia, 1:1 000 000 Geological Series Explanatory Notes, 10p.
- Myers, JS, Shaw, RD and Tyler, IM 1996, Tectonic evolution of Proterozoic Australia: *Tectonics*, v. 15, p. 1431–1446.
- Nebel, O, Nebel-Jacobsen, Y, Mezger, K and Berndt, J 2007, Initial Hf isotope compositions in magmatic zircon from early Proterozoic rocks from the Gawler Craton, Australia: A test for zircon model ages, *Chemical Geology*, v. 241, p. 23–37.
- Nelson, DR, Myers, JS and Nutman, AP 1995, Chronology and evolution of the Middle Proterozoic Albany–Fraser Orogen, Western Australia: *Australian Journal of Earth Sciences*, v. 42, p. 481–495.
- Nelson, DR 1995a, 83662: biotite–hornblende monzogranite gneiss, Poison Creek; Geochronology Record 86: Geological Survey of Western Australia, 4p.
- Nelson, DR 1995b, 112128: muscovite-biotite-sillimanite paragneiss, Point Malcolm; Geochronology Record 499; *in* Compilation of geochronology data, June 2006 update: Geological Survey of Western Australia.
- Nelson, DR 1996a, 112168: fine-grained sandstone, No Tree Hill; Geochronology Record 491: Geological Survey of Western Australia, 4p.
- Nelson, DR 1996b, 112170: metasandstone, Barrons Beach; Geochronology Record 492: Geological Survey of Western Australia, 3p.
- Nelson, DR 2005a, 178071: recrystallized biotite microtonalite, Haig Cave; Geochronology Record 597; *in* Compilation of geochronology data, June 2006 update: Geological Survey of Western Australia.
- Nelson, DR 2005b, 178072: tonalitic gneiss, Haig Cave; Geochronology Record 598; *in* Compilation of geochronology data, June 2006 update: Geological Survey of Western Australia.
- Nelson, DR 2005c, 178070: amphibolite, Haig Cave; Geochronology Record 596; *in* Compilation of geochronology data, June 2006 update: Geological Survey of Western Australia.
- Nutman, AP, Bennett, VC, Kinny, PD and Price, R 1993, Large-scale crustal structure of the northwestern Yilgarn Craton, Western Australia: evidence from Nd isotope data and zircon geochronology: *Tectonics*, v. 12, p. 971–981.
- Ochipinti, SA, Doyle, M, Spaggiari, CV, Korsch, R, Cant, G, Martin, K, Kirkland, CL, Savage, J, Less, T, Bergin, L and Fox, L 2014, Preliminary interpretation of the deep seismic reflection line 12GA–T1: northeastern Albany–Fraser Orogen, *in* Albany–Fraser Orogen seismic and magnetotelluric (MT) workshop 2014: extended abstracts compiled by CV Spaggiari and IM Tyler: Geological Survey of Western Australia, Record 2014/6, p. 44–59.
- Oorschot, CW 2011, P–T–t evolution of the Fraser Zone, Albany–Fraser Orogen, Western Australia: Geological Survey of Western Australia, Record 2011/18, 101p.
- Pawley, MJ, Wingate, MTD, Kirkland, CL, Wyche, S, Hall, CE, Romano, SS and Doublier, MP 2012, Adding pieces to the puzzle: episodic crustal growth and a new terrane in the northeast Yilgarn Craton, Western Australia: *Australian Journal of Earth Sciences*, v. 59, p. 603–623.
- Pearce, JA 2008, Geochemical fingerprinting of oceanic basalts with applications to ophiolite classification and the search for Archean oceanic crust: *Lithos*, v. 100, p. 14–48.
- Peron-Pinvidic, G, Manatschal, G, Minshull, TA and Sawyer, DS 2007, Tectonosedimentary evolution of the deep Iberia-Newfoundland margins: evidence for a complex breakup history: *Tectonics*, v. 26, no. 2, doi: 10.1029/2006TC001970.
- Pidgeon, RT 1990, Timing of plutonism in the Proterozoic Albany Mobile belt, southwestern Australia: *Precambrian Research*, v. 47, p. 157–167.
- Press, WH, Flannery, BP, Teukolsky, SA and Vetterling, WT 1986, Numerical Recipes: Cambridge University Press, Cambridge, UK, 236p.
- Rahl, JM, Reiners, PW, Campbell, IH, Nicolescu, S and Allen, C 2003, Combined single-grain (U–Th)/He and U/Pb dating of detrital zircons from the Navajo Sandstone, Utah: *Geology*, v. 31, no. 9, p. 761–764.
- Rasmussen, B, Bengtson, S, Fletcher, IR and McNaughton, N 2002, Discoidal impressions and trace-like fossils more than 1200 million years old: *Science*, v. 296, p. 1112–1115.
- Rasmussen, B, Fletcher, IR, Bengtson, S and McNaughton, N 2004, SHRIMP U–Pb dating of diagenetic xenotime in the Stirling Range Formation, Western Australia: 1.8 billion year minimum age for the Stirling biota: *Precambrian Research*, v. 133, p. 329–337.
- Rosenbaum, G, Weinberg, RF and Regenauer-Lieb, K 2008, The geodynamics of lithospheric extension: *Tectonophysics*, v. 458, p. 1–8.
- Schellart, WP and Rawlinson, N 2010, Convergent plate dynamics: New perspectives from structural geology, geophysics and geodynamic modelling: *Tectonophysics*, v. 483, p. 4–19.
- Scherer, E, Munker, C and Mezger, K 2001, Calibration of the lutetium–hafnium clock: *Science*, v. 293, p. 683–687.
- Sheppard, S, Ochipinti, SA and Tyler, IM 2004, A 2005–1970 Ma Andean-type batholith in the southern Gascoyne Province, Western Australia: *Precambrian Research*, v. 128, p. 257–277.
- Shervais, JW 1982, Ti–V plots and the petrogenesis of ophiolitic lavas: *Earth and Planetary Science Letters*, v. 32, p. 114–120.
- Sircombe, KN 2000, Quantitative comparison of large sets of geochronological data using multivariate analysis: a provenance study example from Australia: *Geochimica et Cosmochimica Acta*, v. 64, no. 9, p. 1593–1616.

- Sircombe KN and Hazelton, ML 2004, Comparison of detrital zircon age distributions by kernel functional estimation: *Sedimentary Geology*, v. 171, no. 1–4, p. 91–111.
- Smithies, RH, Kirkland, CL, Korhonen, FJ, Aitken, ARA, Howard, HM, Maier, WD, Wingate, MTD, Quentin de Gromard, R and Gessner, K 2014, The Mesoproterozoic thermal evolution of the Musgrave Province in central Australia – Plume vs. the geological record: *Gondwana Research*, doi.org/10.1016/j.gr.2013.12.014.
- Smithies, RH, Howard, HM, Evins, PM, Kirkland, CL, Kelsey, DE, Hand, M, Wingate, MTD, Collins, AS and Belousova, E 2011, High-temperature granite magmatism, crust-mantle interaction and the Mesoproterozoic intracontinental evolution of the Musgrave Province, Central Australia: *Journal of Petrology*, v. 52, p. 931–958.
- Smithies, RH, Spaggiari, CV, Kirkland, Howard, HM and Maier, WD 2013, Petrogenesis of gabbros of the Mesoproterozoic Fraser Zone: constraints on the tectonic evolution of the Albany–Fraser Orogen: *Geological Survey of Western Australia, Record 2013/5*, 29p.
- Smits, RG, Collins, WJ, Hand, M, Dutch, R and Payne, J 2014, A Proterozoic Wilson cycle identified by Hf isotopes in central Australia: Implications for the assembly of Proterozoic Australia and Rodina: *Geology*, v. 42, p.231–234.
- Sofoulis, J 1958, The geology of the Phillips River Goldfield, W.A.: *Geological Survey of Western Australia, Bulletin 110*, 240p.
- Spaggiari, CV, Bodorkos, S, Barquero-Molina, M, Tyler, IM and Wingate, MTD 2009, Interpreted bedrock geology of the south Yilgarn and central Albany–Fraser Orogen, Western Australia: *Geological Survey of Western Australia, Record 2009/10*, 84p.
- Spaggiari, CV, Kirkland, CL, Pawley, MJ, Smithies, RH, Wingate, MTD, Doyle, MG, Blenkinsop, TG, Clark, C, Oorschot, CW, Fox, LJ and Savage, J 2011, The geology of the east Albany–Fraser Orogen — a field guide: *Geological Survey of Western Australia, Record 2011/23*, 97p.
- Spaggiari, CV, Kirkland, CL, Smithies, RH and Wingate, MTD 2012, What lies beneath — interpreting the Eucla basement, in *GSWA 2012 extended abstracts: promoting the prospectivity of Western Australia*: *Geological Survey of Western Australia, Record 2012/2*, p. 25–27.
- Spaggiari, CV and Pawley, MJ 2012, Interpreted pre-Mesozoic bedrock geology of the east Albany–Fraser Orogen and southeast Yilgarn Craton (1:500 000), in *The geology of the east Albany–Fraser Orogen — a field guide compiled by CV Spaggiari, CL Kirkland, MJ Pawley, RH Smithies, MTD Wingate, MG Doyle, TG Blenkinsop, C Clark, CW Oorschot, LJ, Fox and J Savage*: *Geological Survey of Western Australia, Record 2011/23, Plates 1 and 1A*.
- Spaggiari, CV, Kirkland, CL, Smithies, RH, Occhipinti, SA and Wingate, MTD 2014, Geological framework of the Albany–Fraser Orogen, in *Albany–Fraser Orogen seismic and magnetotelluric (MT) workshop 2014: extended abstracts compiled by CV Spaggiari and IM Tyler*: *Geological Survey of Western Australia, Record 2014/6*, p. 12–27.
- Swain, G, Woodhouse, A, Hand, M, Barovich, K, Schwartz, M and Fanning, CM 2005, Provenance and tectonic development of the late Archean Gawler Craton, Australia: U–Pb zircon, geochemical and Sm–Nd isotopic implications: *Precambrian Research*, v. 141, p. 106–136.
- Tillick, D 2011, Final Report of Co-funded Government – Industry Drilling Program at the Haig Prospect, Eucla Project, August 2011, *Teck Australia Pty Ltd*, 24p.
- Tillick, D and Hunt, D 2010, Eucla Project, C283/2008, Combined Annual Report for the Period 1 April 2009 to 31 March 2010, *Teck Australia Pty Ltd*, 13p.
- Thom, R and Chin, RJ (compilers) 1984, Bremer Bay, Western Australia: *Geological Survey of Western Australia, 1:250 000 Geological Series Explanatory Notes*, 20p.
- Thom, R, Chin, RJ and Hickman, AH (compilers) 1984a, Newdegate, Western Australia: *Geological Survey of Western Australia, 1:250 000 Geological Series Explanatory Notes*, 24p.
- Thom, R, Lippie, SL and Sanders, CC (compilers) 1977, Ravensthorpe, Western Australia: *Geological Survey of Western Australia, 1:250 000 Geological Series Explanatory Notes*, 38p.
- Thom, R, Hickman, AH and Chin, RJ 1984b, Newdegate, WA Sheet SI 50-8: *Geological Survey of Western Australia, 1:250 000 Geological Series*.
- Tyler, IM and Hocking, RM 2001, Tectonic units of Western Australia: *Geological Survey of Western Australia, 1:2 500 000 Geological Series*.
- Vallini, DA, Rasmussen, B, Krapež, B, Fletcher, IR and McNaughton, NJ 2002, Obtaining diagenetic ages from metamorphosed sedimentary rocks: U–Pb dating of unusually coarse xenotime cement in phosphatic sandstone: *Geology*, v. 30, p. 1083–1086.
- Vallini, DA, Rasmussen, B, Krapež, B, Fletcher, IR and McNaughton, N 2005, Microtextures, geochemistry and geochronology of authigenic xenotime constraining the cementation history of a Paleoproterozoic metasedimentary sequence: *Sedimentology*, v. 52, p. 101–122.
- Van De Graaff, WJE and Bunting, JA (compilers) 1975, Neale, Western Australia: *Geological Survey of Western Australia, 1:250 000 Geological Series Explanatory Notes*, 23p.
- Van De Graaff, WJE and Bunting, JA (compilers) 1977, Plumridge, Western Australia: *Geological Survey of Western Australia, 1:250 000 Geological Series Explanatory Notes*, 28p.
- Vermeesch, P 2004, How many grains are needed for a provenance study?: *Earth and Planetary Science Letters*, v. 224, p. 441–451.
- Waddell, P-J 2014, Sedimentological and structural evolution of the Mount Ragged Formation, Nornalup Zone, Albany–Fraser Orogen, Western Australia: *Geological Survey of Western Australia, Report 129*, 116p.
- Wang Q, Schiøtte L and Campbell IH 1996, Geochronological constraints on the age of komatiites and nickel mineralisation in the Lake Johnston greenstone belt, Yilgarn Craton, Western Australia: *Australian Journal of Earth Sciences*, v. 43, p. 381–385.
- Wetherley, S 1998, Tectonic evolution of the Mount Barren Group, Albany–Fraser Province, Western Australia: *University of Western Australia, Perth, PhD thesis (unpublished)*.
- Wingate, MTD 2007, Proterozoic mafic dykes in the Yilgarn Craton, in *Proceedings edited by FP Bierlein and CM Knox-Robinson: Geoscience Australia; Kalgoorlie '07 conference, Kalgoorlie, Western Australia, 25 September 2007*, *Record 2007/14*, p. 80–84.
- Wingate, MTD and Bodorkos, S 2007a, 177921: conglomerate, Madoonia Downs Homestead; *Geochronology Record 668, in Compilation of geochronology data: Geological Survey of Western Australia*, 5p.
- Wingate, MTD and Bodorkos, S 2007b, 177910: metamorphosed quartz sandstone, Peters Dam; *Geochronology Record 660, in Compilation of geochronology data: Geological Survey of Western Australia*, 6p.
- Witt, WK 1997, Geology of the Ravensthorpe and Cocanarup 1:100 000 sheets: *Geological Survey of Western Australia, 1:100 000 Geological Series Explanatory Notes*, 26p.
- Witt, WK 1998, Geology and mineral resources of the Ravensthorpe and Cocanarup 1:100 000 sheets: *Geological Survey of Western Australia, Report 54*, 152p.
- Woodhead, JD and Hergt, JM 2005, A preliminary appraisal of seven natural zircon reference materials for in situ Hf isotope determination: *Geostandards and Geoanalytical Research*, v. 29, p. 183–195.
- Wyche, S, Kirkland, CL, Riganti, A, Pawley, MJ, Belousova, E and Wingate, MTD 2012, Isotopic constraints on stratigraphy in the central and eastern Yilgarn Craton, Western Australia: *Australian Journal of Earth Sciences*, v. 59, p. 657–670.

Appendix 1

GSWA geochronology samples cited in this Report. Full references are listed in the References section.

<i>GSWA Sample number</i>	<i>Citation</i>
83662	Nelson, 1995a
112128	Nelson, 1995b
112168	Nelson, 1996a
112170	Nelson, 1996b
165591	Love et al., 2006c
165592	Love et al., 2006d
165593	Love et al., 2006e
177910	Wingate and Bodorkos, 2007b
177921	Wingate and Bodorkos, 2007a
178070	Nelson, 2005c
178071	Nelson, 2005a
178072	Nelson, 2005b
179098	Love et al., 2006a
179602	Love et al., 2006b
182405	Kirkland et al., 2013a
182416	Kirkland et al., 2014b
182424	Kirkland et al., 2012b
182432	Kirkland et al., 2011d
182473	Kirkland et al., 2012d
182474	Kirkland et al., 2012f
182475	Kirkland et al., 2012c
182476	Kirkland et al., 2012e
184122	Bodorkos and Wingate, 2008a
184125	Bodorkos and Wingate, 2008b
192502	Kirkland et al., 2014e
192504	Kirkland et al., 2014f
192557	Kirkland et al., 2013c
192558	Kirkland et al., 2013b
194710	Kirkland et al., 2011g
194714	Kirkland et al., 2011f
194718	Kirkland et al., 2011e
194722	Kirkland et al., 2010d
194731	Kirkland et al., 2010b
194733	Kirkland et al., 2010c
194735	Kirkland et al., 2010e
194736	Kirkland et al., 2010a
194742	Kirkland et al., 2012g
194743	Kirkland et al., 2012h
194777	Kirkland et al., 2014c
194778	Kirkland et al., 2012i
194784	Kirkland et al., 2012a
194785	Kirkland et al., 2014d

Appendix 2

Detrital zircon U–Pb dating

All detrital zircon U–Pb ages compiled in this work are $^{207}\text{Pb}^*/^{206}\text{Pb}^*$ dates that are greater than or equal to 95% concordant ($\text{Pb}^* = \text{radiogenic Pb}$). All mean U–Pb ages are quoted with 95% uncertainties, except where noted otherwise. On average, each dataset contains about 50 detrital zircon analyses, providing 95% certainty of identifying a component that constitutes at least 10% of the true age population (e.g. Vermeesch, 2004). In some cases a smaller number of concordant detrital analyses were obtained due to intense metamorphic overprinting and new zircon growth. Nonetheless, Andersen (2005) has shown the relevant statistics for lower ‘n’ sample sets, which indicate that for 16 measured ages, only detrital components more abundant than about 15% will exceed the detection limit at the 95% confidence level. Hence, each zircon age component recognized in low-number datasets by one or more analyses is likely to be an important constituent of the sediment and of importance in defining provenance trends (e.g. Andersen, 2005; Kinnaird et al., 2007).

List of GSWA geochronology samples used in this publication

On the following pages is a list of GSWA zircon geochronology and Lu–Hf samples used in this publication. External datasets used are also listed.

GSWA Sample ID	Lithology	Unit	Location	Lu-Hf data	MGA Zone	Easting	Northing	Latitude	Longitude
Magmatic rocks									
83701A	Monzogranitic gneiss	Munglinup Gneiss, Northern Foreland	Young River		51	311153	6289569	-33.51678	120.96666
83691	Biotite monzogranite gneiss	Munglinup Gneiss, Northern Foreland	Young River North		51	300162	6296744	-33.45012	120.84998
83702	Biotite tonalite gneiss	Munglinup Gneiss, Northern Foreland	Young River South		51	320787	6271264	-33.68345	121.06666
184314	Leucocratic granodioritic gneiss	Munglinup Gneiss, Northern Foreland	Lort River		51	338711	6274811	-33.65435	121.26058
184120	Monzogranitic gneiss	Munglinup Gneiss, Northern Foreland	Pallinup River	Yes	50	658727	6191757	-34.40345	118.72691
184127	Monzodiorite	Munglinup Gneiss, Northern Foreland	Powell Point		51	274527	6243949	-33.92078	120.56098
184128	Leucocratic tonalite gneiss	Munglinup Gneiss, Northern Foreland	Powell Point	Yes	51	274332	6243706	-33.92292	120.55881
184334	Migmatitic granitic gneiss	Munglinup Gneiss, Northern Foreland	Quagi Beach		51	342339	6254715	-33.83607	121.29611
184329	Leucosome vein crosscutting F3 folds	Munglinup Gneiss, Northern Foreland	Powell Point		51	274342	6243778	-33.92228	120.55894
192507	Granitic gneiss	Munglinup Gneiss, Northern Foreland	Salmon Gums core SGD005	Yes	51	365139	6326588	-33.19116	121.55327
182435	Metagranite	Northern Foreland	Northwest of Tropicana	Yes	51	650037	6770831	-29.18231	124.54304
194791	Metamonzogranite	Northern Foreland	Southeast of Coonana Hill	Yes	51	524664	6542735	-31.24934	123.25903
194792	Metagranite	Northern Foreland	Southeast of Coonana Hill		51	513623	6542261	-31.25380	123.14308
194793	Metamonzogranite	Northern Foreland	Southeast of Coonana Hill	Yes	51	517278	6551730	-31.16832	123.18130
192521	Metagranite	Northern Foreland	Theofrastos prospect		51	485252	6489010	-31.73425	122.84431
179644	Foliated monzogranite	Northern Foreland	About 40 km southwest of Cave Rock		51	469474	6348760	-32.99915	122.67323
194709	Metasyenogranite	Northern Foreland	Cave Rock, north of Mount Andrew	Yes	51	492878	6392895	-32.60143	122.92410
194784	Mylonitic metagranite	Northern Foreland	Newman Shear Zone	Yes	51	516435	6447139	-32.11198	123.17421
194785	Migmatitic granitic gneiss	Northern Foreland	East of Boingaring Rocks	Yes	51	532246	6407415	-32.47000	123.34315
192502	Granitic gneiss	Eastern Biranup Zone	Salmon Gums core SGD001	Yes	51	361984	6319310	-33.25639	121.51833
192504	Granitic gneiss	Eastern Biranup Zone	Salmon Gums core SGD002		51	361774	6318751	-33.26141	121.51599
192505	Granitic gneiss	Eastern Biranup Zone	Salmon Gums core SGD003		51	363782	6320534	-33.24558	121.53781
192508	Granitic gneiss	Eastern Biranup Zone	Salmon Gums core SGD005	Yes	51	365139	6326588	-33.19116	121.55327
83666	Garnet-biotite monzogranitic gneiss	Southeastern Biranup Zone	Garnet Ice Quarry		51	468777	6450787	-32.07876	122.66916

GSWA Sample ID	Lithology	Unit	Location	Lu-Hf data	MGA Zone	Easting	Northing	Latitude	Longitude
83676A	Hornblende syenogranite gneiss	Southeastern Biranup Zone	North of Mount Andrew		51	491769	6400828	-32.52986	122.91235
194701	Granitic gneiss	Southeastern Biranup Zone	Crystal Lake	Yes	51	419829	6330456	-33.16172	122.14022
194702	Granitic gneiss	Southeastern Biranup Zone	Dingo rock		51	421293	6341711	-33.06031	122.15689
194703	Pegmatitic leucosome in quartzofeldspathic gneiss	Southeastern Biranup Zone	Double Tank		51	421073	6352936	-32.95905	122.15550
194704	Plagioclase-quartz-hornblende biotite-garnet gneiss	Southeastern Biranup Zone	Double Tank	Yes	51	421073	6352936	-32.95905	122.15550
194705	Syenogranite gneiss	Southeastern Biranup Zone	Fraser Range Track, Cowalinya	Yes	51	437572	6388116	-32.64280	122.33439
194706	Hornblende syenogranite gneiss	Southeastern Biranup Zone	North of Mount Andrew		51	491769	6400828	-32.52986	122.91235
194707	Metamonzogranite	Southeastern Biranup Zone	Mount Andrew Track		51	490951	6397970	-32.55563	122.90361
194708	Leucosome in metamonzogranite	Southeastern Biranup Zone	Mount Andrew Track		51	490951	6397970	-32.55563	122.90361
194713	Metamonzogranite gneiss	Southeastern Biranup Zone	Garnet Ice Quarry	Yes	51	468777	6450787	-32.07876	122.66916
194720	Rapakivi metagranite	Eddy Suite; Eastern Biranup Zone	Southwest of Harris Lake	Yes	51	546153	6534950	-31.31893	123.48507
194721	Biotite-augite norite	Eddy Suite; Eastern Biranup Zone	Southwest of Harris Lake	Yes	51	546142	6535047	-31.31806	123.48495
194739	Granitic dyke	Eddy Suite; Eastern Biranup Zone	Southwest of Harris Lake		51	545937	6534910	-31.31930	123.48280
194744	Gabbroic-intermediate dyke	Eddy Suite; Eastern Biranup Zone	Southwest of Harris Lake		51	541365	6531323	-31.35184	123.43490
194723	Monzogranite gneiss	Eddy Suite; Eastern Biranup Zone	Southwest of Harris Lake	Yes	51	546022	6535898	-31.31038	123.48365
194724	Syenogranite gneiss	Eddy Suite; Eastern Biranup Zone	Southwest of Harris Lake	Yes	51	545951	6535999	-31.30948	123.48290
194725	Granitic gneiss	Eastern Biranup Zone	South of Urarylie Rock	Yes	51	540851	6541647	-31.25871	123.42907
194726	Granitic gneiss	Eastern Biranup Zone	Urarylie Rock	Yes	51	540239	6549701	-31.18606	123.42232
194727	Syenogranitic gneiss	Eastern Biranup Zone	Urarylie Rock	Yes	51	540166	6549845	-31.18476	123.42155
194788	Granitic leucosome cutting foliation	Eastern Biranup Zone	Torvil and Dean Lake		51	545939	6535995	-31.30951	123.48277

GSWA Sample ID	Lithology	Unit	Location	Lu-Hf data	MGA Zone	Easting	Northing	Latitude	Longitude
194789	Migmatitic granitic gneiss	Eastern Biranup Zone	Southwest of Uraryie Rock		51	534276	6539006	-31.28275	123.36010
194728	Quartzofeldspathic gneiss	Eastern Biranup Zone	Ponton Creek	Yes	51	560358	6583678	-30.87863	123.63144
194729	Leucosome in metamonzogranite	Eastern Biranup Zone	Ponton Creek		51	562765	6582098	-30.89276	123.65672
194730	Monzogranite gneiss (migmatized)	Eastern Biranup Zone	Ponton Creek	Yes	51	562765	6582098	-30.89276	123.65672
194732	Metagranodiorite	Eastern Biranup Zone	Ponton Creek	Yes	51	561511	6579817	-30.91341	123.64374
194733	Porphyritic metamonzogranite	Eastern Biranup Zone	Ponton Creek	Yes	51	561598	6579812	-30.91345	123.64465
194734	Migmatitic granitic gneiss	Eastern Biranup Zone	Ponton Creek	Yes	51	561862	6579939	-30.91229	123.64740
194790	Garnet-bearing leucosome	Eastern Biranup Zone	Ponton Creek		51	561872	6579911	-30.91254	123.64751
194736	Metasyenogranite	Northeastern Biranup Zone	East of Tropicana	Yes	51	667696	6772873	-29.16167	124.72428
194737	Metasyenogranite	Northeastern Biranup Zone	Bobbie Point	Yes	51	662415	6792732	-28.98319	124.66711
182424	Metasyenogranite	Northeastern Biranup Zone	McKay Creek	Yes	51	675563	6802915	-28.88958	124.80043
182426	Syenogranitic dyke	Northeastern Biranup Zone	Pleiades Lakes area	Yes	51	683549	6770104	-29.18445	124.88767
182411	Megacrystic foliated metagranite	Northeastern Biranup Zone	Pleiades Lakes area	Yes	51	684379	6769891	-29.18625	124.89624
182428	Megacrystic foliated metagranite	Northeastern Biranup Zone	Pleiades Lakes area	Yes	51	684613	6770517	-29.18057	124.89854
184311	Opx-Cpx granitic gneiss	Central Biranup Zone	Fisherys headland, Bremer Bay	Yes	50	720773	6187931	-34.42654	119.40249
184310	Leucocratic granodiorite in boudin neck	Central Biranup Zone	Fisherys headland, Bremer Bay		50	720773	6187931	-34.42654	119.40249
184312	Granodioritic gneiss	Central Biranup Zone	Short Beach headland, Bremer Bay	Yes	50	720437	6186221	-34.44202	119.39927
184326	Pegmatitic leucogranite in boudin neck	Central Biranup Zone	Short Beach headland, Bremer Bay		50	720546	6186078	-34.44328	119.40050
184119	Monzogranitic gneiss	Central Biranup Zone	Point Henry, Bremer Bay		50	719139	6181985	-34.48046	119.38624
184307	Pegmatitic granodiorite in boudin neck	Central Biranup Zone	Point Henry, Bremer Bay		50	719234	6182133	-34.47911	119.38724
83658	Hornblende-biotite granodiorite gneiss	Central Biranup Zone	Dalyup Creek		51	368735	6268345	-33.71678	121.58332

GSWA Sample ID	Lithology	Unit	Location	Lu-Hf data	MGA Zone	Easting	Northing	Latitude	Longitude
83652	Biotite–hornblende granodioritic gneiss	Central Biranup Zone	Lake Gidong headland		51	355032	6255207	-33.83345	121.43332
83651	Biotite–hornblende granodioritic gneiss	Central Biranup Zone	Lake Gidong headland		51	355032	6255207	-33.83345	121.43332
83649	Granite pegmatite	Central Biranup Zone	Lake Gidong headland		51	355032	6255207	-33.83345	121.43332
184123	Garnet–monzogranitic gneiss	Central Biranup Zone	Butty Head	Yes	51	377419	6251030	-33.87395	121.67462
183671	Granitic gneiss	Fraser Range Metamorphics	Track to northeastern gabbro quarry;		51	507214	6464176	-32.95837	122.07634
194781	Mafic granulite	Fraser Range Metamorphics	East of Mount Pleasant	Yes	51	490607	6452803	-32.06096	122.90049
194776	Metagranite	Fraser Range Metamorphics	North of Southern Hills HSD	Yes	51	484476	6437595	-32.19809	122.83529
183653	Pegmatite	Fraser Range Metamorphics	Mount Malcolm	Yes	51	486546	6433715	-32.23312	122.85720
194782	Pegmatite	Fraser Range Metamorphics	Gold Leaf Black Quarry	Yes	51	502575	6447072	-32.11270	123.02790
194717	Norite and K-spar–quartz metagabbro	Fraser Range Metamorphics	Fraser Range Black Quarry		51	502080	6447098	-32.11247	123.02205
194719	Metasyenogranite	Fraser Range Metamorphics	Symons Hill	Yes	51	503090	6475794	-31.85357	123.03266
194711	Metamonzogranite	Fraser Range Metamorphics	Newman Shear Zone (south)	Yes	51	492904	6418535	-32.37013	122.92457
194787	Granitic pegmatite	Fraser Range Metamorphics	Small quarry NW of Newman Rocks		51	510398	6453926	-32.05082	123.11014
194718	Mafic granulite	Fraser Range Metamorphics	American Granulite Quarry	Yes	51	489105	6462896	-31.96989	122.88469
177909	Monzogranite gneiss	Fraser Range Metamorphics	Fantasia Quarry	Yes	51	491173	6465549	-31.94597	122.90660
194779	Metagranite	Fraser Range Metamorphics	Near Fraser Range Station	Yes	51	480664	6454348	-32.04690	122.79519
194780	Granitic pegmatite	Fraser Range Metamorphics	Near Fraser Range Station		51	482656	6456347	-32.02889	122.81632
194783	Metagranite	Recherche Supersuite	Newman Shear Zone	Yes	51	516133	6446900	-32.11414	123.17101
83690	Biotite granodiorite gneiss	Recherche Supersuite	Bald Rock		51	349076	6302425	-33.40690	121.37698
83700A	Hornblende–biotite syenogranite gneiss	Recherche Supersuite	Coramup Hill Quarry		51	399681	6263175	-33.76678	121.91666

GSWA Sample ID	Lithology	Unit	Location	Lu-Hf data	MGA Zone	Easting	Northing	Latitude	Longitude
83697	Biotite monzogranite gneiss	Recherche Supersuite	Mount Burdett	Yes	51	420371	6297714	-33.45705	122.14315
83662	Biotite-hornblende monzogranite gneiss	Recherche Supersuite	Poison Creek	Yes	51	532545	6248117	-33.90685	123.35203
83663	Granodiorite gneiss	Recherche Supersuite	Israelite Bay	Yes	51	585617	6283235	-33.58717	123.92266
194710	Syenogranite gneiss	Recherche Supersuite	East of Mount Andrew	Yes	51	502814	6389122	-32.63548	123.03000
194712	Syenogranite gneiss	Recherche Supersuite	East of Mount Andrew	Yes	51	506467	6410544	-32.44222	123.06880
184125	Opx-dioritic gneiss	Recherche Supersuite	Observatory Point, Esperance	Yes	51	388659	6247378	-33.90813	121.79566
83659	Metagranite	Recherche Supersuite	Observatory Point, Esperance	Yes	51	388659	6247378	-33.90813	121.79566
194786	Metamonzogranite	Recherche Supersuite	East of Boigaring Rocks	Yes	51	531632	6402882	-32.51091	123.33677
182477	Mafic granulite	Recherche Supersuite	Big Red drillcore	Yes	51	688400	6649200	-30.27426	124.95861
182476	Granitic gneiss	Recherche Supersuite	Big Red drillcore	Yes	51	688400	6649200	-30.27426	124.95861
Metasedimentary rocks									
194722	Semipellitic schist	Eddy schist; intruded by Eddy Suite	Southwest of Harris Lake		51	546046	6534694	-31.32125	123.48396
194731	Psammitic gneiss	Pontoon Creek gneiss	Pontoon Creek		51	561726	6579780	-30.91373	123.64599
184122	Psammitic gneiss	Coramup Gneiss	Butty Head		51	377419	6251030	-33.87395	121.67462
182405	Metaconglomerate	Lindsay Hill Formation	East of Tropicana	Yes	51	677352	6802234	-28.89548	124.81887
182416	Quartzite	Lindsay Hill Formation	McKay Creek	Yes	51	663584	674594	-29.14668	124.68176
182473	Sedimentary gneiss	Unnamed	Big Red drill core	Yes	51	690500	6649200	-30.27393	124.98043
182475	Sedimentary gneiss	Unnamed	Big Red drill core	Yes	51	690500	6649200	-30.27393	124.98043
194742	Psammitic gneiss	Fly Dam Formation	South of Udarra Soak	Yes	51	535727	6531076	-31.35425	123.37563
194743	Semipellitic gneiss	Fly Dam Formation	South of Udarra Soak	Yes	51	535652	6530467	-31.35975	123.37487
165592	Quartz sandstone	Woodline Formation	Madoonia Downs		51	474130	6519050	-31.46302	122.72769
165591	Quartz sandstone	Woodline Formation	Madoonia Downs		51	474130	6519050	-31.46302	122.72769
179098	Quartz sandstone	Woodline Formation	Madoonia Downs		51	475900	6520210	-31.45259	122.74635
165593	Quartz sandstone	Woodline Formation	Madoonia Downs		51	475900	6520210	-31.45259	122.74635
179602	Quartz sandstone	Woodline Formation	Madoonia Downs		51	462640	6533390	-31.33332	122.60729
179097	Quartz sandstone	Woodline Formation	Madoonia Downs		51	462640	6533390	-31.33332	122.60729
177921	Metaconglomerate	Woodline Formation	Madoonia Downs		51	476294	6516878	-31.48260	122.71883
112170	Metasandstone	Kundip Quartzite, Mount Barren Group	Barrens Beach		51	225774	6241259	-33.93344	120.03332
112168	Fine-grained metasandstone	Kundip Quartzite, Mount Barren Group	No Tree Hill		51	228381	6257986	-33.78345	120.06666

GSWA Sample ID	Lithology	Unit	Location	Lu-Hf data	MGA Zone	Easting	Northing	Latitude	Longitude
112128	Muscovite–biotite–sillimanite paragneiss	Malcolm Metamorphics	Southwest of Point Malcolm		51	565292	6257865	-33.81741	123.70551
194735	Quartzofeldspathic gneiss	Gwynne Creek Gneiss	Gwynne Creek	Yes	51	688969	6743276	-29.42565	124.94797
182432	Semipelite gneiss	Gwynne Creek Gneiss	Gwynne Creek	Yes	51	688992	6745016	-29.40995	124.94791
194777	Metasedimentary gneiss	Snowys Dam Formation	West of Mount Malcolm	Yes	51	483364	6433838	-32.23197	122.82343
194778	Migmatitic garnet–biotite gneiss	Snowys Dam Formation	West of Mount Malcolm		51	483448	6433883	-32.23157	122.82432
177910	Quartzite	Snowys Dam Formation	Near Peters Dam	Yes	51	484173	6464384	-31.95641	122.83252
194714	Psammitic gneiss	Snowys Dam Formation	Near Gnamma Hill	Yes	51	471675	6440359	-32.17291	122.69956
194867	Interlayered psammitic and pelitic gneiss	Malcolm Metamorphics	Point Malcolm	Yes	51	570136	6259972	-33.79810	123.75768
194869	Interlayered psammitic and pelitic gneiss	Malcolm Metamorphics	Point Malcolm	Yes	51	564857	6257310	-33.82244	123.70085

Data from external sources:

Sample ID	Lithology	Unit	Location	References*
Sr-01	Semipelite schist	Kybulup Schist	Near Steere River	Dawson et al., 2002
Sr-02	Semipelite schist	Kybulup Schist	Near Steere River	Dawson et al., 2002
Tr-02	Metasandstone	Kundip Quartzite	Trilogy drill core MYCD058	Dawson et al., 2002
Tr-011	Metasandstone	Steere Formation	Trilogy drill core MYCD058	Dawson et al., 2002
9510101	Quartzite	Mount Ragged Formation	Mount Ragged	Clark et al., 2000
PM-11-011	Migmatitic semipelite schist	Malcolm Metamorphics	Point Malcolm	Adams, 2012

NOTE: *Full references for external sources can be found in the References section

Appendix 3

List of GSWA geochemistry samples used in this publication. MGA coordinates are in Zone 52.

GSWA Sample ID	Magmatic series/core ID	Depth (m)	Lithology	Latitude	Longitude	Easting	Northing	250k map
201175	Haig gabbro HDDH001	464.5 – 464.75	Medium- to coarse-grained acicular-textured leucogabbro; hornblende to 1cm	-31.0534	126.0791	221250	6560810	SH 52-10
201176	Haig gabbro HDDH001	463.7 – 464.1	Medium-grained meso-melanocratic gabbro	-31.0534	126.0791	221250	6560810	SH 52-10
201177	Haig gabbro HDDH001	475 – 475.15	Coarse-grained acicular-textured leucogabbro; hornblende to 2cm	-31.0534	126.0791	221250	6560810	SH 52-10
201178	Haig gabbro HDDH001	491.5 – 491.75	Fine- to medium-grained leucogabbro; acicular hornblende	-31.0534	126.0791	221250	6560810	SH 52-10
201179	Haig gabbro HDDH001	498.75 – 498.95	Medium-grained leucogabbro; acicular hornblende	-31.0534	126.0791	221250	6560810	SH 52-10
201180	Haig gabbro HDDH001	502.1 – 502.7	Fine- to medium-grained leucogabbro; acicular hornblende	-31.0534	126.0791	221250	6560810	SH 52-10
201181	Haig gabbro HDDH001	513.2 – 513.4	Inhomogeneous mix of fine-grained, fine- to medium-grained and medium-grained acicular-textured leucogabbro	-31.0534	126.0791	221250	6560810	SH 52-10
201182	Haig gabbro HDDH001	514.25 – 514.5	Inhomogeneous mix of fine- to medium-grained and medium-grained acicular-textured leucogabbro	-31.0534	126.0791	221250	6560810	SH 52-10
201183	Haig gabbro HDDH001	520.1 – 520.3	Fine-grained gabbro	-31.0534	126.0791	221250	6560810	SH 52-10
201184	Haig gabbro HDDH001	523.6 – 523.8	Medium-grained acicular-textured leucogabbro	-31.0534	126.0791	221250	6560810	SH 52-10
201185	Haig gabbro HDDH001	529.85 – 530	Fine-grained gabbro	-31.0534	126.0791	221250	6560810	SH 52-10
201186	Haig gabbro HDDH001	531.55 – 531.7	Medium- to coarse-grained acicular-textured leucogabbro	-31.0534	126.0791	221250	6560810	SH 52-10
201187	Haig gabbro HDDH001	542.5 – 542.7	Mesocratic homogeneous gabbro	-31.0534	126.0791	221250	6560810	SH 52-10
201189	Haig gabbro HDDH001	561.75 – 562	Medium- to coarse-grained acicular-textured leucogabbro	-31.0534	126.0791	221250	6560810	SH 52-10
201190	Haig gabbro HDDH001	570.5 – 570.7	Medium- to coarse-grained acicular-textured leucogabbro	-31.0534	126.0791	221250	6560810	SH 52-10
201191	Haig gabbro HDDH001	579.3 – 579.6	Medium-grained mesocratic gabbro	-31.0534	126.0791	221250	6560810	SH 52-10
201192	Haig gabbro HDDH001	582.8 – 583	Fine- to medium-grained mesocratic to leucocratic gabbro	-31.0534	126.0791	221250	6560810	SH 52-10
201193	Haig gabbro HDDH001	591.4 – 591.7	Coarse-grained acicular-textured leucogabbro; hornblende to 2cm	-31.0534	126.0791	221250	6560810	SH 52-10
201194	Haig gabbro HDDH002	319.45 – 319.65	Medium-grained, mesocratic, equigranular gabbro	-30.9451	126.1035	223271	6572880	SH 52-10
201195	Haig gabbro HDDH002	330.9 – 331.1	Medium-grained, mesocratic, equigranular gabbro	-30.9451	126.1035	223271	6572880	SH 52-10
201196	Haig gabbro HDDH002	340.35 – 340.52	Fine- to medium-grained meso-melanocratic gabbro	-30.9451	126.1035	223271	6572880	SH 52-10
201197	Haig gabbro HDDH002	356.8 – 357.2	Fine- to medium-grained gabbro	-30.9451	126.1035	223271	6572880	SH 52-10
201198	Haig gabbro HDDH002	366.65 – 366.9	Medium-grained meso-melanocratic gabbro	-30.9451	126.1035	223271	6572880	SH 52-10
201199	Haig gabbro HDDH002	374.8 – 375.1	Fine- to medium-grained mesocratic gabbro	-30.9451	126.1035	223271	6572880	SH 52-10
201200	Haig gabbro HDDH002	379.68 – 379.88	Fine- to medium-grained mesocratic gabbro	-30.9451	126.1035	223271	6572880	SH 52-10
201201	Haig gabbro HDDH002	383.6 – 383.85	Medium-grained melanocratic gabbro	-30.9451	126.1035	223271	6572880	SH 52-10
201203	Haig gabbro HDDH002	392.9 – 392.65	Medium-grained melanocratic gabbro	-30.9451	126.1035	223271	6572880	SH 52-10

GSWA Sample ID	Magmatic series/core ID	Depth (m)	Lithology	Latitude	Longitude	Easting	Northing	250k map
201204	Haig gabbro HDDH002	401.1 – 401.35	Medium-grained melanocratic gabbro	-30.9451	126.1035	223271	6572880	SH 52-10
201205	Haig gabbro HDDH002	404.65 – 404.85	Fine- to medium-grained mesocratic gabbro	-30.9451	126.1035	223271	6572880	SH 52-10
201206	Haig gabbro HDDH002	407 – 407.25	Medium-grained meso-melanocratic gabbro	-30.9451	126.1035	223271	6572880	SH 52-10
201207	Haig gabbro HDDH002	416.7 – 416.9	Medium-grained melanocratic gabbro	-30.9451	126.1035	223271	6572880	SH 52-10
201208	Haig gabbro HDDH002	422.4 – 422.65	Fine- to medium-grained mesocratic gabbro	-30.9451	126.1035	223271	6572880	SH 52-10
201210	Haig gabbro HDDH002	459.35 – 459.5	Medium-grained mesocratic gabbro	-30.9451	126.1035	223271	6572880	SH 52-10
201211	Haig gabbro HDDH002	466.35 – 466.5	Fine- to medium-grained meso-melanocratic gabbro	-30.9451	126.1035	223271	6572880	SH 52-10
201212	Haig gabbro HDDH002	474.25 – 474.45	Medium-grained mesocratic gabbro	-30.9451	126.1035	223271	6572880	SH 52-10
201188	Haig plagiogranite HDDH001	159.15 – 159.3	30cm wide leucogranite vein in gabbro	-31.0534	126.0791	221250	6560810	SH 52-10
201202	Haig plagiogranite HDDH002	391.05 – 391.3	Granite dyke	-30.9451	126.1035	223271	6572880	SH 52-10
201209	Haig plagiogranite HDDH002	442.2 – 442.35	Granite dyke	-30.9451	126.1035	223271	6572880	SH 52-10
201111	Loongana gabbro LNGD001	277 – 277.4	Fine- to medium-grained gabbro	-30.8197	126.415	252720	6587520	SH 52-09
201112	Loongana gabbro LNGD001	280.24 – 280.4	Fine- to medium-grained gabbro	-30.8197	126.415	252720	6587520	SH 52-09
201113	Loongana gabbro LNGD001	282.55 – 282.72	Medium-grained equigranular gabbro	-30.8197	126.415	252720	6587520	SH 52-09
201114	Loongana gabbro LNGD001	283 – 283.3	Fine- to medium-grained equigranular gabbro	-30.8197	126.415	252720	6587520	SH 52-09
201115	Loongana gabbro LNGD001	284.05 – 284.24	Fine- to medium-grained equigranular gabbro	-30.8197	126.415	252720	6587520	SH 52-09
201116	Loongana gabbro LNGD001	284.58 – 284.71	Pegmatoidal gabbro/pyroxenite	-30.8197	126.415	252720	6587520	SH 52-09
201117	Loongana gabbro LNGD001	285 – 285.2	Fine- to medium-grained equigranular gabbro	-30.8197	126.415	252720	6587520	SH 52-09
201118	Loongana gabbro LNGD001	286.1 – 286.5	Fine- to medium-grained olivine-rich equigranular gabbro	-30.8197	126.415	252720	6587520	SH 52-09
201119	Loongana gabbro LNGD001	286.7 – 286.92	Fine- to medium-grained olivine-rich equigranular gabbro	-30.8197	126.415	252720	6587520	SH 52-09
201120	Loongana gabbro LNGD001	288 – 288.3	Fine- to medium-grained equigranular olivine gabbro or peridotite	-30.8197	126.415	252720	6587520	SH 52-09
201121	Loongana gabbro LNGD001	288.45 – 288.7	Fine- to medium-grained equigranular olivine gabbro or peridotite	-30.8197	126.415	252720	6587520	SH 52-09
201122	Loongana gabbro LNGD001	288.75 – 288.95	Fine- to medium-grained equigranular gabbro	-30.8197	126.415	252720	6587520	SH 52-09
201123	Loongana gabbro LNGD001	290.75 – 291	Fine- to medium-grained equigranular gabbro	-30.8197	126.415	252720	6587520	SH 52-09
201124	Loongana gabbro LNGD001	291.7 – 291.9	Fine- to medium-grained equigranular gabbro	-30.8197	126.415	252720	6587520	SH 52-09
201125	Loongana gabbro LNGD001	292.45 – 292.7	Fine- to medium-grained equigranular gabbro	-30.8197	126.415	252720	6587520	SH 52-09
201126	Loongana gabbro LNGD001	293.25 – 293.4	Pegmatoidal gabbro/pyroxenite	-30.8197	126.415	252720	6587520	SH 52-09
201127	Loongana gabbro LNGD001	293.6 – 293.8	Fine- to medium-grained equigranular gabbro	-30.8197	126.415	252720	6587520	SH 52-09

GSWA Sample ID	Magmatic series/core ID	Depth (m)	Lithology	Latitude	Longitude	Easting	Northing	250k map
201128	Loongana gabbro LNGD001	294.45 – 294.7	Fine- to medium-grained equigranular gabbro	-30.8197	126.415	252720	6587520	SH 52-09
201129	Loongana gabbro LNGD001	295.5 – 295.7	Fine- to medium-grained equigranular gabbro	-30.8197	126.415	252720	6587520	SH 52-09
201130	Loongana gabbro LNGD001	296.8 – 297	Fine- to medium-grained equigranular gabbro	-30.8197	126.415	252720	6587520	SH 52-09
201131	Loongana gabbro LNGD001	297.3 – 297.45	Fine- to medium-grained equigranular leucocratic gabbro	-30.8197	126.415	252720	6587520	SH 52-09
201132	Loongana gabbro LNGD001	298.4 – 298.6	Fine- to medium-grained equigranular leucocratic gabbro	-30.8197	126.415	252720	6587520	SH 52-09
201133	Loongana gabbro LNGD001	300 – 300.28	Fine- to medium-grained equigranular leucocratic gabbro	-30.8197	126.415	252720	6587520	SH 52-09
201134	Loongana gabbro LNGD001	301 – 301.3	Fine- to medium-grained equigranular leucocratic gabbro	-30.8197	126.415	252720	6587520	SH 52-09
201135	Loongana gabbro LNGD001	302.2 – 302.6	Fine- to medium-grained equigranular leucocratic gabbro	-30.8197	126.415	252720	6587520	SH 52-09
201136	Loongana gabbro LNGD001	304 – 304.3	Fine- to medium-grained equigranular leucocratic gabbro	-30.8197	126.415	252720	6587520	SH 52-09
201137	Loongana gabbro LNGD001	305.1 – 305.45	Fine- to medium-grained equigranular leucocratic gabbro	-30.8197	126.415	252720	6587520	SH 52-09
201138	Loongana gabbro LNGD001	307.15 – 307.55	Fine- to medium-grained equigranular leucocratic gabbro	-30.8197	126.415	252720	6587520	SH 52-09
201139	Loongana gabbro LNGD001	309.75 – 310	Fine- to medium-grained equigranular leucocratic gabbro	-30.8197	126.415	252720	6587520	SH 52-09
201140	Loongana gabbro LNGD001	313.1 – 313.4	Pegmatoidal gabbro/pyroxenite	-30.8197	126.415	252720	6587520	SH 52-09
201141	Loongana gabbro LNGD001	316.5 – 316.8	Medium-grained equigranular gabbro	-30.8197	126.415	252720	6587520	SH 52-09
201142	Loongana gabbro LNGD001	318.2 – 318.5	Medium-grained gabbro	-30.8197	126.415	252720	6587520	SH 52-09
201143	Loongana gabbro LNGD001	320 – 320.4	Fine- to medium-grained equigranular gabbro	-30.8197	126.415	252720	6587520	SH 52-09
201144	Loongana gabbro LNGD001	323.1 – 323.4	Fine- to medium-grained equigranular gabbro	-30.8197	126.415	252720	6587520	SH 52-09
201145	Loongana gabbro LNGD001	325.25 – 325.7	Medium-grained equigranular leucogabbro	-30.8197	126.415	252720	6587520	SH 52-09
201146	Loongana gabbro LNGD001	329.6 – 329.75	Medium-grained equigranular leucogabbro	-30.8197	126.415	252720	6587520	SH 52-09
201147	Loongana gabbro LNGD001	329.8 – 330.15	Medium-grained equigranular gabbro	-30.8197	126.415	252720	6587520	SH 52-09
201148	Loongana gabbro LNGD001	332.8 – 333	Medium-grained equigranular gabbro	-30.8197	126.415	252720	6587520	SH 52-09
201150	Loongana gabbro LNGD001	344.5 – 344.8	Fine- to medium-grained equigranular gabbro	-30.8197	126.415	252720	6587520	SH 52-09
201152	Loongana gabbro LNGD001	382.1 – 382.3	Fine- to medium-grained gabbro	-30.8197	126.415	252720	6587520	SH 52-09
201153	Loongana gabbro LNGD001	385.4 – 385.65	Medium-grained acicular textured gabbro	-30.8197	126.415	252720	6587520	SH 52-09
201158	Loongana gabbro LNGD001	510.2 – 510.4	Medium-grained equigranular to acicular gabbro	-30.8197	126.415	252720	6587520	SH 52-09
201171	Loongana gabbro LNGD001	331.5 – 331.7	Gabbro	-30.8197	126.415	252720	6587520	SH 52-09
201165	Loongana gabbro LNGD002	315.5 – 315.8	Medium-grained equigranular to acicular gabbro	-30.8003	126.4277	253880	6589701	SH 52-09
201170	Loongana gabbro LNGD002	564.2 – 564.4	Fine- to medium-grained equigranular gabbro	-30.8003	126.4277	253880	6589701	SH 52-09
201149	Loongana plagiogranite LNGD001	335.3 – 335.6	Weakly foliated granite – blue quartz	-30.8197	126.415	252720	6587520	SH 52-09

GSWA Sample ID	Magmatic series/core ID	Depth (m)	Lithology	Latitude	Longitude	Easting	Northing	250k map
201151	Loongana plagiogranite LNGD001	362.8 – 363.1	Weakly foliated granite – blue quartz to 6 mm; schlieren or mafic-rich lenses	-30.8197	126.415	252720	6587520	SH 52-09
201154	Loongana plagiogranite LNGD001	465.8 – 466	Weakly foliated medium- to coarse-grained mesocratic granite– blue quartz	-30.8197	126.415	252720	6587520	SH 52-09
201155	Loongana plagiogranite LNGD001	468.85 – 469.05	Weakly foliated leucogranite (syenogranite)	-30.8197	126.415	252720	6587520	SH 52-09
201156	Loongana plagiogranite LNGD001	474.6 – 474.96	Massive mesocratic granodiorite	-30.8197	126.415	252720	6587520	SH 52-09
201157	Loongana plagiogranite LNGD001	499.25 – 499.5	Weakly foliated mesocratic granite – blue quartz	-30.8197	126.415	252720	6587520	SH 52-09
201159	Loongana plagiogranite LNGD001	511.9 – 512.1	Weakly foliated mesocratic granite – blue quartz	-30.8197	126.415	252720	6587520	SH 52-09
201160	Loongana plagiogranite LNGD001	514.4 – 514.55	Foliated mesocratic granodiorite	-30.8197	126.415	252720	6587520	SH 52-09
201161	Loongana plagiogranite LNGD001	526.6 – 526.9	Weakly foliated medium- to coarse-grained mesocratic granite – blue quartz	-30.8197	126.415	252720	6587520	SH 52-09
201162	Loongana plagiogranite LNGD001	560.4 – 560.65	Weakly foliated medium- to coarse-grained mesocratic granite – blue quartz	-30.8197	126.415	252720	6587520	SH 52-09
201163	Loongana plagiogranite LNGD001	575.7 – 575.95	Weakly foliated medium- to coarse-grained mesocratic granite – blue quartz	-30.8197	126.415	252720	6587520	SH 52-09
201164	Loongana plagiogranite LNGD001	642.7 – 643	Foliated medium- to coarse-grained mesocratic granite – blue quartz	-30.8197	126.415	252720	6587520	SH 52-09
201166	Loongana plagiogranite LNGD002	356.7 – 357	Equigranular leucogranite	-30.8003	126.4277	253880	6589701	SH 52-09
201168	Loongana plagiogranite LNGD002	467.8 – 468.2	Weakly foliated equigranular leucogranite	-30.8003	126.4277	253880	6589701	SH 52-09
201169	Loongana plagiogranite LNGD002	543.7 – 544	Foliated equigranular leucogranite	-30.8003	126.4277	253880	6589701	SH 52-09
182466	Serpent gabbro SDDH1	536.4 – 537	Metagabbro	-31.2139	126.0715	221001	6543000	SH 52-10
182467	Serpent gabbro SDDH1	552.8 – 553.3	Metagabbro	-31.2139	126.0715	221001	6543000	SH 52-10
182468	Serpent gabbro SDDH1	571.3 – 571.9	Metagabbro	-31.2139	126.0715	221001	6543000	SH 52-10
182469	Serpent gabbro SDDH1	583.4 – 583.9	Metagabbro	-31.2139	126.0715	221001	6543000	SH 52-10
182470	Serpent gabbro SDDH2	456.1 – 456.2	Metagabbro	-31.2276	126.0816	222001	6541500	SH 52-10
182471	Serpent gabbro SDDH2	472.8 – 473	Metagabbro	-31.2276	126.0816	222001	6541500	SH 52-10
182472	Serpent gabbro SDDH2	512.05 – 512.4	Metagabbro	-31.2276	126.0816	222001	6541500	SH 52-10

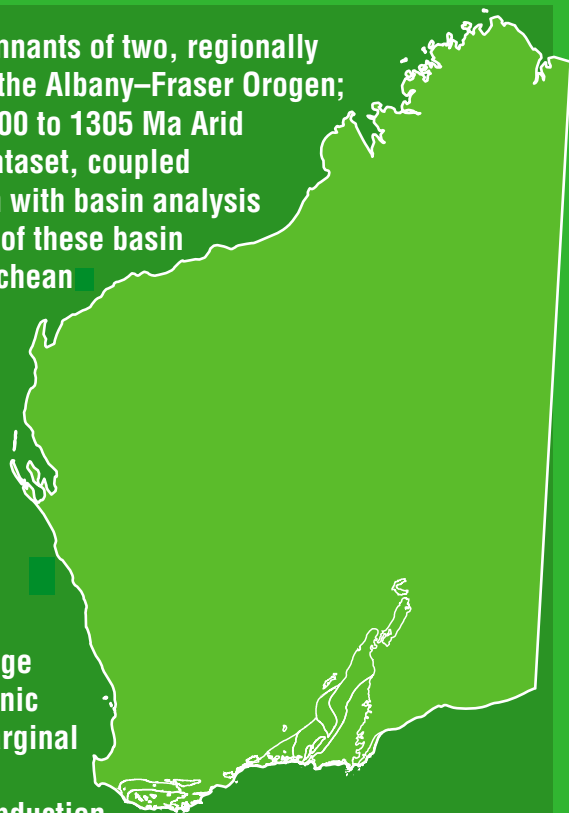
Appendix 4

Lu–Hf data collection and methods

Hafnium isotope analyses were conducted on previously dated zircons using a New Wave/Merchantek LUV213 laser-ablation microprobe, attached to a Nu Plasma multi-collector inductively coupled plasma mass spectrometer (LA-MC-ICPMS). The methodology of this approach has been detailed elsewhere (Griffin et al., 2000). In brief, the analyses employed a beam diameter of c. 40 μm with ablation pits 40–60 μm deep. The ablated sample material was transported from the laser cell to the ICP–MS torch in a helium gas flow. Interference of ^{176}Lu on ^{176}Hf was corrected by measurement of the interference-free ^{175}Lu and using an invariant $^{176}\text{Lu}/^{175}\text{Lu}$ correction factor (De Bièvre and Taylor, 1993). Isobaric interference of ^{176}Yb on ^{176}Hf was corrected by measurement of the interference-free ^{172}Yb isotope and using the $^{176}\text{Yb}/^{172}\text{Yb}$ ratio to calculate the intensity of interference free ^{176}Yb . The appropriate value of $^{176}\text{Yb}/^{172}\text{Yb}$ was determined by successive doping of the JMC475 Hf standard with various amounts of Yb.

Hf isotopic measurements for this project were conducted over four separate analytical sessions. Zircons from the Mud Tank carbonatite locality were analysed, together with the samples, as a measure of the accuracy of the results. Most of the data and the mean $^{176}\text{Hf}/^{177}\text{Hf}$ value in all sessions (session 1 = 0.282522 ± 15 , $n = 15$; session 2 = 0.282523 ± 21 , $n = 38$; session 3 = 0.282519 ± 12 , $n = 14$; session 4 = 0.282525 ± 18 , $n = 97$) are within 2 standard deviations (SD) of the recommended value (0.282522 ± 0.000042 (2σ); (Griffin et al., 2007). Temora-2 zircon was run as an independent check on the accuracy of the Yb correction during sessions 2, 3, and 4. Temora zircon has an average $^{176}\text{Yb}/^{177}\text{Hf}$ ratio of 0.037, which is similar to the average $^{176}\text{Yb}/^{177}\text{Hf}$ ratio of zircon in this study of 0.031. The average $^{176}\text{Hf}/^{177}\text{Hf}$ ratio for Temora-2 is (session 2 = 0.282722 ± 48 , $n = 8$; session 3 = 0.282672 ± 11 , $n = 2$; session 4 = 0.282685 ± 19 , $n = 30$) consistent with the published value for the Temora-2 standard (0.282686 ± 8 , solution ICPMS, Woodhead and Hergt (2005); 0.282687 ± 24 , LA-ICPMS, Hawkesworth and Kemp (2006). During session one 91500 was analysed as a secondary standard and yielded a $^{176}\text{Hf}/^{177}\text{Hf}$ value (0.282321 ± 19 , $n = 6$) well within the range of reported values for this standard (Griffin et al., 2007). Calculation of εHf values employs the decay constant of Scherer et al. (2001) and the CHUR values of Blichert-Toft and Albarède (1997).

This Report presents a detailed analysis of the remnants of two, regionally extensive Proterozoic basin systems preserved in the Albany–Fraser Orogen; the c. 1815 to 1600 Ma Barren Basin and the c. 1600 to 1305 Ma Arid Basin. An extensive U–Pb zircon geochronology dataset, coupled with Lu–Hf isotope analysis, is used in conjunction with basin analysis to interpret the provenance and tectonic evolution of these basin systems. The Barren Basin is dominated by Neoarchean zircon detritus from the Yilgarn Craton, and Paleoproterozoic zircon detritus from magmatic events within the orogen. The abundance of locally derived sediment deposited onto a reworked Archean Yilgarn Craton substrate indicates a largely extensional tectonic setting, consistent with a broad continental rift basin or alternatively, a long-lived back-arc basin system along the craton margin. The relatively quiescent period from c.1600 to c. 1455 Ma indicates a change from active, rift-related extension, to a proto-oceanic rift, through to a passive-margin and adjoining marginal basin, marking the initiation of the Arid Basin. Closure of this marginal basin via east-dipping subduction led to accretion of the Loongana oceanic-arc at c. 1330 Ma, and dispersal of the detritus into a foreland basin system, marking a second phase of the Arid Basin. The two basin systems reflect a distinct change in tectonic regime from Paleoproterozoic rifting of the Yilgarn Craton, to the formation of a marginal basin that was subsequently closed during the Mesoproterozoic.



Further details of geological products and maps produced by the Geological Survey of Western Australia are available from:

Information Centre
Department of Mines and Petroleum
100 Plain Street
EAST PERTH WA 6004
Phone: (08) 9222 3459 Fax: (08) 9222 3444
www.dmp.wa.gov.au/GSWApublications